CONTRACTOR REPORT

SAND89—7064
Unlimited Release
UC—~~900~~ 700

Slotted-Wall Research With Disk and Parachute Models in the DSMA Low-Speed Wind Tunnel

David Van Every, John L. Harris
DSMA International Inc.
Mississauga, Ontario
CANADA

Prepared by Sandia National Laboratories Albuquerque, New Mexico 87185
and Livermore, California 94550 for the United States Department of Energy
under Contract DE-AC04-76DP00789

Printed June 1990

Issued by Sandia National Laboratories, operated for the United States Department of Energy by Sandia Corporation.

Available to DOE and DOE contractors from
Office of Scientific and Technical Information
PO Box 62
Oak Ridge, TN 37831

Prices available from (615) 576-8401, FTS 626-8401

Available to the public from
National Technical Information Service
US Department of Commerce
5285 Port Royal Rd
Springfield, VA 22161

NTIS price codes
Printed copy: A06
Microfiche copy: A01

SAND89-7064
Unlimited Release
Printed June 1990

SAND--89-7064

DE90 013631

Slotted-Wall Research with Disk and Parachute Models in the DSMA Low-Speed Wind Tunnel

David Van Every
John L. Harris

DSMA International Inc.
Mississauga, Ontario, Canada

Abstract

A test program investigated the effects of wall open area ratio (OAR) and model axial position on the measured drag of disk and parachute models in a low-speed wind tunnel. The data and discussion presented in this report provide new insight into the nature of slotted-wall interference for bluff bodies in steady flow and give the first quantitative information on nonsteady wall interference and airflow response during the inflation of a parachute. The report concludes that a fixed OAR of between 5% and 15% should eliminate wall interference during inflation and greatly reduce steady-flow interference for geometric blockages up to 15%. Preliminary arguments suggest that an optimum OAR may be found that alleviates wall interference for large models at low speeds while providing for acceptable testing of smaller models in the transonic speed range.

*The work described in this report was performed for Sandia National Laboratories under Contract No. 75-5888.

(this page intentionally left blank)

TABLE OF CONTENTS

LIST OF TABLES

LIST OF FIGURES

LIST OF SYMBOLS

A - test section cross sectional area (0.72m x 0.72m)

C_D - drag coefficient

C_p - pressure coefficient (defined by the following equation for wall pressures)

$$C_p = \frac{P_{wall\ (disk\ in)} - P_{wall\ (empty)}}{(P_{c1} - P_{c2}) \times K_q}$$

K_m - Maskell blockage correction factor (defined by the following equation)

$$\frac{q_c}{q} = \frac{C_D}{C_{Dc}} = 1 + K_m \frac{C_D S_u}{A}$$

K_q - test section dynamic pressure calibration factor (see Appendix A for definition)

K/h - slotted wall boundary condition parameter (see reference 6 for further explanation)

M_{int} - the Mach number at which a change in test section wall porosity is required due to increasing wall interference

OAR - open area ratio

P - static pressure

P_{c1} - reference static pressure at inlet of the contraction

P_{c2} - reference static pressure at outlet of the contraction

P_t - total pressure

q - dynamic pressure

S - model frontal area

SD - standard deviation

sqrt() - square root of the quantity in the brackets

X - axial location measured from the nozzle exit

Subscripts

c - corrected quantity

ref - reference quantity

u - uncorrected quantity

1 INTRODUCTION

Sandia National Laboratories have identified a need for a ground test facility to be used in the development of high performance parachute systems. A feasibility study[1] for this facility has been conducted by DSMA. During the final meetings for that study the idea of using a slotted wall test section to relieve or eliminate wall interference for subsonic tests was discussed.

Subsequently a contract was awarded to DSMA to perform a test program jointly with Sandia in DSMA's low speed model wind tunnel (MWT) to explore the possibility of using slotted walls to minimize parachute blockage. This test program was conducted in a 0.72 metre x 0.72 metre test section which was designed and constructed by DSMA for these tests. DSMA supplied the test facility with a complete calibration of all the test section configurations, while Sandia supplied the parachute models, the disk models, the data acquisition system, a balance, model support strut and sting, and pressure transducers. The calibration of the test sections was completed before Sandia personnel and equipment arrived at the MWT and this calibration program is described in Appendix A.

The purpose of the program was to establish wall interference characteristics for several open area ratios (OAR) using disk models and to establish the effect of wall OAR on the drag time history for parachute models during an infinite mass inflation. The test program did not include any moving model tests. In addition to this experimental work, DSMA also examined the compatibility of slotted walls for transonic testing and blockage reduction in subsonic testing for the proposed Sandia Parachute Wind Tunnel.

The experimental program was carried out during the weeks of August 21 and August 28, 1989. This report presents and evaluates the results of the test program and is the final deliverable required by the Sandia contract.

2 WIND TUNNEL TEST PROGRAM

2.1 DSMA Wind Tunnel

The DSMA MWT is a fan driven, closed circuit wind tunnel with a design maximum speed of 52 m/s with the original test section. The wind tunnel was designed for the testing of fifth scale passenger vehicles and tenth scale trucks and buses. The original test section has three slotted walls (solid floor) with a 30% open area ratio and the test section dimensions are 1240 mm wide x 720 mm high. The fan is manually operated. The fan speed is continuously variable to 1600 rpm and the fan is driven through a belt drive by a 94 hp DC motor. Rotor blade pitch is adjustable wind-off. Wind tunnel air temperature is controlled by a low loss, unfinned, aluminum airfoil heat exchanger in the second cross leg.

There are 3 flow conditioning screens and a honeycomb in the settling chamber, with contraction ratio of 6 to 1 to the original test section. These flow conditioning elements and a well designed circuit combine to yield very good flow uniformity and low test section turbulence. An airline diagram of the facility with the original test section is shown in Figure 1.

The existing airline was modified for the test program by installing several screens on the upstream face of the corner upstream of the fan section (see Appendix A). The purpose of these screens was to increase the circuit loss factor in order to reduce the change in dynamic pressure during a parachute inflation. The installation of the screens increased the overall circuit loss factor from 0.56 of the test section dynamic pressure to 3.29.

2.2 Test Section Configurations

A special test section which is 0.72 metres x 0.72 metres in cross-section and 2.0 metres long was designed and fabricated for these tests (Figures 2 to 7). This test section, complete with a secondary contraction, replaced the existing test section in the model wind tunnel, the effective contraction ratio then being 10.3 to 1. The test section diffuser was modified by adding internal walls to accommodate the reduced test section width. Four wall configurations were used for the tests; solid, and nominal wall porosities of 10% OAR, 20% OAR and 30% OAR. The test section airline is shown in Figure 2 and slot/slat geometries are shown in Figure 3. Also given in Figure 3 are the actual as-built average wall porosity for each wall configuration. The nominal wall porosities have been used to identify the different wall configurations in this report and in test documentation, but the actual wall porosities have been used in the analysis.

Changes in wall OAR are achieved by changing the centre three slats on each wall. The new test section does not have a plenum in order to simplify construction and provide more convenient access. Elimination of the plenum also eliminates any uncertainties due to plenum wall flows which is desirable for this type of fundamental investigation. Downstream adjustable flaps are provided to control the portion of the flow forced out through the slots which bypasses the remainder of the test section and re-enters the circuit through the flap opening. The test section has fillets which taper from an inlet hypotenuse of 100 mm to an exit hypotenuse of 0 mm. These fillets were designed to compensate for boundary layer growth in the solid wall configuration and were left installed for all wall configurations. With the solid wall configuration the re-entry flap was opened by a small amount to serve as the test section breather.

2.3 Models

Four disk models were tested with nominal diameters of 4.5 inches, 7.2 inches, 10.1 inches and 12.4 inches. All of the disks were 1/8 inch thick with a 45^{o} chamfer. The disk dimensions and area blockages in the MWT are given in the table below. Reference data for these models, with essentially zero wall interference, was collected in the Lockheed-Georgia wind tunnel by Sandia prior to the DSMA-Sandia tests. The Lockheed-Georgia data as well as actual disk dimensions are given in Table 1.

Disk Diameter	S	S/A
4.52 inches	16.06 in^2	0.02
7.15 inches	40.15 in^2	0.05
10.11 inches	80.28 in^2	0.10
12.39 inches	120.57 in^2	0.15

Three parachute models were also tested and these had constructed diameters of 10 inches, 14.5 inches and 18 inches. Suspension line lengths for each model were the same as the constructed diameter. Both steady state data and inflation data for the parachutes were collected at Lockheed-Georgia and this data is also summarized in Table 1.

Both the parachute models and the disk models were supported in the test section using a sting and strut arrangement (shown in Figures 4 and 5). The sting could be translated in the strut to permit the disks and parachutes to be positioned at any axial station. The parachute models had holes in the centre of the canopy to permit the sting to pass through. The ends of the suspension lines were captured in a special nose piece which attached to the metric side of the balance (see Figure 6).

2.4 Instrumentation

Disk drag and parachute drag were measured using an internal strain gage balance which had a maximum drag force capacity of 25 lbs force. Dynamic pressure and total pressure were measured with two Validyne 0.1 psid pressure transducers close coupled to a pitot tube and a wall static pressure hole located in the nozzle exit. This system was used in order to minimize lags and measure the dynamic pressure as close as possible to the model for the inflation tests. The location of the pitot tube and the static hole is indicated in Figure 2. A redundant measurement of reference dynamic pressure was made using four static pressure holes in the settling chamber, pneumatically averaged, and a second static tap in the nozzle. This pressure difference was measured using a 2000 Pa Datametrics differential pressure transducer.

The two dynamic pressure signals, the total pressure signal and five balance signals (rolling moment was omitted) were fed through an 8 channel signal conditioning rack to a PC based data acquisition system (shown in Figure 7). Signal conditioning included a 3 Hz low pass filter for all channels. This system was used to record the steady state data only.

All 8 channels were also input, before signal conditioning, to an FM tape recorder to permit later analysis of the inflation transients. The dynamic pressure and drag signal were input to a Nicolet digital oscilloscope for real time viewing of the parachute inflation transient. Hard copies of the oscilloscope traces were made using an HP plotter. A schematic of the instrumentation set-up is shown in Figure 8.

At the end of the test program a series of runs was made to measure the static pressure distribution on the left wall of the test section. The wall static taps were made using a 0.063" O.D.

Scanivalve tubulation pressed into a 1/16" hole drilled in the centre wall slat. The wall pressures were measured with the DSMA data acquisition system using a Scanivalve with a 0.5 psid Setra pressure transducer cross-referenced to the Datametrics reference transducer.

2.5 Test Procedure

For each slotted wall configuration initial runs were made with the 10.1 inch disk to determine a flap setting for the remainder of the runs with that wall configuration. Beginning at the most downstream position of 4.92 feet, disk drag was measured for flap positions of 1" through 5" in 1" increments. The convention for defining flap position is indicated in Figure 2. These runs were repeated with successive upstream disk positions until the flap effect was no longer significant. An optimum flap position was then selected; this position was chosen as the one for which opening the flaps further had negligible effect on the measured drag. The optimum flap selection rational was based on previous DSMA experience and is strictly correct only for the 10.1" disk; however, the specious effects of using this flap position for the other disks would be small and significant only for axial positions close to the flap. Further discussion regarding flap position is presented in section 3.1 of this report. These initial runs also served to define the extent of upstream flap influence. This procedure gave a flap position of 4" for all open area ratios.

With the flap setting of 4", measurements of disk drag for all 4 disks were made at axial positions which spanned the length of the test section. The data from the disk runs was used to determine an optimum position for the parachute inflations. In general steady state data for the parachutes and inflation data were collected during the same wind tunnel run in order to reduce parachute fatigue.

Parachute inflation was initiated through use of a light reefing line tied with a slip knot. The reefing line was tied tightly around the suspension lines just upstream of the parachute skirt (Figure 6). The end of the reefing line that ran through the slip knot was carried downstream over and around the main strut and then down to a weight suspended underneath the floor of the test section. The weight was suspended from a secondary line. To initiate deployment of the parachute, the secondary line was cut causing the weight to drop, thus pulling out the slip knot and undoing the reefing line. It was found that in general this deployment method gave acceptable repeatability. There were some deployments where the knot in the reefing line fouled with the parachute canopy. When this occurred it was immediately apparent from the transient data and the run was repeated.

For all disk and parachute runs the wind tunnel dynamic pressure was set to give the same steady state drag force that was measured at the Lockheed-Georgia wind tunnel. This was done for the parachutes, before the inflation run, by running the wind tunnel and allowing the chute to inflate. The wind speed was adjusted to give the correct drag as indicated by the voltage from the balance drag element. The fan rpm for this condition was noted and the same fan speed set for the inflation run. Data was not recorded during this pre-run procedure nor was this designated as a test run. This was necessary for the parachute inflations in order that the inflations be comparable with the reference data.

The test matrix is summarized in Table 2.

3 RESULTS

3.1 Disk Models

The solid wall test section data is summarized in Table 3 and plotted in Figure 9. The repeatability of this data is between 0.5

and 1.0%. In Figure 9 the measured uncorrected drag is plotted against the Maskell[2] blockage parameter. According to Maskell the effective increase in the free stream dynamic pressure due to the presence of the model is given by,

$$\frac{q_c}{q} = \frac{C_D}{C_{Dc}} = 1 + K_m \frac{C_D S_u}{A} \qquad (1)$$

A linear fit of the data was made (i.e. a fit to equation 1) and the result extrapolated to zero blockage. The trend of the correction with blockage will be non-linear for higher blockages but this was not considered in the analysis, as the effect will be small for the largest disk tested. A zero blockage disk drag coefficient of 1.148 was calculated. This compares very favourably with the values measured in the Lockheed-Georgia facility which ranged from 1.158 to 1.168. The small difference between the zero blockage drag measured in this test program and the reference drag may be the result of the effect of incorrect geometric similarity when extrapolating the results to zero blockage. Specifically the sting diameter was not scaled for the different disks and this may also be the cause of the difference in the drag coefficients measured at Lockheed-Georgia.

Figure 10 shows solid wall data for the largest disk (S/A = 0.15) as a function of axial position in the test section. It is seen that the blockage correction is constant over the axial range tested which is as expected. This confirms that the test section static pressure gradient is negligible and that the q measuring station in the contraction is not affected by the proximity of the model (i.e. the q calibration does not change).

The data for the slotted wall configurations is summarized in Tables 4 through 6 and plotted in Figures 11 through 18. The blockage correction tabulated and plotted was calculated using the drag areas measured at Lockheed-Georgia for each disk as the

interference free drag area.

Figures 11, 13 and 15 show the influence that moving the flaps has on the drag for the 10.1 inch disk. The flap influence decreases as the disk is moved toward the nozzle and the flap effect is minimal by the time the middle of the test section (X/sqrt(A) = 1.39) is reached.

The variation of wall constraint with axial position for the range of blockages is shown in Figures 12, 14, and 16. These figures show very similar trends for all three test sections. Near the nozzle exit the flow is constrained by the nozzle solid walls and the blockage correction is in the solid wall direction. Further downstream wall constraint is relieved by the slots and the blockage correction is in the open jet direction. It is interesting to note that for the 20% OAR wall and the 30% OAR wall all of the curves cross at a common (albeit different for each OAR) axial location and at a blockage correction near 1.0.

The data plotted at the last two downstream axial positions does not in general represent wall effects, as at these two locations the results are dominated by the effect of the collector flaps. However at X/sqrt(A) = 1.74 (second last axial position) the data trend indicates that the flap position for the 10.1 inch disk is approximately correct. It is clear from the data that at this position the cross-sectional area at the flaps is too small for the largest disk while the flap area is too large for the 4.5 inch and 7.2 inch disk.

This is the result of choosing the "optimum" position based on data from the 10.1 inch disk, as discussed previously. Clearly it would be possible to choose a different "optimum" flap position for each S/A which would improve the data for the downstream model positions. Such a procedure is suspect, however, once the "near wake" from the model approaches the pressure field affected by the

flaps. In this regime, the model drag can be "tailored" by using the flaps to influence the wake and hence the basic wall effects can not be determined.

Clearly this test section regime of "end effects" is not useable for normal testing. Hence the flap position only needs to be approximately correct but the extent of the "end effects" regime needs to be known.

If the slotted walls extended far upstream and far downstream the blockage correction for a given model would be insensitive to axial position (i.e. the test section would be effectively infinitely long). In a long but finite test section there will be three regimes for wall effects. Near the nozzle exit the blockage effect will approach that for a solid wall as the nozzle exit is approached. Far downstream the model flow field will be influenced by the diffuser/flap configuration. The wall interference effect could be either in the solid wall direction or the open jet direction in this regime depending on the geometry. In between this "entry regime" and "exit regime" there must be a section were wall constraint does not change appreciably with axial position and further, if the test section is long enough, the wall correction will be near that for an infinitely long test section. These three regimes are shown in Figure 19. Therefore the blockage correction should approach asymptotically a constant value if the model is moved sufficiently far downstream of the nozzle exit. This asymptotic value for the blockage correction would indicate the interference characteristic for an infinitely long test section.

The 30% OAR test section shows this characteristic. In Figure 16 the three smallest disks appear to approach their asymptotic value. It is apparent from this figure that the axial position at which the asymptotic value is reached depends upon model size. The 12.4 inch disk blockage correction may not be at the asymptotic value before the influence of the flaps dominates. The dashed lines in

Figure 16 indicate how these curves might appear if the test section were longer and the last two axial positions were not influenced by the flaps.

In the 20% OAR test section the location at which the asymptotic blockage correction is reached has moved further downstream than for the 30% OAR (Figure 14). The 12.4 inch and 10.1 inch disks may not have reached the asymptotic value. As in Figure 16 a possible extrapolation of the data for no flap influence has been included in Figure 14. Figure 14 also indicates that the asymptotic value of blockage correction is slightly closer to 1.0 for this wall configuration as compared to the 30% OAR wall, and the spread in the correction for the different model sizes is less.

It is clear from Figure 12 that the test section is not long enough when configured with the 10% OAR wall. In this configuration the region of nozzle influence and flap influence overlap for the 12.4, 10.1 and 7.2 inch disks. The length of the entrance regime has increased from that observed with the 20% OAR test section. Blockage correction for the 4.5 inch disk has reached an asymptote. The trends found with the other two OAR's when applied to the 10% OAR indicate that this wall configuration may give a blockage correction that is nearer to but still less than 1.0 given a sufficiently long test section. In addition the correction may be less sensitive to model size than the other two OAR's. However the above comments are made with reservation as there is insufficient data to allow definite conclusions to be made.

Conversely to the trend of the length of the entrance regime with OAR discussed above, the extent of flap influence appears to be invariant with OAR. This can be seen by comparing Figures 11, 13, and 15.

If the model is placed too near the nozzle exit, the wall interference effect is similar to that of wall with a lower OAR.

This can be demonstrated quite clearly by plotting the disk data, for one axial location, against OAR as has been done in Figure 17 and Figure 18. In these figures some of the data is influenced by either the nozzle or the flaps so the points plotted do not necessarily indicate the asymptotic characteristic of the particular wall configuration. Specifically, the two largest disks in the 10% OAR test section are strongly influenced by the nozzle at both axial positions. Comparison of these two figures with Figure 14 shows a great deal of similarity.

Wall pressure signatures were measured for the solid wall configuration and the 20% OAR slotted wall configuration, for all of the disks, positioned at two different axial locations. This data was collected to facilitate possible future numerical modelling of the slotted wall test section. The data is summarized in Tables 7 through 10. The data for the most upstream position tested is plotted in Figures 20 and 21.

The pressure coefficients tabulated and plotted were calculated by subtracting the empty test section wall pressure signature from the disk wall pressure signature. This procedure eliminates hole errors and local wall effects. The pressure differences were normalized by the freestream dynamic pressure using the following calculation,

$$C_p = \frac{P_{wall\ (disk\ in)} - P_{wall\ (empty)}}{(P_{c1} - P_{c2}) \times K_q} \qquad (2)$$

P_{c1} and P_{c2} are defined in Figure 8 and K_q is defined in Appendix A. The flaps were set at 1 inch for all solid test section runs and for the 20% OAR test section empty run. The sting and sting support were also installed for the 20% OAR run. A 4 inch flap setting was used for all 20% OAR runs with the disks installed.

It is apparent in Figure 21 that the flap setting is not correct for the 2 smallest disks as the wall pressure should approach, asymptotically, a small negative value downstream of the model. The reduction in blockage effect offered by the 20% OAR is clear from these two figures.

3.2 Parachute Models

The data collected with the parachutes is summarized in Tables 11 through 14. The steady state drag areas reported in the tables were computed using the data recorded by the microcomputer and represent the average of 10 different readings recorded over a 10 to 15 second period. The peak inflation drag areas were determined by manually reading the peak value on the drag trace using the curser on the oscilloscope. The peak drags for runs that were judged not acceptable (most often because the release line fouled) are not included in the summary tables. Typical traces from the oscilloscope are shown in Figures 22 through 27. The output from the total pressure transducer and the dynamic pressure transducer is also given in these figures.

There is marked difference in the measured dynamic pressure and total pressure trace between the solid wall test section and the slotted wall test sections. In the solid wall test section the drop in dynamic pressure is initiated almost immediately after the inflation begins. (It is not possible to distinguish a time difference between the two events at the scale used in Figures 22, 23 and 24.) The dynamic pressure change is also accompanied by a noticeable rise in total pressure. For the slotted wall test sections there is a lag of 0.1 to 0.2 seconds before the dynamic pressure change begins. Also in the slotted wall test sections there is slight drop in total pressure. At the end of the transient the drop in dynamic pressure was about the same for a given parachute model regardless of the test section wall configuration. The actual overall dynamic pressure change was less

than measured for disks during the pretest commissioning phase (see Appendix A).

Approximate Overall Q Change
10" Parachute - 1%
14.5" Parachute - 3%
18" Parachute - 6%

A possible explanation for this difference in transient behaviour is as follows. In the solid wall test section the inflation of the parachute has an immediate throttling effect on the flow due to the wall constraint. This causes the flow just upstream of the parachute to decelerate and the static pressure to increase. The mass flow is no longer constant around the wind tunnel circuit due to the effect of compressibility. Mass and energy are transferred from the area just downstream of the test section to just upstream of the test section via compression waves. Therefore both static and total pressure increase just upstream of the model. The reduction in mass flow is local to the test section area until sometime after the inflation has been initiated. During the initial stages of the transient the mass flow through the fan section of the circuit is higher than the mass flow through the test section. Eventually conditions all around the wind tunnel circuit change and the fan operating point settles out to some new value (lower mass flow and higher pressure rise) due to the overall increase in circuit losses. At the end of the transient the mass flow is the same at any axial station around the circuit.

In the slotted wall test sections the throttling effect is much reduced as a result of the relief that the slots offer to the flow. There is therefore a minimal change in local mass flow and the drop in dynamic pressure does not occur until the circuit can respond

to the increase in circuit loss factor caused by the inflated parachute.

Parachute drag area measured in the DSMA MWT is compared to the reference data as a function of wall open area ratio in Figures 28, 29 and 30. The variation in blockage correction for the inflation data is also indicated in these figures. The scatter in the data for the 10 inch parachute and the 14.5 inch parachute is on the order of ± 5%. The scatter for the 18 inch parachute results is less than this for the 10% and 20% wall OAR's. There is evidence that the characteristics of the 14.5 inch parachute changed during the test program. This was primarily due to the fabric sliding up on the suspension lines. The change was evidenced by a significant decrease in the steady state drag (compare run 89 with run 90). After testing was completed with all four wall OAR's, an attempt was made to repair this parachute. It was subsequently retested with the 20% OAR wall (runs 188 to 190) and the drag level returned to near the original value.

The steady state parachute data is well behaved and repeatable (within 2% except for the problem with the 14.5 inch parachute). Data for all of the models tested are compared in Figures 31 through 34. Note that in these figures the peak inflation data has been plotted against the steady state drag area. A straight line has been fitted to each of the three types of data (disks, steady state parachute, and parachute inflations) in Figure 31 and a Maskell blockage correction factor calculated for each of these lines. Note that in this figure the uncorrected drag area has been normalized by the drag area measured at Lockheed-Georgia. Two possible straight line fits have been shown for the steady state parachute data as result of the scatter in the data. Straight line fits for the steady state only are also shown on the plots for the other wall configurations. This presumes that the behaviour of the blockage correction factor is nearly linear over this range of aerodynamic blockage. There cannot be much confidence in the

values of K_m derived from this analysis due to the uncertainty of the data. However, the straight line fits have been presented in order to show the possible trend of wall interference with wall OAR. The trend of K_m with OAR is discussed in section 3.3. Points on the plots that were judged to be influenced by the flaps or proximity to the test section nozzle were not weighted very heavily or not used at all. The data for the smallest disk does not agree with the trends indicated by the other disks. In all of the test sections the drag for the small disk appears to be too small. This could be a result of experimental error in the reference data. As the same instrumentation was used for all the disks, the error in measurement will be proportionally higher for the smallest disk. The small disk data was not included for the estimation of the Maskell blockage factor.

A Maskell blockage factor of 1.85 was reported in reference 5 for single parachutes in solid wall test sections. This is near the value for the largest parachute in Figure 31. In the solid wall test section it can be seen that there is wall interference during the inflation process but that the wall constraint is much reduced as compared to the steady state measurements. When the uncertainty on the data is considered, the measurements made in the slotted wall test sections indicate that the peak drag during an inflation does not need to be corrected for wall interference. For all test sections the wall interference for the parachutes is less than that seen for the disks for the same drag area.

In the slotted wall test sections it can be seen that the magnitude of the Maskell blockage correction parameter reduces with OAR for both the disk models and the parachute models. In the solid wall section K_m is positive. This suggests that, if OAR were decreased below 10%, K_m must pass through zero and then become positive. In other words there must be an OAR (less than 10%) for which there is no blockage correction for a range of model sizes.

3.3 Application to the PWT

The data collected in this test program clearly reveals that slotted walls almost eliminate wall interference during an infinite mass parachute inflation for parachutes that have a steady state drag area as large as 19% of the test section area. These tests also demonstrated that slotted walls delay the perturbation in freestream dynamic pressure that the inflation transient causes. Although the full scale facility will be an intermittent wind tunnel with a dynamic pressure control system that is quite different from the model wind tunnel used for these tests, the slots should provide the same relief in full scale as the initial effect of parachute inflation is local.

The requirements for the parachute wind tunnel are quite different than previous low speed applications of slotted wall test sections. In this application the model is moving and it therefore may be important that the variation of wall boundary condition with axial location be minimized. In past applications where the model is fixed, the variation of blockage effect with axial position is not important, as the model can be positioned correctly to give blockage free results (references 3 and 4). The initial stage of parachute inflation for the full scale moving model tests should be very similar to the infinite mass inflation tests in the way the slot and plenum flow develops. During this initial stage the model will not have moved very much and there will be a large, fast, flow field transient. After the initial stage the parachute geometry will be changing at much slower rate but the model will now be moving at a significant velocity. Now the test section flow field will be changing rapidly in space. The effect of wall constraint on the flow around the model under these conditions is of course unknown. This flow field transient may be similar to the infinite mass inflation and it may be that the wall effects are much reduced as compared to steady state testing. If this is true the asymptotic value of blockage correction may not be very important

for full scale moving model tests. However the full scale wind tunnel will very likely be used for other types of unsteady testing as well, and therefore it is desirable that the test section give blockage free results over most of its length.

There will be one OAR for a given model which gives blockage free results far downstream of the nozzle exit. It is not possible to determine what the correct OAR should be for a long test section from the data gathered in this test program. However an indication of a possible range of OAR's to achieve blockage free testing can be estimated from the trends presented in section 3.2. The Maskell blockage correction factor previously calculated is plotted as a function of OAR in Figure 35. Also shown in this figure are possible trends for the disk data and parachute data between OAR's of 0.0 and 0.2. This figure shows that the OAR for blockage free testing probably lies somewhere between 5% and 10%. Also if the assumption that the blockage correction is a linear function of aerodynamic blockage, for slotted wall test sections, is correct, the proper OAR will be suitable for a range of model sizes. The data collected in this test program is too limited to verify this assumption; however, the disk data for 30% OAR plotted in Figure 34 (this data has minimal flap influence) supports this.

Historically, there has been a considerable theoretical effort to calculate wall corrections for all of the types of wall boundary conditions. The early efforts employed transonic small perturbation theory with the appropriate boundary conditions for the wall type. Solid blockage, wake blockage, and lift interference were calculated by representing the model with singularities. A summary of the results from these efforts is given in reference 6. These results were used in an attempt to predict the incompressible flow blockage correction as function of OAR for the disk models used in the test program. This prediction is presented in Figure 36. To obtain these curves each disk was initially represented by a sphere of the same diameter (the

inviscid theory uses a doublet to represent the body) to obtain the solid blockage correction and the freestream drag area was used to estimate the wake blockage. Note that the theory predicts a wake blockage term only for the solid wall test section. It was found that using this representation of the body gave blockage corrections far smaller than were measured. This would be expected as the effective flow displacement caused by the disks is much larger than given by a sphere of the same diameter in an inviscid flow field. (See for example reference 7.) To improve the prediction the sphere was scaled to give, approximately, the blockage correction measured for the largest disk in the solid wall test section. This resulted in a sphere about twice the diameter of the disk which is not unreasonable[7]. The same scaling factor was then used for all the disks and all OAR's.

The theoretical estimate of the relationship between the slotted wall boundary condition coefficient (K/h, which is defined in reference 6) and test section geometry was used to generate Figure 36. However experimental evidence[8] indicates that the theory under-predicts the magnitude of this coefficient. If the magnitude of K/h is increased, the curves in Figure 36 will be stretched to the right.

The trends shown by the theoretical analysis agree qualitatively with the trends observed in this experimental program. The theory predicts that the correct OAR for blockage free testing would be the same for all model sizes. It also predicts this OAR to be about 3%, which is on the correct side of the curve shown in Figure 35, given the probable error in K/h used in the analysis.

The selection of an OAR for the full scale wind tunnel will require a compromise between the wall interference attained and the flow development length for the nozzle. The upstream length required will also be dependent upon model blockage. However because the

effect of the walls during a transient is less severe, the flow development length required can be relaxed for inflation testing. The 10% OAR test section used in this program is too short for steady state testing but is long enough for infinite mass inflations (see Figure 30 for example). In the full scale facility the model could be started at an upstream location where the nozzle still affects wall interference and by the time peak inflation drag occurred the model would have moved out of the region of nozzle influence.

The trends from the data collected in this test program show that low OAR's are required to give an asymptotic value of K_m which is near zero. The use of smaller OAR is also desirable in the full scale facility because of the length of the test section. Smaller OAR will give less shear layer growth in the test section and in the plenum which will reduce circuit losses, give a larger potential core at the end of the test section, and reduce the size of the plenum.

The discussion above and the results from this test program indicates that OAR's in the range of 5% to 15% are of the most interest for the full scale facility. The test section geometry should be further investigated through additional model scale tests with a longer test section. This test program should also include moving model tests as this is the next logical step in exploring the slotted wall concept for the low speed inflation testing of parachutes.

3.4 Compatibility with Transonic Test Requirements

Slotted walls have been used to relieve choking near sonic speeds ever since the first successful transonic wind tunnel tests were done[9]. Consequently there has been a abundance of knowledge generated in the intervening years relating optimal slot geometry to test requirements for transonic tests. However most of this

experience has been with streamlined, lifting shapes tested at small blockage ratios (less than 1% of the test section area). There is little experience, either experimental or theoretical, to draw upon for bluff bodies at high blockages at transonic speeds. DSMA's experience in transonic testing has been primarily with perforated wall transonic test sections, due to their excellent shock cancellation properties. All of the transonic test sections that DSMA has designed or tested in have been designed for the testing of streamlined bodies. As a consequence of this it is not possible to address conclusively the compatibility of subsonic and transonic inflation testing of parachutes. However some preliminary thoughts will be given in this report. Test section design for the transonic speed regime must be eventually confirmed through pilot wind tunnel tests.

The 3D transonic slotted wall test sections in use in the world have porosities that range from about 4% to 12%. These test sections are primarily used for the testing of lifting models and therefore both the blockage correction and the correction to freestream flow angle are important. Existing test sections would consequently have been optimized to minimize both types of correction simultaneously. The optimum OAR to minimize blockage correction only for a large bluff body may not correspond to the wall configurations currently in use for transonic testing. Nevertheless, it would seem very likely that the optimum porosity for the PWT in the transonic speed range should not fall too far outside of the OAR's currently in use for transonic testing.

The theoretical calculation that was discussed in section 3.2 was originally derived for compressible flow. Given that the test section flow can be computed using small perturbation theory for area blockages as large as 15%, the compressible flow solution can be calculated from the incompressible flow solution using the Prandtl-Glauert rule. The result of this transformation is that only the vertical scale in Figure 36 changes as a function of Mach

number and therefore, the OAR to give blockage free testing is independent of Mach number, in this flow regime.

As the test Mach number approaches Mach 1.0 there will be a point at which increasing wall interference requires a reduction in wall porosity. The Mach number at which this occurs (M_{int}) will depend upon model size, model aerodynamic characteristics, and the level of wall interference which is judged to be acceptable. The value of M_{int} should be bounded by the Mach number at which sonic flow is established on the model ($M_{critical}$) and the Mach number at which sonic flow is established at the wall ($M_{wall\ critical}$). A large change in wall interference will occur when the local Mach number at the wall approaches 1.0. The actual value of M_{int} can only be accurately determined through an experimental test program.

The trends from this test program show that an OAR of 5% to 15% is of the most interest for low speed testing, which is in the same range as existing transonic test sections. This further supports the conclusion that the correct OAR will be independent of Mach number (for $M_\infty \leq M_{int}$).

For small models (less than 1% blockage) M_{int} will be near Mach 1.0. Above M_{int} a change in wall geometry is required in order to minimize wall interference. For example in reference 10 it was found that constant wall OAR gave very good results up to Mach 0.9 for a 1% blockage cone cylinder model. At Mach 0.95 a reduction in wall OAR from 4.0% to 2.75% was required, while at Mach 1.0 near closure of the wall was indicated. Although the test section studied in reference 10 had adjustable porosity it was not possible to completely eliminate wall interference at Mach 1.0. This test was done in a perforated wall test section but it is expected that about the same critical Mach number would be obtained for the 1% cone cylinder model in a slotted wall test section.

A fixed geometry slotted wall test section for the full scale parachute wind tunnel would not preclude testing very near or at Mach 1.0 but wall interference may become significant above M_{int}. It should be possible to estimate the bounds for this Mach number, for a parachute, if the extent of supersonic flow in the region of the parachute is known as a function of freestream Mach number. Above Mach 1.0 slotted wall test sections do not have the required wave cancellation properties necessary to minimize wall interference and in this speed regime perforated walls are the preferred wall configuration. Perforated walls were not considered for the parachute wind tunnel during the previous feasibility study[1] because of cost and the assumption that subsonic testing would be emphasized for this facility. Whether or not wall interference will be a significant problem from M_{int} through Mach 1.2 for the unique transient tests for which the facility will be used can only be determined through an experimental test program. The value of M_{int} for a given parachute model size is also best determined experimentally.

The potential problem of wall interference at these speeds is not an indication of an incompatibility between low speed requirements and transonic speed requirements for a slotted wall parachute wind tunnel, but it is an indication of the deficiency of a fixed geometry slotted test section used near Mach 1.0 and at low supersonic speeds.

4 CONCLUSIONS

A test program to investigate the effect of OAR and model position for flat disks in steady flow and the effect of OAR on parachutes in steady state and during infinite mass inflations has been successfully completed. The results of this test program show that:

1. There was no measurable wall interference, for all slotted wall test sections, for parachutes with steady state drag areas as large as 19% of test section area during infinite mass inflations.

2. Slotted walls provide the additional advantage of delaying the change in reference dynamic pressure until well after the peak inflation drag has occurred.

3. The optimum OAR should be between 5% and 15% for geometric blockages up to 15% in steady state testing with a sufficiently long test section. This result needs to be further explored through a follow-on test program.

4. The wall OAR to give minimum wall interference for low speed tests should also be correct for transonic testing. There should not be any incompatibility between transonic test requirements and low speed test requirements for the full scale facility. This initial conclusion is subject to confirmatory pilot wind tunnel tests.

5 RECOMMENDATIONS

A follow-on test program should be conducted to further explore the properties of wall OAR in a longer test section. As was done in this test program the variation of wall interference with OAR and

model axial position should be determined using disk models of different sizes. Wall OAR's between 5% and 15% should be investigated. This test program should also take the investigation of wall effect on transient tests to the next stage with a moving parachute model.

6 REFERENCES

1. "Feasibility Study for a Parachute Wind Tunnel", DSMA Report No. 4099-R214, Sandia Contract No. 01-8202A, May 31, 1988.

2. E. C. Maskell, "Theory of the Blockage Effects on Bluff Bodies and Stalled Wings in a Closed Wind Tunnel", Royal Aircraft Establishment Report No. Aero 2685, UK, November 1963.

3. S. Raimondo and P. J. F. Clark, "Slotted Wall Test Section for Automotive Aerodynamic Test Facilities", AIAA 12th Aerodynamic Testing Conference, Williamsburg, VA, 1982.

4. R. G. J. Flay, G. M. Elfstrom, and P. J. F. Clark, "Slotted-Wall Test Section for Automotive Aerodynamic Tests at Yaw", SAE 830302, 1983.

5. J. M. Macha, and R. J. Buffington, "An Experimental Investigation of Wall-Interference Effects for Parachutes in Closed Wall Wind Tunnels", Sandia report SAND89-1485, Sandia National Laboratories, Albuquerque, NM, September 1989.

6. M. Pindzola and C. F. Lo, "Boundary Interference at Subsonic Speeds in Wind Tunnels with Ventilated Walls". AEDC-TR-69-47, May 1969.

7. J. E. Hackett, D. J. Wilsden and D. E. Lilley, "Estimation of Tunnel Blockage from Wall Pressure Signatures: A Review and Data Correlation", NASA CR-15224, March 1979.

8. J. L. Everhart and R. W. Barnwell, "A Parametric Experimental Study of the Interference Effects and the Boundary-Condition Coefficient of Slotted Wall Wind Tunnels". AIAA Paper No. 78-805, 1978.

9. B. H. Goethert, "Transonic Wind Tunnel Testing", AGARD, 1961.

10. G. M. Elfstrom, B. Medved, W. J. Rainbird, "Wave Cancellation Properties of a Splitter-Plate Porous Wall Configuration", Journal of Aircraft, Volume 26, Number 10, October 1989.

TABLES

Table 1: Reference Data - from Lockheed-Georgia Wind Tunnel (23.25 ft x 16.25 ft test section)

a) Disk Data

Run	Diameter (inches)	Geometric Blockage (%)	Dynamic Pressure (lb/ft^2)	Drag Area (ft^2)	C_D
31	4.52	0.03	10.01	0.130	1.1682
32	7.20	0.07	10.01	0.325	1.1657
33	10.11	0.15	10.06	0.646	1.1607
34	12.39	0.22	10.07	0.969	1.1583

b) Parachute Data

Part 1 - Full Open, Steady State

Run	Diameter (inches)	Dynamic Pressure (lb/ft^2)	Drag Area (ft^2)
35	10.0	10.02	0.320
40	10.0	10.02	0.323
41	14.5	10.03	0.668
44	14.5	10.02	0.663
46	18.0	6.03	1.044
49	18.0	6.05	1.045

Part 2 - Infinite Mass Inflation

Run	Diameter (inches)	Dynamic Pressure (lb/ft^2)	C_DS_{peak} (ft^2)	C_DS_{peak}/C_DS
39	10.0	10.00	0.630	1.957
45	10.0	9.98	0.585	1.817
42	14.5	10.00	1.194	1.793
43	14.5	10.02	1.141	1.713
47	18.0	6.01	2.018	1.931
48	18.0	6.02	1.923	1.840

Table 2: Test Matrix

OAR	Flap Setting	Model	Axial Position
30%	1", 2", 3", 4", 5"	10.1" disk	4.92', 4.1', 3.62'
	4"	4.5", 7.2",10.1", 12.4" disks	4.1', 3.28', 2.46', 1.64', 0.82'
	4"	10", 14.5", 18" chutes	3.28'
20%	1", 2", 3", 4", 5"	10.1" disk	4.92', 4.1', 3.62'
	4"	4.5", 7.2",10.1", 12.4" disks	4.1', 3.28', 2.46', 1.64', 0.82'
	4"	10", 14.5", 18" chutes	3.28'
10%	1", 2", 3", 4", 5"	10.1" disk	4.92', 4.1', 3.62'
	4"	4.5", 7.2",10.1", 12.4" disks	4.1', 3.28', 2.46', 1.64', 0.82'
	4"	10", 14.5", 18" chutes	3.28'
solid	1"	4.5", 7.2",10.1", 12.4" disks	3.28'
		10", 14.5", 18" chutes	3.28'

Table 3: Summary of Solid Wall Disk Data

Run	Disk Diameter (inches)	Axial Position (feet)	Drag Area (ft^2)	Cd	Av Cd	SD (%)
96	4.5	3.28	.135	1.212		
175	4.5	3.28	.134	1.203	1.206	.43
176	4.5	2.46	.134	1.203		
98	7.2	3.28	.379	1.340		
174	7.2	3.28	.378	1.337	1.339	.15
177	7.2	2.46	.379	1.340		
99	10.1	3.28	.930	1.668		
173	10.1	3.28	.926	1.661	1.667	.33
178	10.1	2.46	.932	1.672		
100	12.4	3.28	1.695	2.024		
172	12.4	3.28	1.692	2.021		
171	12.4	3.28	1.684	2.011	2.025	.57
170	12.4	3.28	1.684	2.011		
108	12.4	2.46	1.703	2.034		
109	12.4	1.64	1.705	2.036		
110	12.4	.82	1.707	2.039		

Table 4: Summary of 10 % OAR Disk Data

Run	Disk Diameter (inches)	Flap Position	Axial Position (feet)	Drag Area (ft^2)	CdSu/CdS
138	4.5	4	.82	.132	1.015
137			1.64	.129	.992
130			2.46	.127	.977
129			3.28	.127	.977
143			4.10	.122	.938
144			4.85	.120	.923
139	7.2		.82	.361	1.111
136			1.64	.338	1.040
131			2.46	.331	1.018
128			3.28	.318	.978
145			3.28	.319	.982
140			4.10	.303	.932
135	10.1		1.64	.760	1.176
132			2.46	.706	1.093
125			3.28	.661	1.023
118			4.10	.640	.991
115			4.85	.651	1.008
134	12.4		1.64	1.362	1.406
133			2.46	1.215	1.254
127			3.28	1.116	1.152
142			4.10	1.061	1.095
148	4.50	1	4.10	.124	.954
147		2	4.10	.124	.954
146		3	4.10	.124	.954
145		3	4.10	.120	.923
167	7.20	1	3.28	.322	.991
122	10.1	1	3.28	.672	1.040
121			4.10	.674	1.043
112			4.85	.721	1.116
123		2	3.28	.671	1.039
120			4.10	.652	1.009
113			4.85	.679	1.051
124		3	3.28	.670	1.037
119			4.10	.647	1.002
114			4.85	.662	1.025
126		5	3.28	.660	1.022
117			4.10	.639	.989
116			4.85	.643	.995

Table 5: Summary of 20 % OAR Disk Data

Run	Disk Diameter (inches)	Flap Position	Axial Position (feet)	Drag Area (ft^2)	CdSu/CdS	Repeatability diff from mean(%)
80	4.5	4	.82	.131	1.008	
79			1.64	.129	.992	
71			2.46	.128	.985	.79
194			2.46	.126	.969	-.79
70			3.28	.126	.969	0
187			3.28	.126	.969	0
86			4.10	.124	.954	
81	7.2		.82	.349	1.074	
78			1.64	.329	1.012	
72			2.46	.318	.978	-.16
195			2.46	.319	.982	.16
69			3.28	.315	.969	0
			3.28	.315	.969	0
85			4.10	.301	.926	
82	10.1		.82	.762	1.180	
77			1.64	.675	1.045	
73			2.46	.634	.981	.48
196			2.46	.628	.972	-.48
66			3.28	.612	.947	.66
185			3.28	.604	.935	-.66
59			4.10	.605	.937	
56			4.85	.619	.958	
83	12.4		.82	1.308	1.350	
76			1.64	1.078	1.112	
75			2.46	.961	.992	.10
197			2.46	.959	.990	-.10
68			3.28	.921	.950	.41
184			3.28	.911	.940	-.68
183			3.28	.920	.949	.30
182			3.28	.917	.946	-.03
84			4.10	.920	.949	

Table 6: Summary of 30 % OAR Disk Data

Run	Disk Diameter (inches)	Flap Position	Axial Position (feet)	Drag Area (ft^2)	CdSu/CdS
30	4.5	4	.82	.130	1
29			1.64	.128	.985
23			2.46	.126	.969
37			3.28	.126	.969
38			4.10	.123	.946
31	7.2		.82	.342	1.052
28			1.64	.323	.994
24			2.46	.314	.966
36			3.28	.313	.963
39			4.10	.304	.935
32	10.1		.82	.720	1.115
27			1.64	.642	.994
21			2.46	.604	.935
14			3.28	.589	.912
11			4.10	.595	.921
33	12.4		.82	1.182	1.220
26			1.64	.966	.997
25			2.46	.894	.923
34			3.28	.864	.892
41			4.10	.896	.925
18	10.1	1	2.46	.615	.952
17			3.28	.605	.937
8			4.10	.623	.964
1			4.85	.692	1.071
19		2	2.46	.607	.940
16			3.28	.600	.929
9			4.10	.609	.943
2			4.85	.660	1.022
20		3	2.46	.606	.938
15			3.28	.592	.916
10			4.10	.597	.924
3			4.85	.632	.978
13		5	3.28	.597	.924
12			4.10	.593	.918
6			4.85	.602	.932

Table 7: Summary of wall pressure signature data, solid wall test section, X/sqrt(A) = 1.39

Tap Pos	Cp			
X/sqrt(A)	4.5" disk	7.2" disk	10.1" disk	12.4" disk
.14	.001	.001	.003	.003
.56	.000	.001	.003	.004
.97	-.004	-.010	-.014	-.017
1.18	-.021	-.048	-.082	-.111
1.39	-.059	-.155	-.309	-.481
1.60	-.096	-.294	-.661	-1.081
1.81	-.080	-.300	-.807	-1.352
2.01	-.051	-.202	-.654	-1.245
2.22	-.036	-.132	-.433	-.893
2.43	-.030	-.099	-.295	-.636
2.64	-.028	-.089	-.253	-.479

Table 8: Summary of wall pressure signature data, solid wall test section, X/sqrt(A) = 1.04

Tap Pos	Cp			
X/sqrt(A)	4.5" disk	7.2" disk	10.1" disk	12.4" disk
.14	-.001	-.000	.000	.001
.56	-.002	-.006	-.008	-.009
.97	-.045	-.110	-.205	-.306
1.18	-.094	-.266	-.544	-.898
1.39	-.089	-.320	-.748	-1.264
1.60	-.062	-.234	-.622	-1.306
1.81	-.042	-.148	-.447	-.954
2.01	-.034	-.106	-.305	-.668
2.22	-.034	-.090	-.248	-.515
2.43	-.034	-.087	-.229	-.453
2.64	-.030	-.084	-.217	-.427

Table 9: Summary of wall pressure signature data,
20 % OAR test section, X/sqrt(A) = 1.39

Tap Pos	Cp			
X/sqrt(A)	4.5" disk	7.2" disk	10.1" disk	12.4" disk
.14	-.000	.001	-.000	-.001
.56	.006	.018	.050	.089
.97	.017	.058	.154	.241
1.18	.022	.077	.197	.298
1.39	.004	.037	.126	.187
1.60	-.023	-.054	-.059	-.089
1.81	-.020	-.077	-.152	-.215
2.01	-.009	-.043	-.140	-.265
2.22	-.003	-.021	-.104	-.188
2.43	-.002	-.012	-.060	-.094
2.64	-.001	-.014	-.055	-.089

Table 10: Summary of wall pressure signature data,
20 % OAR test section, X/sqrt(A) = 1.04

Tap Pos	Cp			
X/sqrt(A)	4.5" disk	7.2" disk	10.1" disk	12.4" disk
.14	-.000	-.002	.001	.012
.56	.011	.040	.110	.177
.97	.008	.048	.142	.219
1.18	-.020	-.041	-.035	-.052
1.39	-.026	-.089	-.176	-.266
1.60	-.014	-.056	-.159	-.266
1.81	-.001	-.021	-.103	-.230
2.01	.005	-.010	-.072	-.170
2.22	.013	-.002	-.044	-.097
2.43	.030	.015	-.021	-.068
2.64	.068	.051	.006	-.053

Table 11: Summary of parachute data, solid wall test section

(a) Full-open steady drag

Run	Model (dia inches)	q (psf)	CdSu	Repeatability diff from mean (%)	CdSu,mean
101	10.0	6.73	.349	0	
102		6.91	.349	0	.349
103	14.5	8.59	.772	-1.3	
104		8.57	.791	1.2	
111		8.57	.783	.1	.782
105	18.0	3.99	1.550	-.4	
106		4.00	1.557	.0	
107		3.99	1.562	.4	1.556

(b) Infinite mass inflations

Run	Model (dia inches)	q (psf)	CdSu (peak)	Repeatability diff from mean (%)	CdSu,mean (peak)	CdSu,peak / CdSu,steady
101	10.0	6.81	.629	-2.0		1.802
102		6.97	.655	2.0	.642	1.877
103	14.5	8.83	1.336	2.8		1.708
104		8.81	1.238	-4.7		1.583
111		8.80	1.324	1.9	1.299	1.693
105	18.0	4.27	2.348	3.8		1.509
106		4.27	2.213	-2.1		1.422
107		4.26	2.222	-1.7	2.261	1.428

Table 12: Summary of parachute data, 10% OAR test section

(a) Full-open steady drag

Run	Model (dia inches)	Axial Position (feet)	q (psf)	CdSu	Repeatability diff from mean (%)	CdSu,mean
153	10.0	2.36	6.34	.321	-.3	
154			9.96	.323	.3	.322
155		3.42	10.00	.319	.4	
156			9.98	.316	-.5	
157			10.20	.318	.1	.318
149		3.98	6.35	.307	-1.8	
150			6.37	.309	-1.2	
* 151			6.40	.317	1.4	
* 152			6.33	.318	1.7	.313
158	14.5	3.54	10.67	.610	-1.3	
163			10.75	.610	-1.3	
164			10.72	.629	1.7	
165			10.72	.624	.9	.618
160	18.0	3.54	5.68	1.080	-.2	
161			5.70	1.081	-.1	
162			5.70	1.084	.2	1.082

(b) Infinite mass inflations

Run	Model (dia inches)	Axial Position (feet)	q (psf)	CdSu (peak)	Repeatability diff from mean (%)	CdSu,mean (peak)	CdSu,peak / CdSu,steady
153	10.0	2.36	6.40	.598	2.5		1.86
154			10.11	.569	-2.5	.584	1.77
155		3.42	10.12	.510	-5.3		1.61
156			10.10	.554	2.8		1.74
157			10.14	.552	2.5	.539	1.74
149		3.98	6.41	.620	7.3		1.98
150			6.42	.596	3.1		1.91
* 151			6.48	.546	-5.5		1.75
* 152			6.44	.550	-4.8	.578	1.76
158	14.5	3.54	11.06	1.160	2.8		1.84
163			11.13	1.139	1.0		
164			11.06	1.093	-3.1		1.77
165			11.05	1.121	-.6	1.128	1.81
162	18.0	3.54	6.08	2.013		2.013	1.86

* flaps set to 1" for these runs

Table 13: Summary of parachute data, 20% OAR test section

(a) Full-open steady drag

Run	Model (dia inches)	Axial Position (feet)	q (psf)	CdSu	Repeatability diff from mean (%)	CdSu,mean
94	10.0	3.43	10.14	.320	.2	
95			10.09	.319	-.2	.320
89	14.5	3.54	10.52	.638	6.3	
90			10.49	.585	-2.5	
91			10.56	.586	-2.3	
92			10.52	.591	-1.5	.600
* 188			10.08	.625	.1	
* 189			10.10	.631	1.0	
* 190			10.04	.618	-1.1	.625
87	18.0	3.54	5.95	1.018	-.2	
88			5.93	1.022	.2	1.020

(b) Infinite mass inflations

Run	Model (dia inches)	Axial Position (feet)	q (psf)	CdSu (peak)	Repeatability diff from mean (%)	CdSu,mean (peak)	CdSu,peak / CdSu,steady
94	10.0	3.43	10.27	.588	-3.8		1.84
95			10.21	.635	3.8	.612	1.99
89	14.5	3.54	10.80	1.256	-1.6		2.09
90			10.80	1.297	1.6	1.277	2.16
* 188			10.37	1.223	1.3		1.96
* 189			10.34	1.198	-.8		1.92
* 190			10.32	1.201	-.5	1.207	1.92
87	18.0	3.54	6.30	2.036	.02		2.00
88			6.31	2.035	-.02	2.036	2.00

* 14.5 inch diameter chute repaired for these runs

Table 14: Summary of parachute data, 30% OAR test section

(a) Full-open steady drag

Run	Model (dia inches)	Axial Position (feet)	q (psf)	CdSu	Repeatability diff from mean (%)	CdSu,mean
42	10.0	3.43	10.19	.315	-.3	
43			10.22	.316	0	
45			10.21	.317	.3	.316
46	14.5	3.54	10.41	.635	3.6	
47			10.29	.602	-1.8	
48			10.27	.603	-1.6	
49			10.41	.612	-.2	.613
50	18.0	3.54	5.88	.988	-.9	
51			5.90	1.011	1.4	
52			5.89	.992	-.5	.997

(b) Infinite mass inflations

Run	Model (dia inches)	Axial Position (feet)	q (psf)	CdSu (peak)	Repeatability diff from mean (%)	CdSu,mean (peak)	CdSu,peak / CdSu,steady
43	10.0	3.43	10.34	.684	4.5		2.16
44			10.36	.654	-.1		2.07
45			10.21	.626	-4.4	.655	1.98
48	14.5	3.54	10.56	1.187	-3.0		1.82
49			10.69	1.117	-3.0	1.152	1.82
50	18.0	3.54	6.20	2.239	1.7		2.25
52			6.19	2.165	-1.7	2.202	2.17

FIGURES

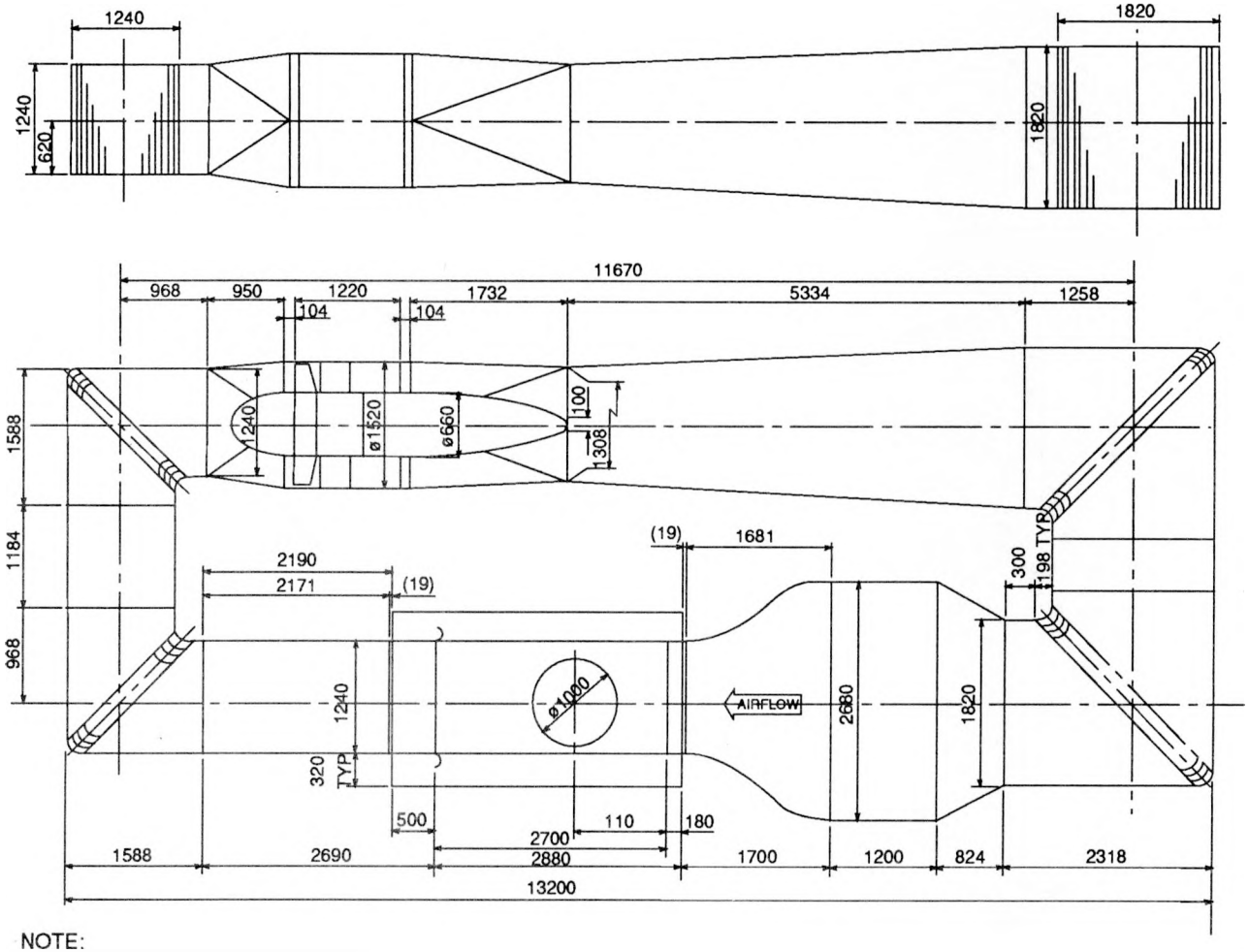

NOTE:
ALL DIMENSIONS IN MILLIMETRES

Figure 1. DSMA Model Wind Tunnel Airline Diagram

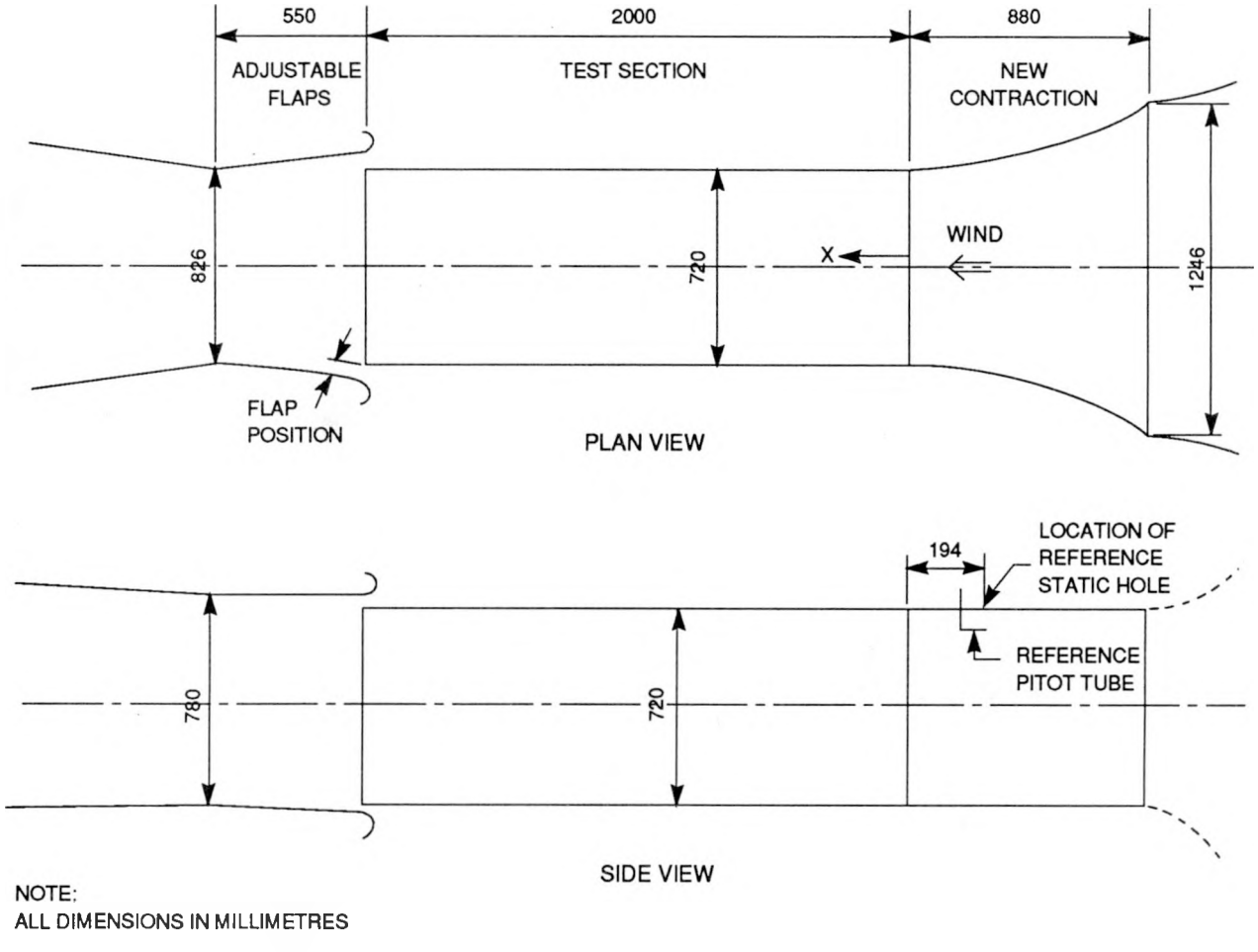

Figure 2. 0.72m x 0.72m Test Section

DSMA International engineers constructors

Sandia National Laboratories

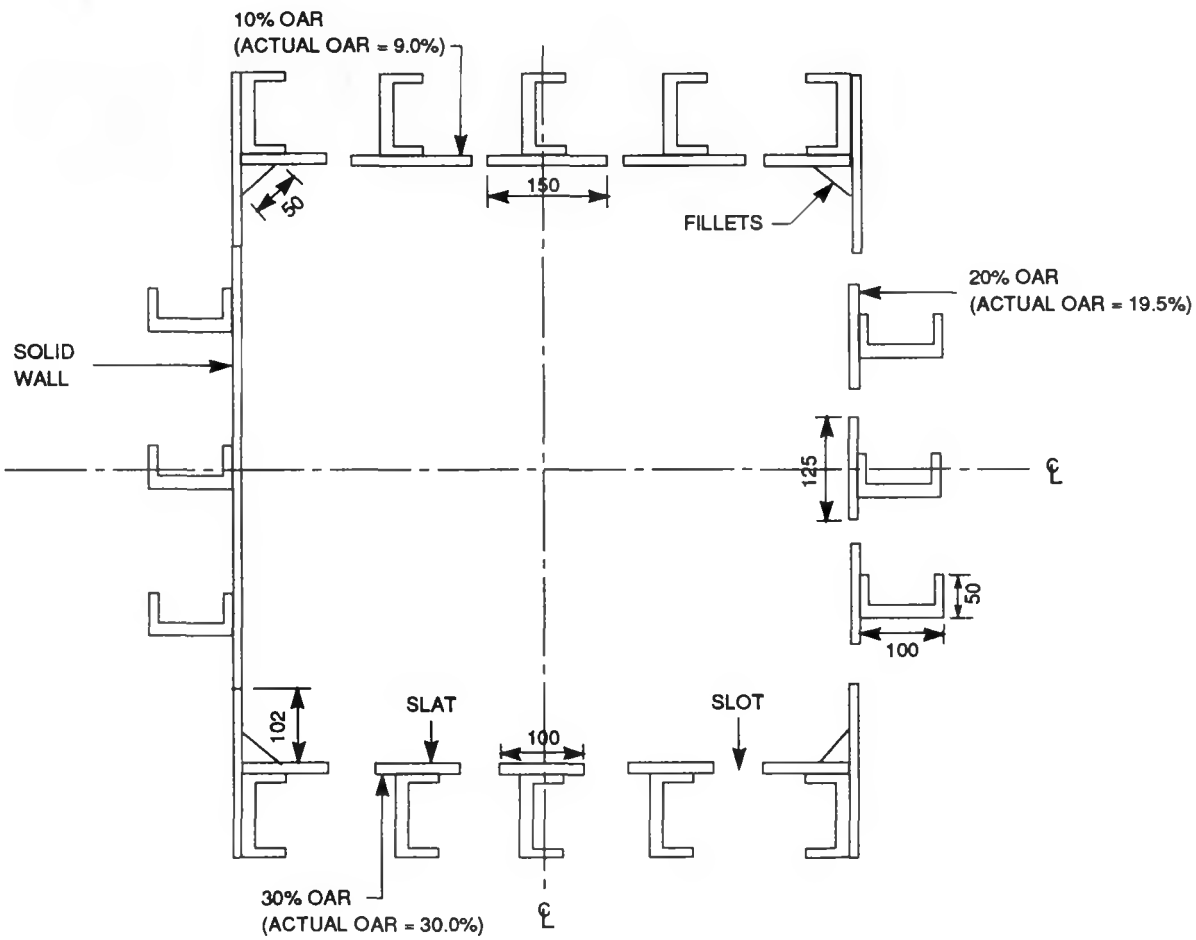

NOTE:
THE ABOVE SKETCH IS A COMPOSITE OF CONFIGURATION OPTIONS. THE ACTUAL CONFIGURATION SHOWN ABOVE WAS NOT TESTED.

Figure 3. Sectional View of Test Section At X = 1000mm (3.28 ft)

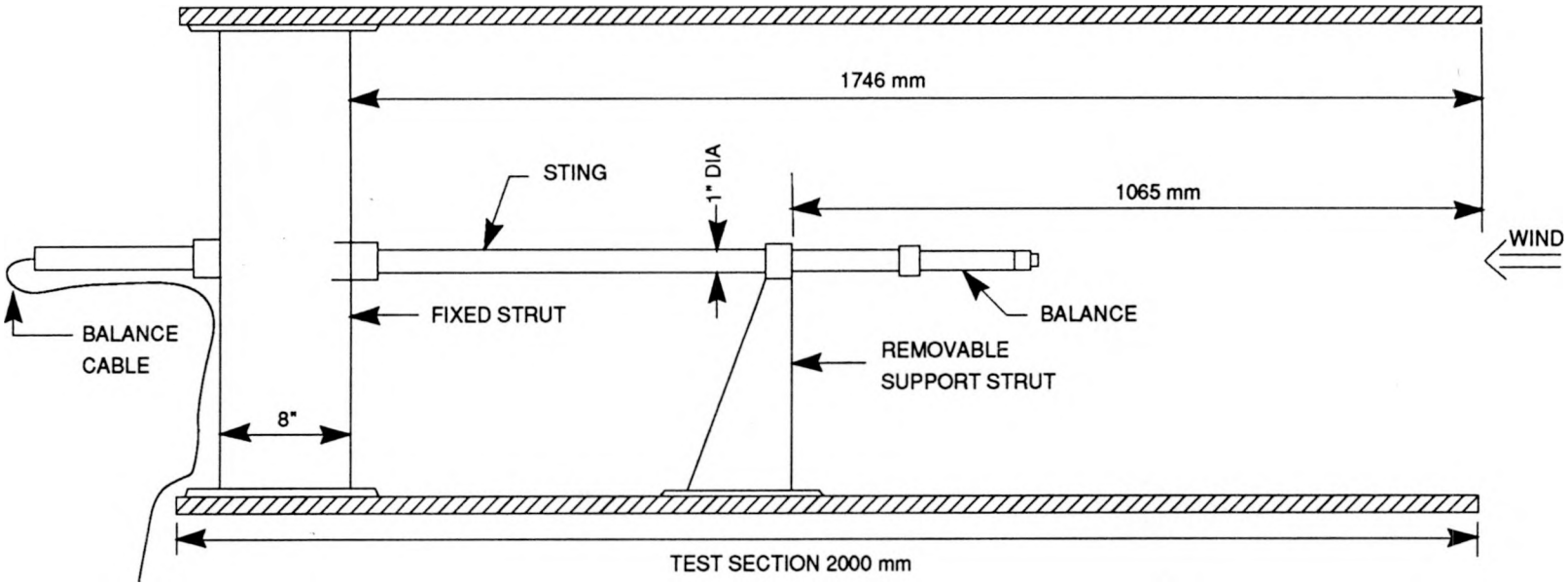

Figure 4. Parachute and Disk Model Support System

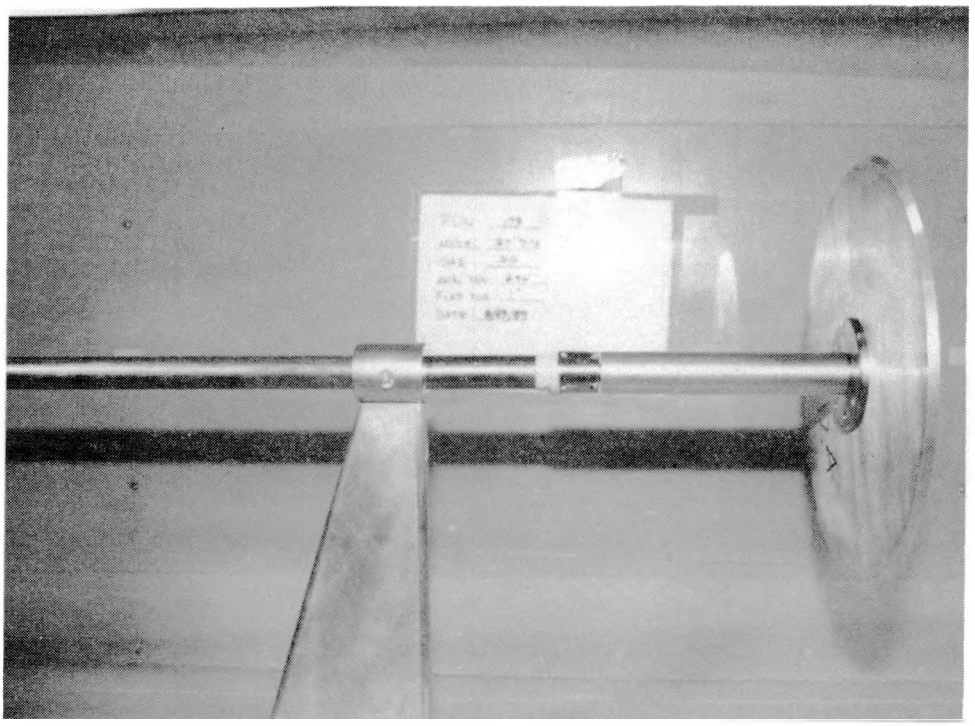

(a). with removable support strut installed

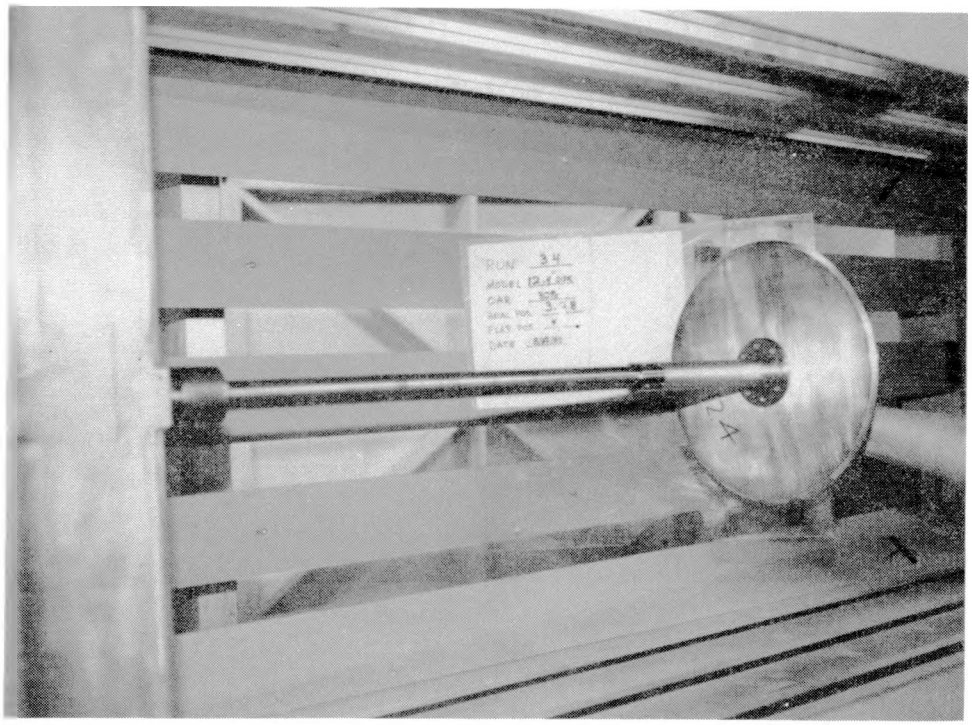

(b). without removable support strut

Figure 5. View of 12.4" Disk Model Installed on The Model Support System

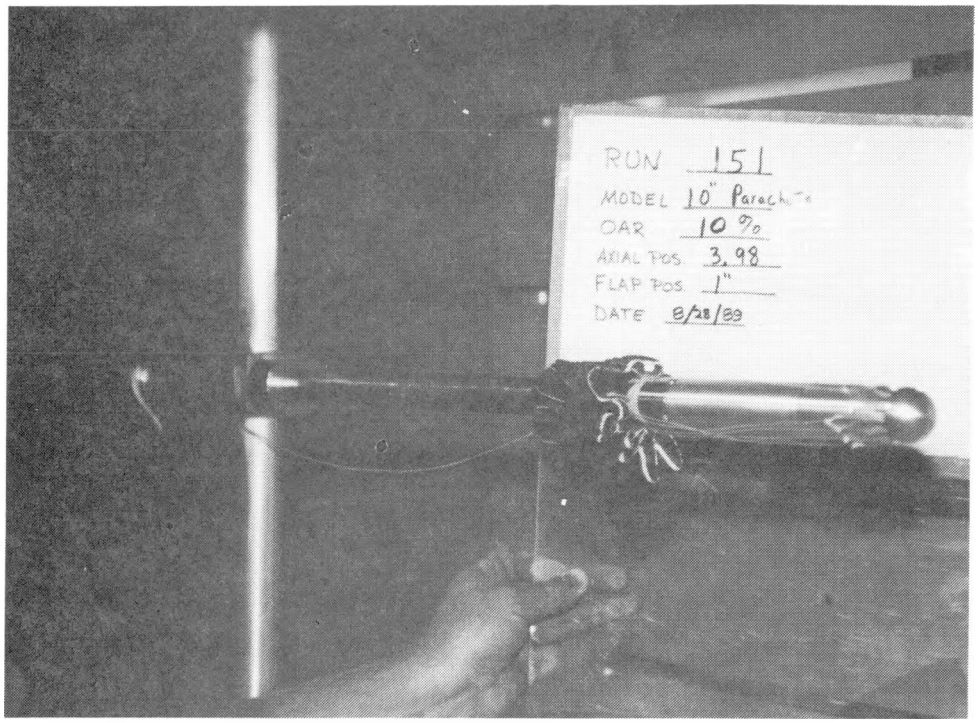

(a). 10" parachute reefed

(b). 14.5" parachute inflated

Figure 6. Parachute Installed on the Model Support System

Figure 7. Data Aquisition System

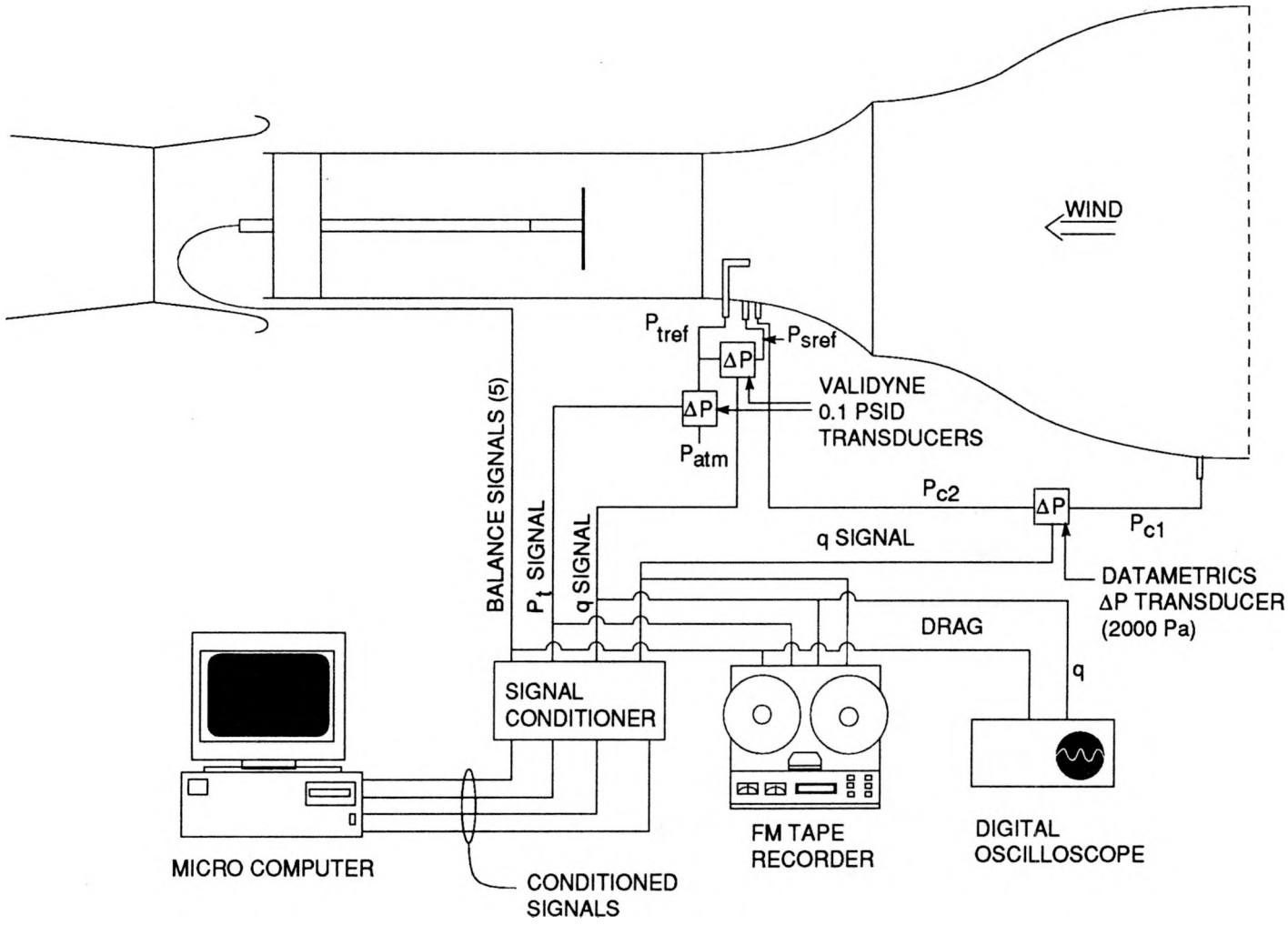

Figure 8. Instrumentation Schematic

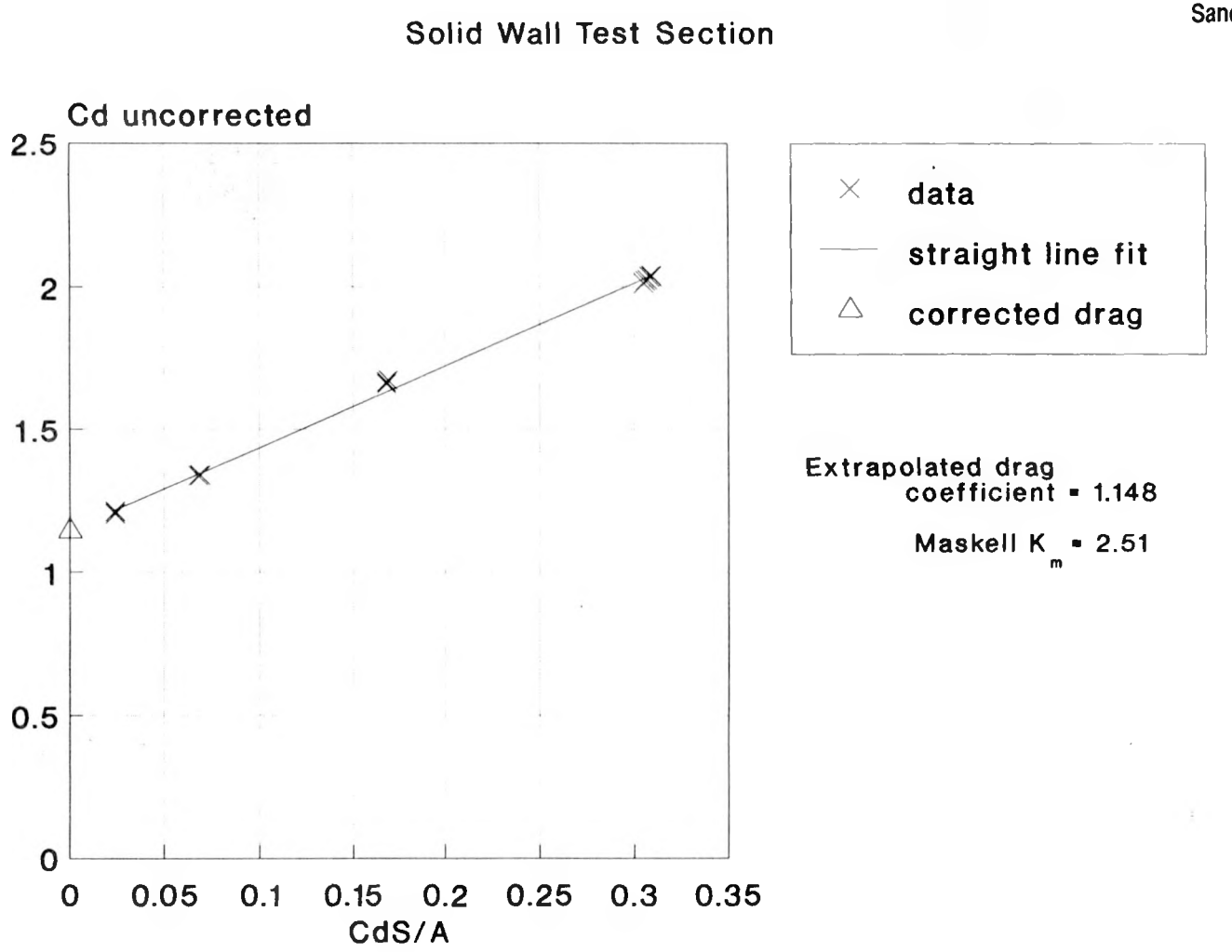

Figure 9. Variation in Uncorrected Blockage with Aerodynamic Drag (Disk Data)

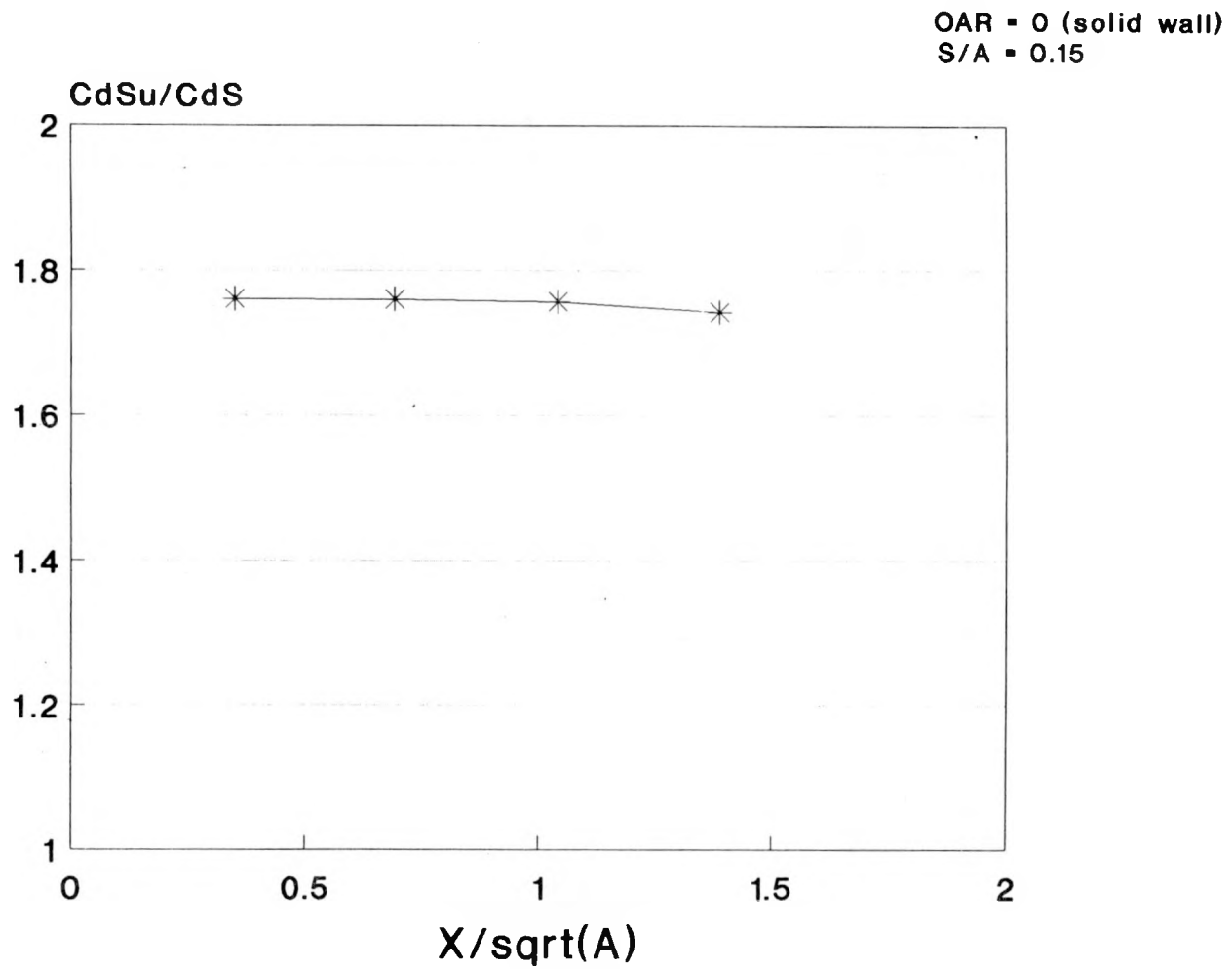

Figure 10. Effect of Axial Position on Blockage Correction for Solid Wall Test Section (Disk Data)

DSMA International engineers constructors

Sandia National Laboratories

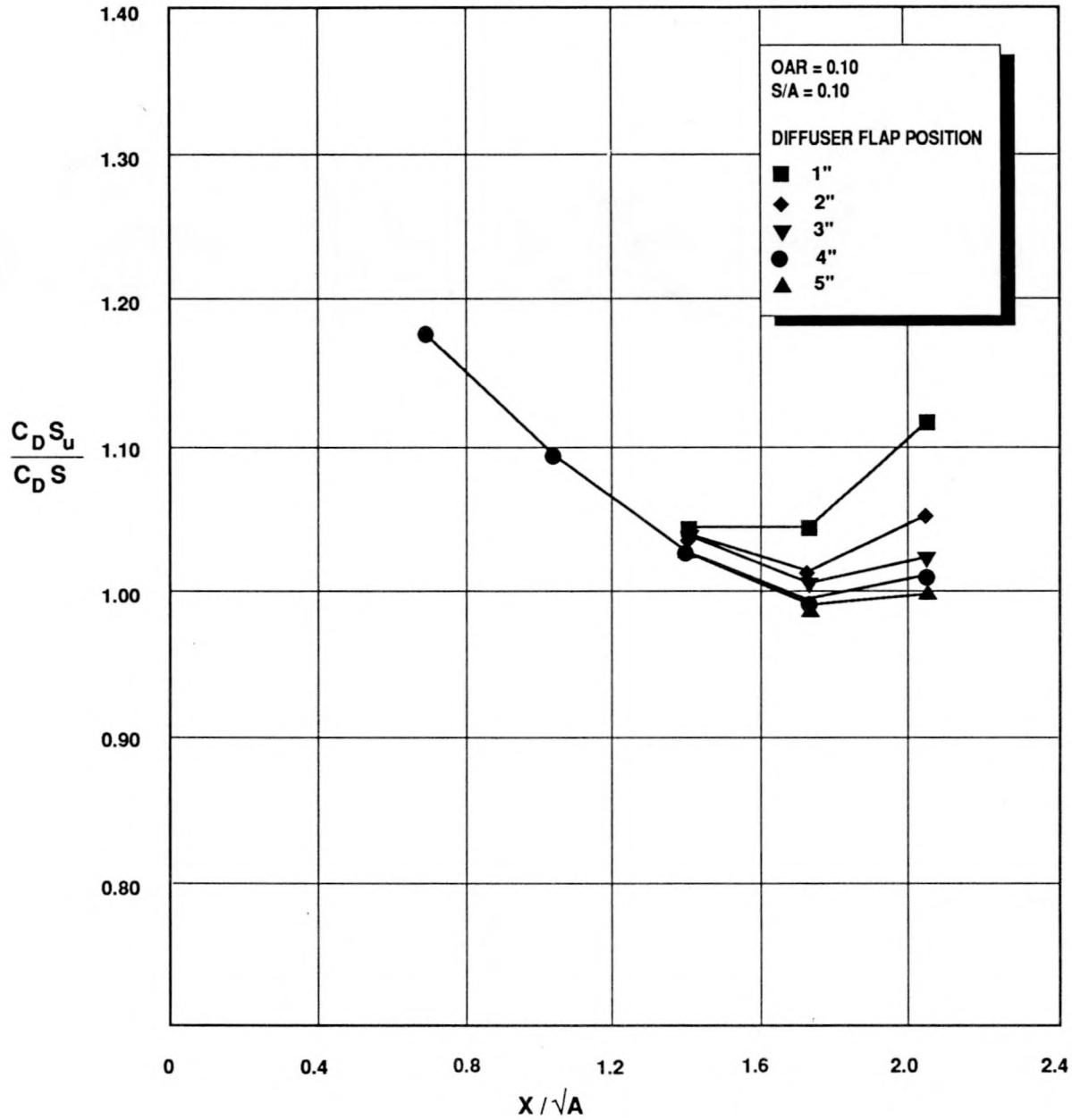

Figure 11. Effect of Axial Position and Flap Variation for 10% Wall OAR (Disk Data)

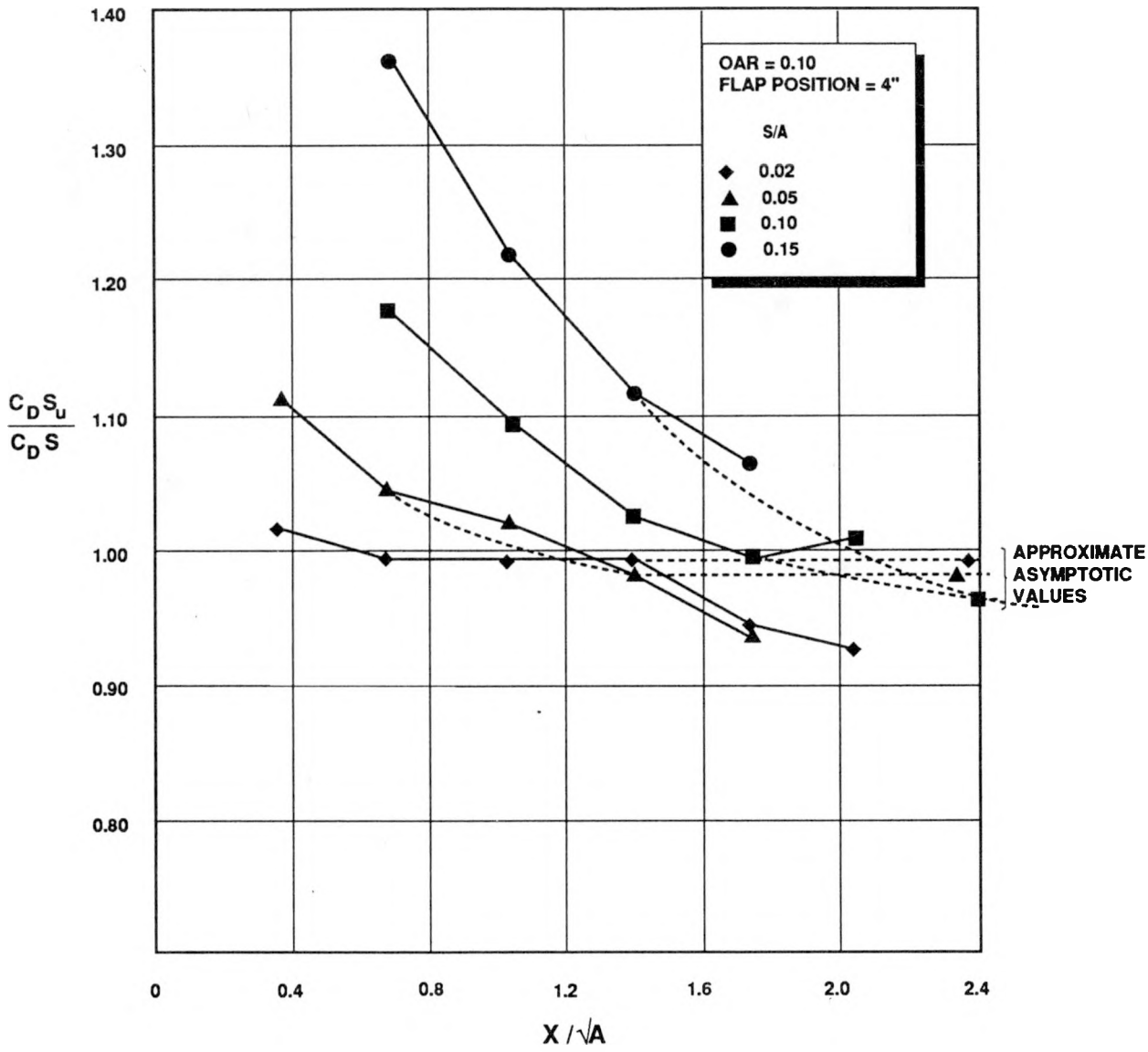

Figure 12. Variation of Blockage Correction with Axial Position in 10% Wall OAR Test Section (Disk Data)

DSMA International engineers constructors

Sandia National Laboratories

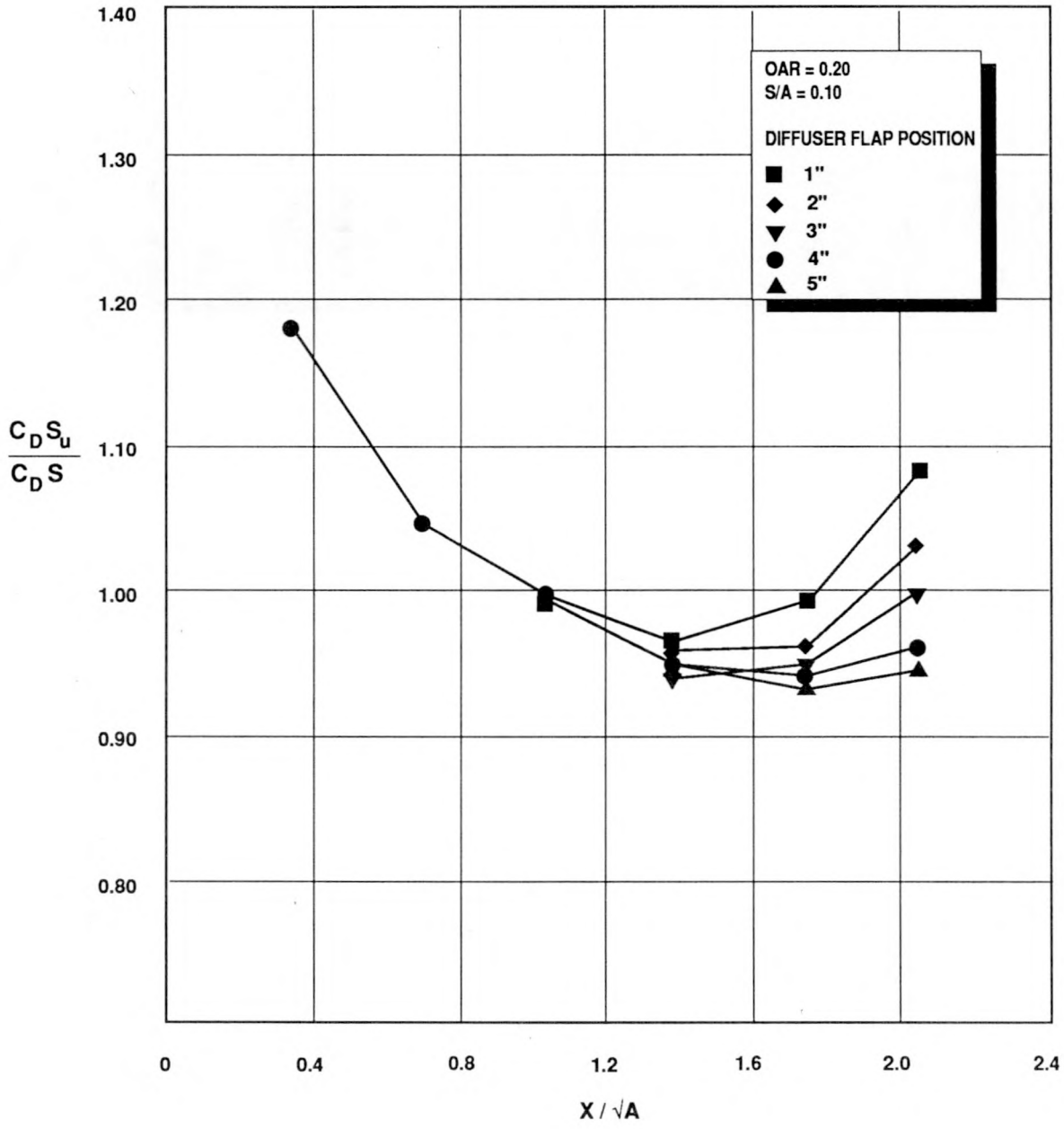

Figure 13. Effect of Flap Variation for 20% Wall OAR (Disk Data)

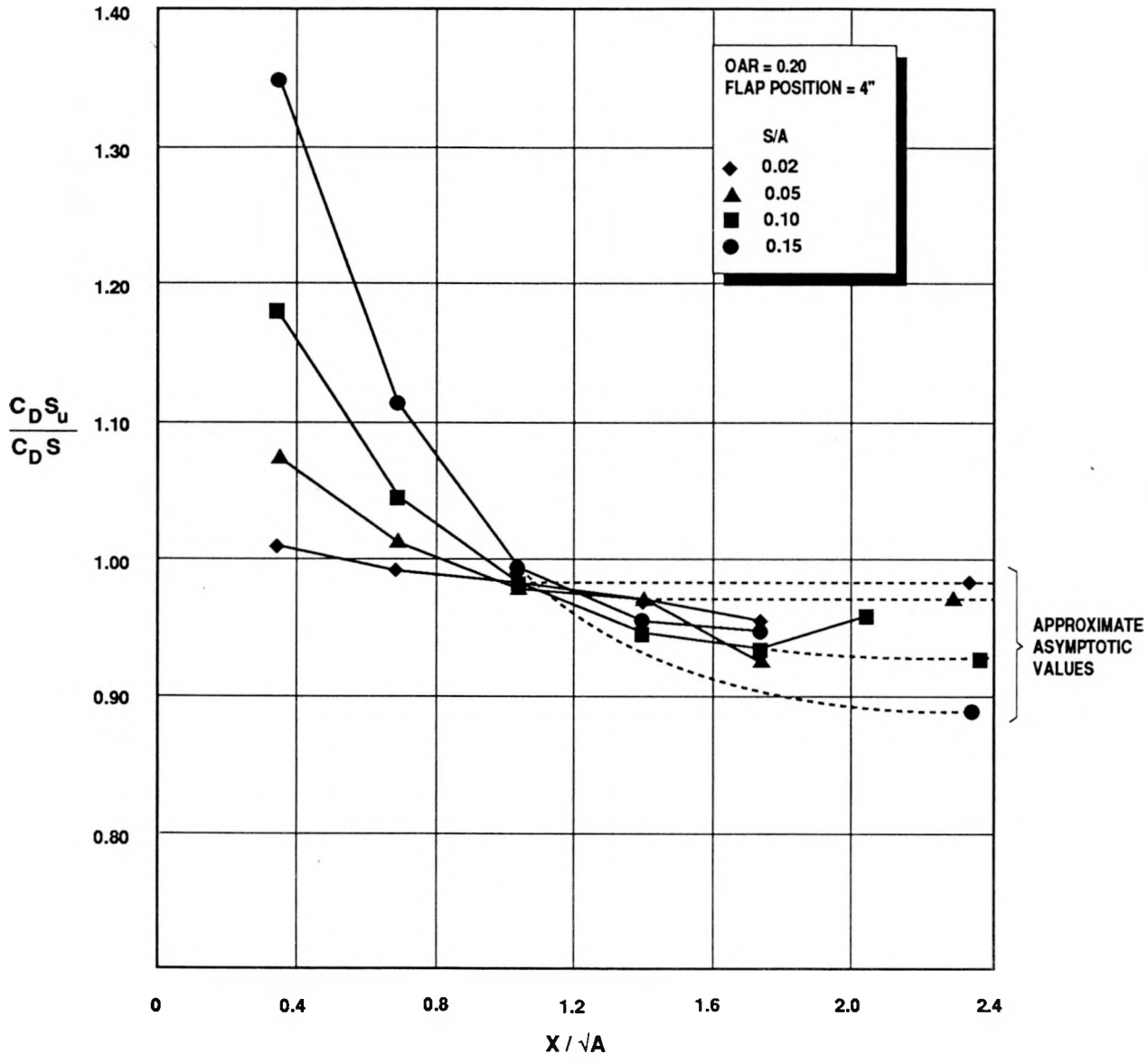

Figure 14. Variation of Blockage Correction with Axial Position in the 20% Wall OAR Test Section (Disk Data)

DSMA International engineers constructors

Sandia National Laboratories

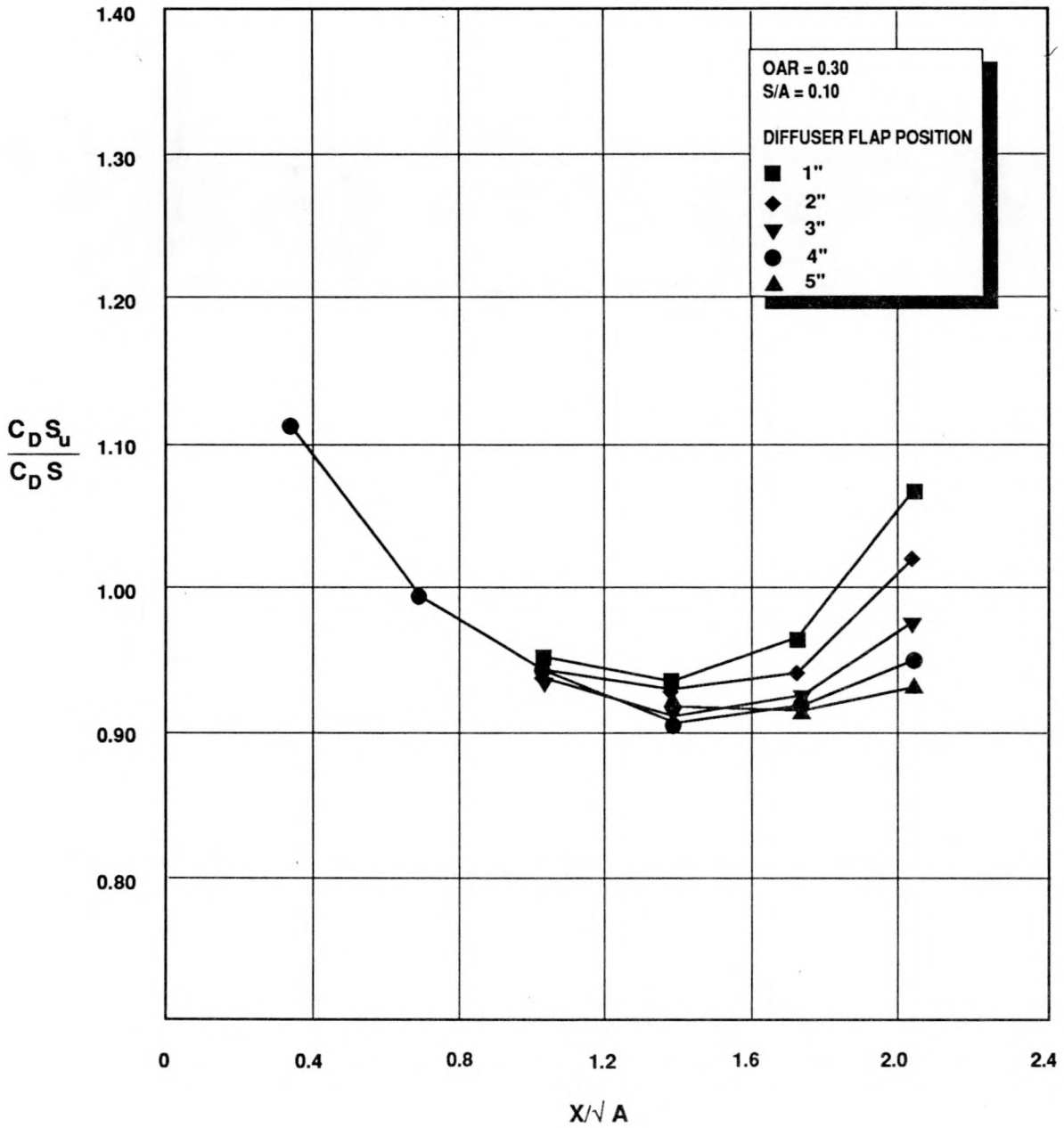

Figure 15. Effect of Flaps Variation for 30% Wall OAR (Disk Data)

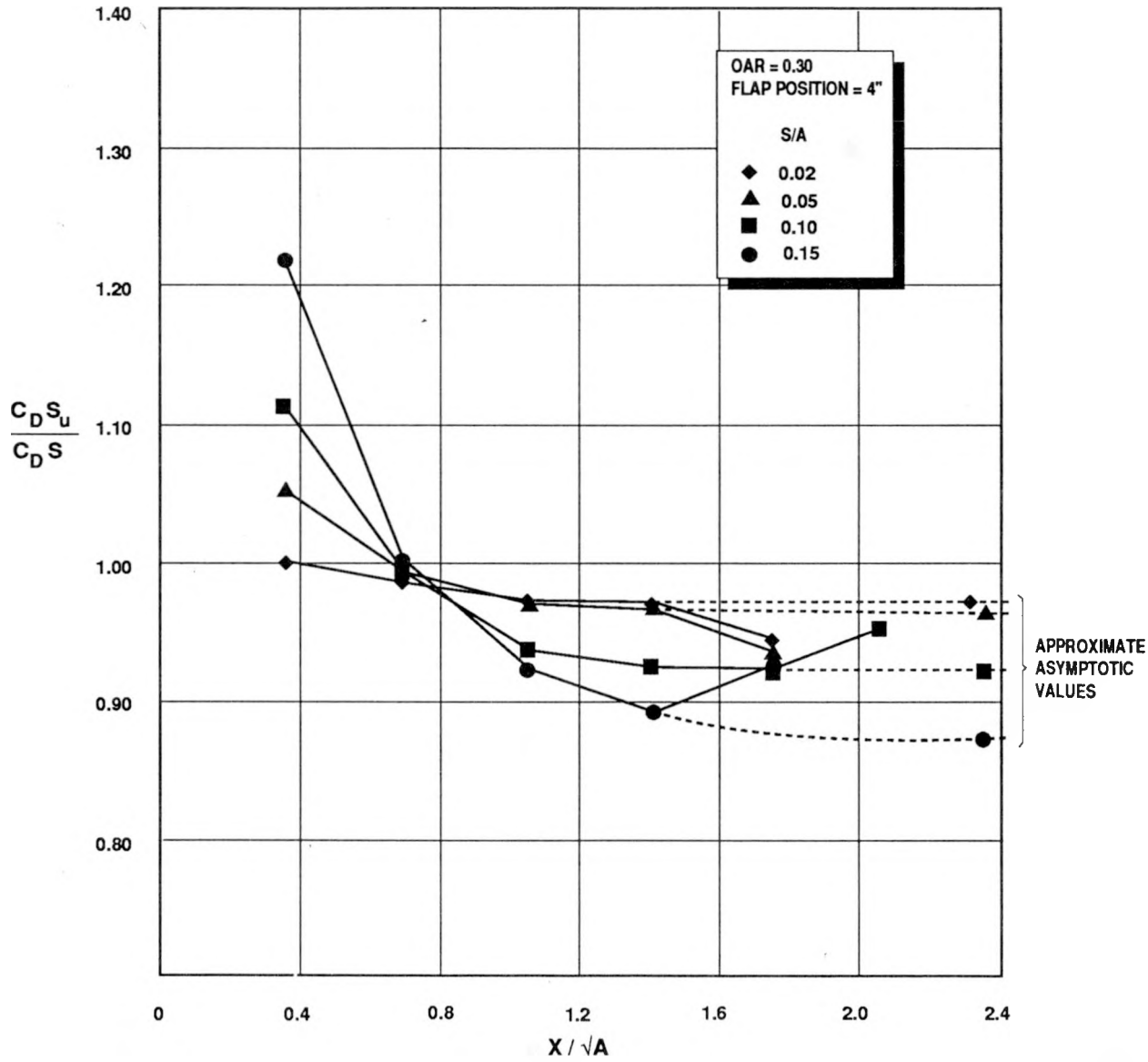

Figure 16. Variation of Blockage Correction with Axial Position in the 30% Wall OAR Test Section (Disk Data)

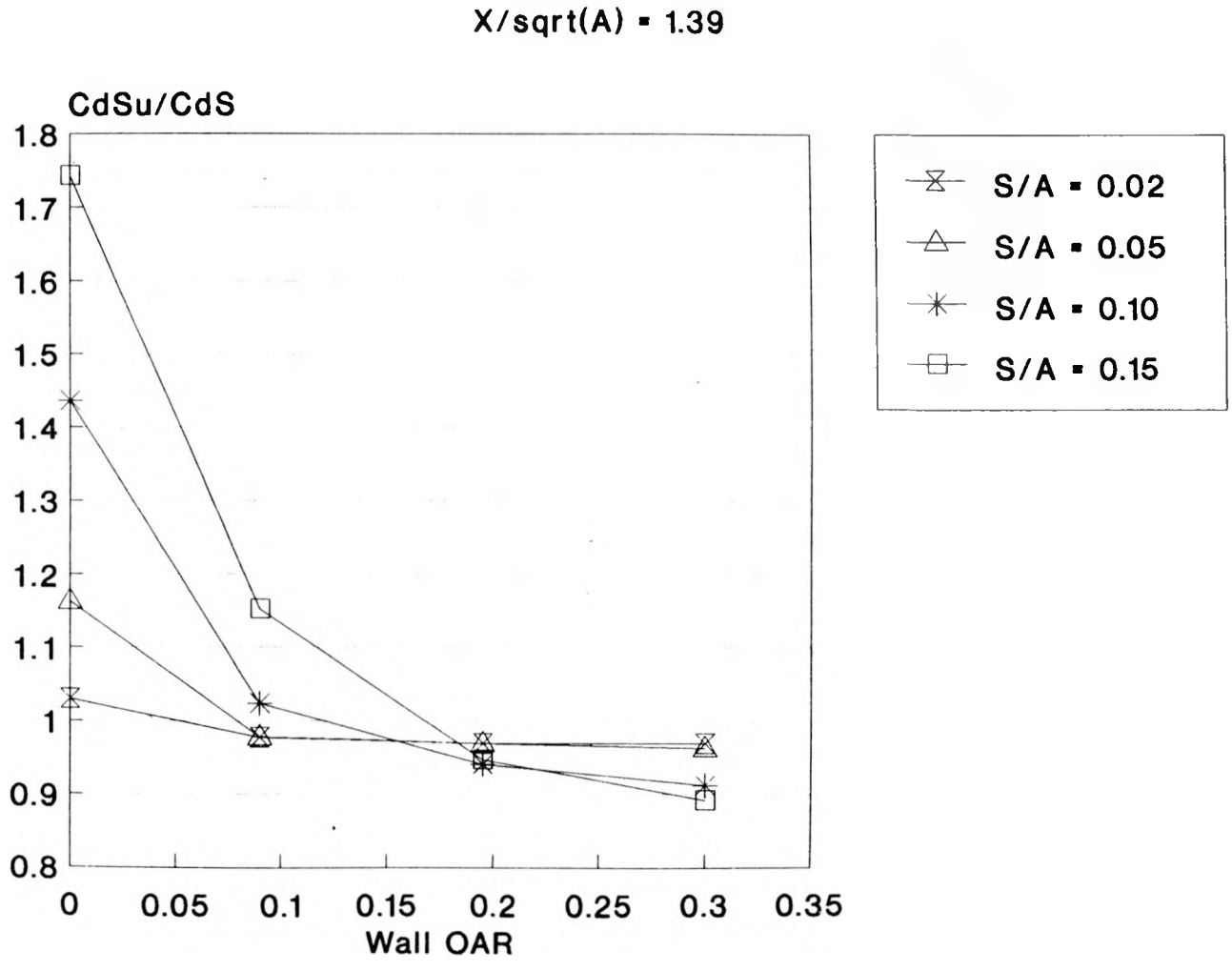

Figure 17. Variation of Blockage Correction with OAR at X/sqrt (A) = 1.39 (Disk Data)

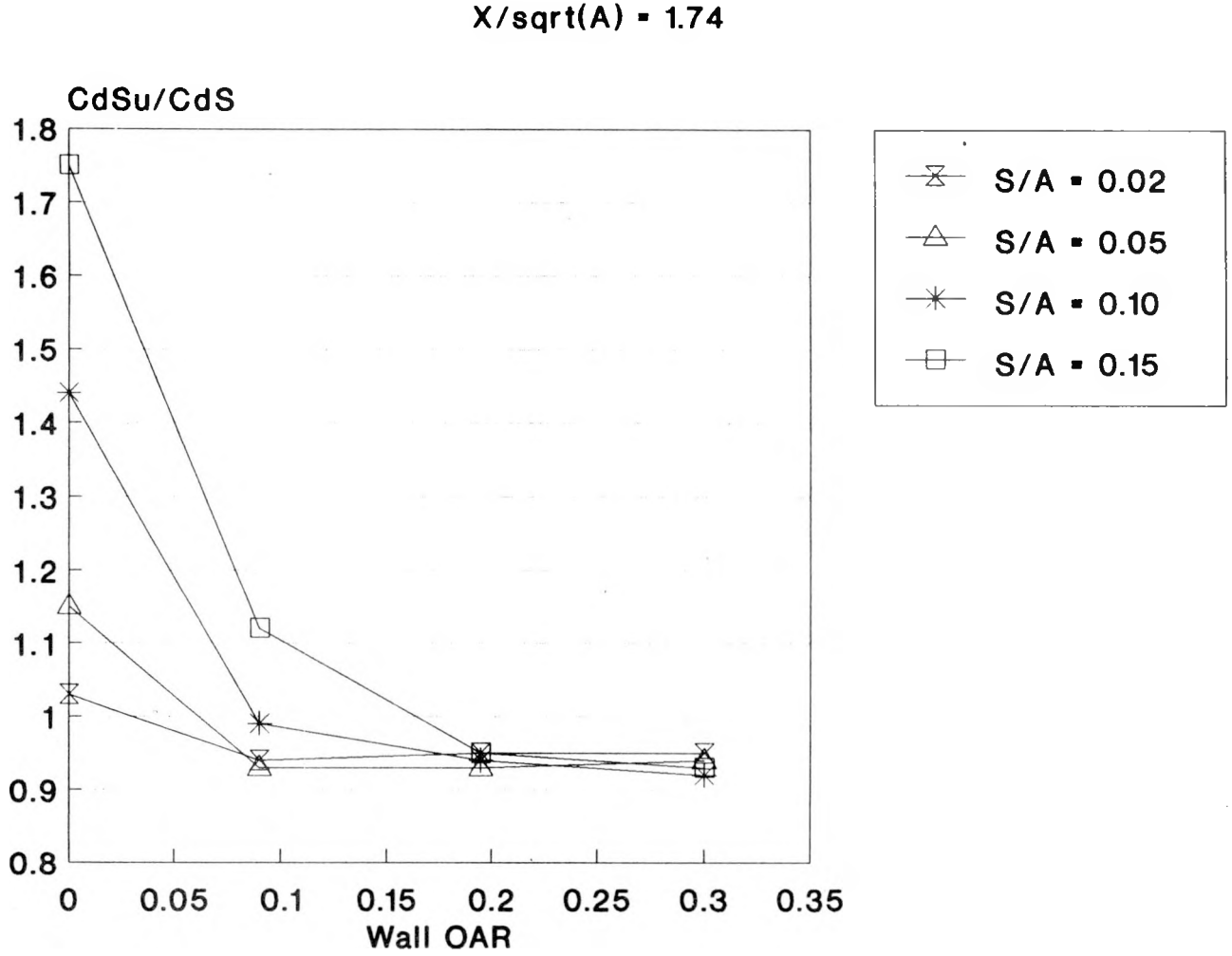

Figure 18. Variation of Blockage Correction with Axial Position at X/sqrt (A) = 1.74 (Disk Data)

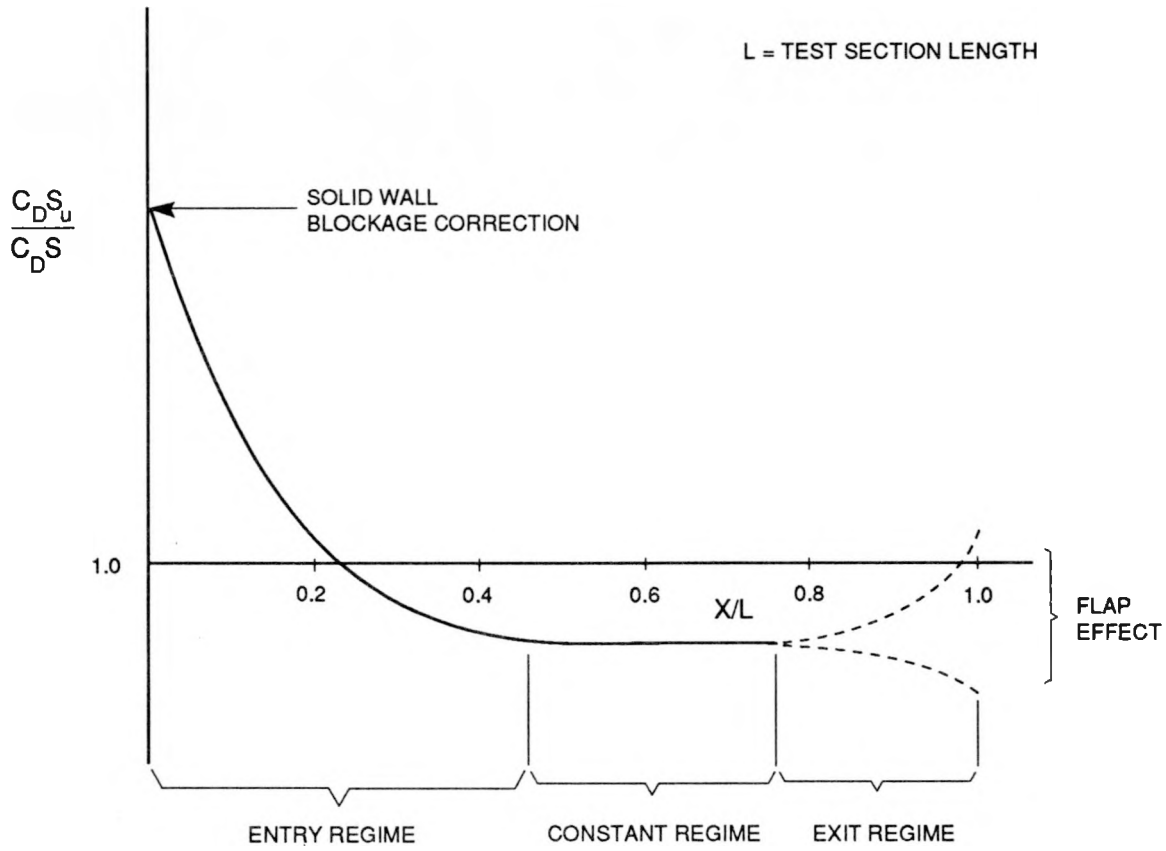

Figure 19. Test Section Boundary Constraint Regimes

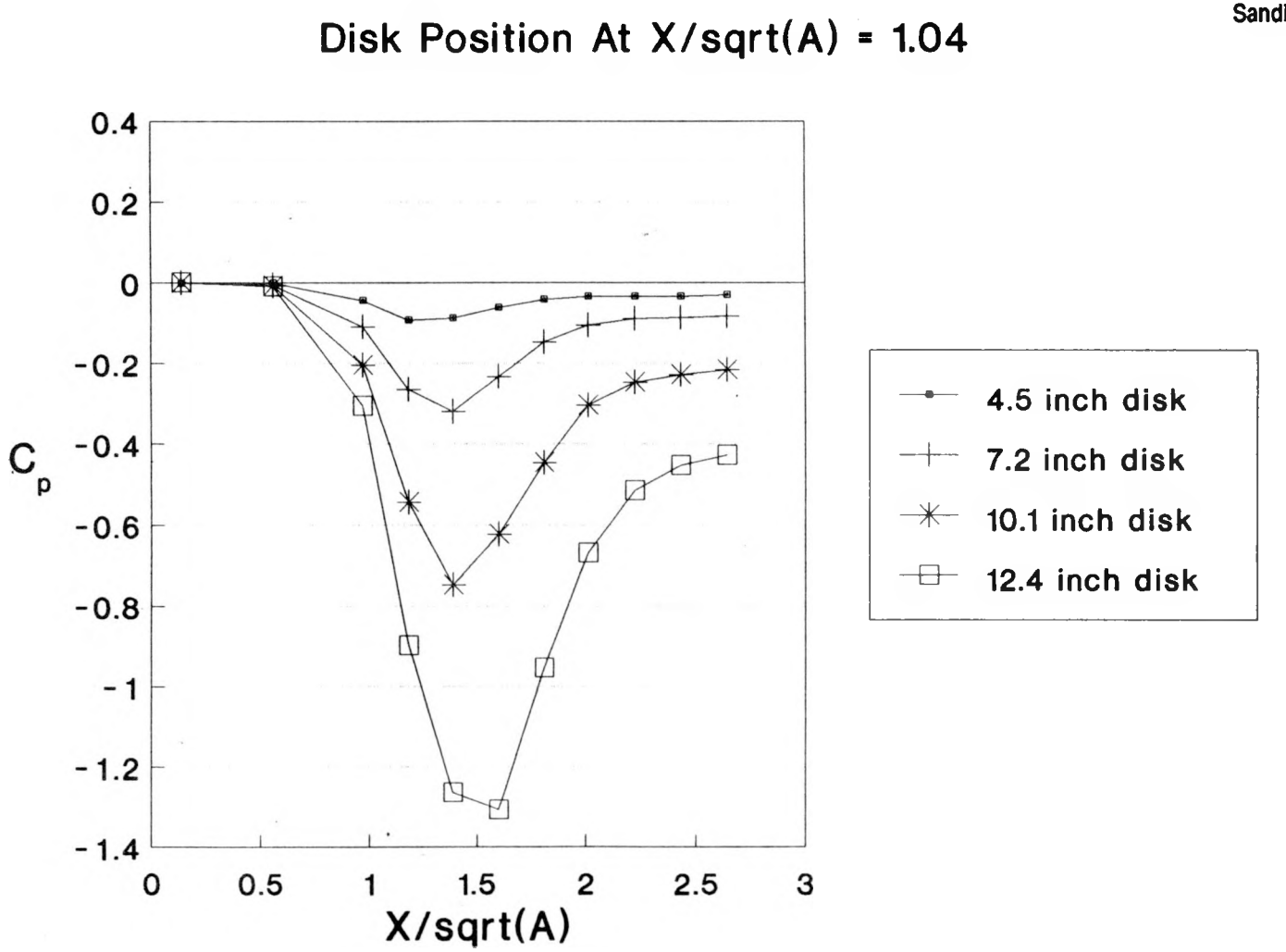

Figure 20. Wall Pressure Signature for The Solid Wall Test Section

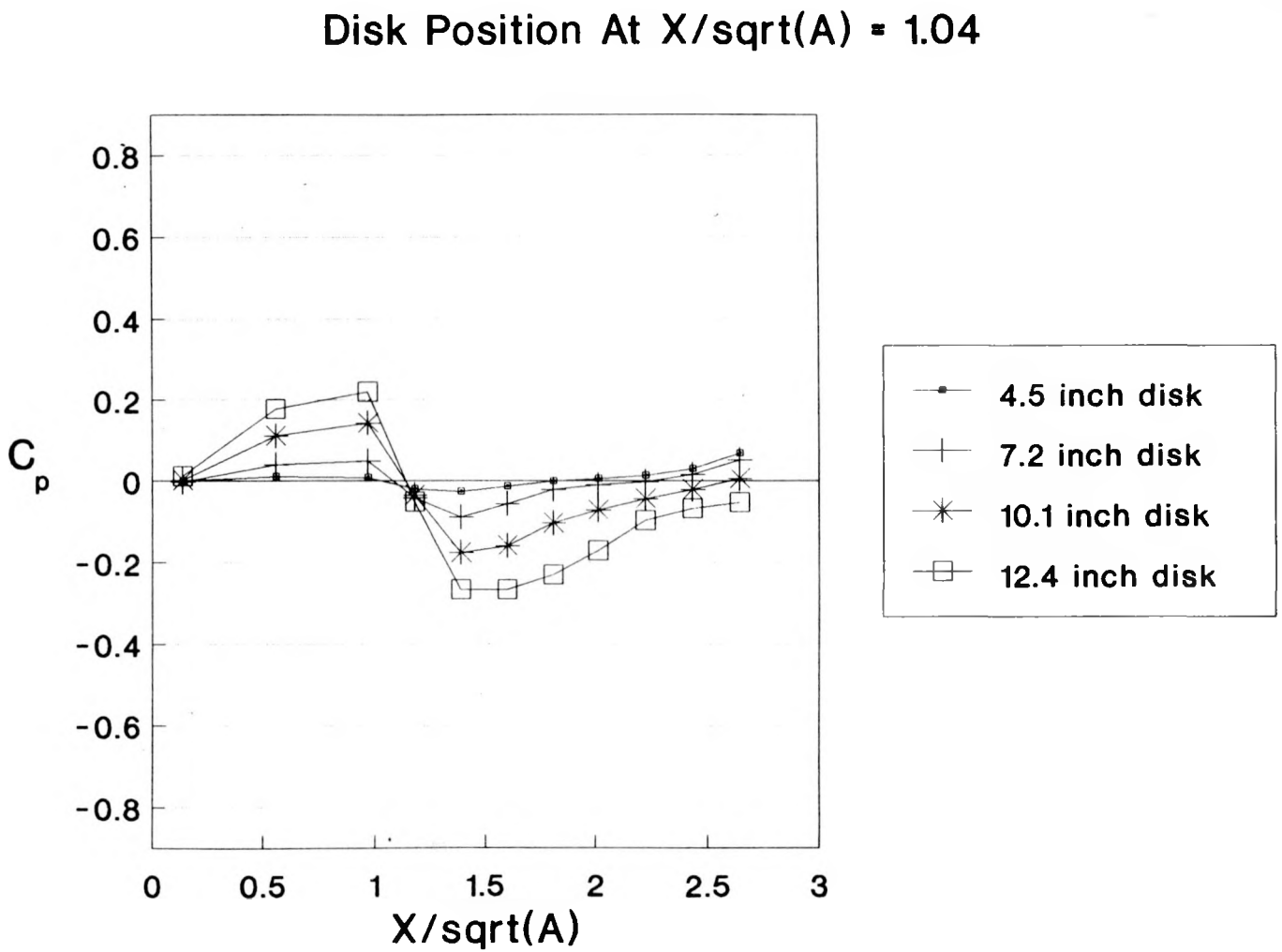

Figure 21. Wall Pressure Signature for The 20% OAR Test Section

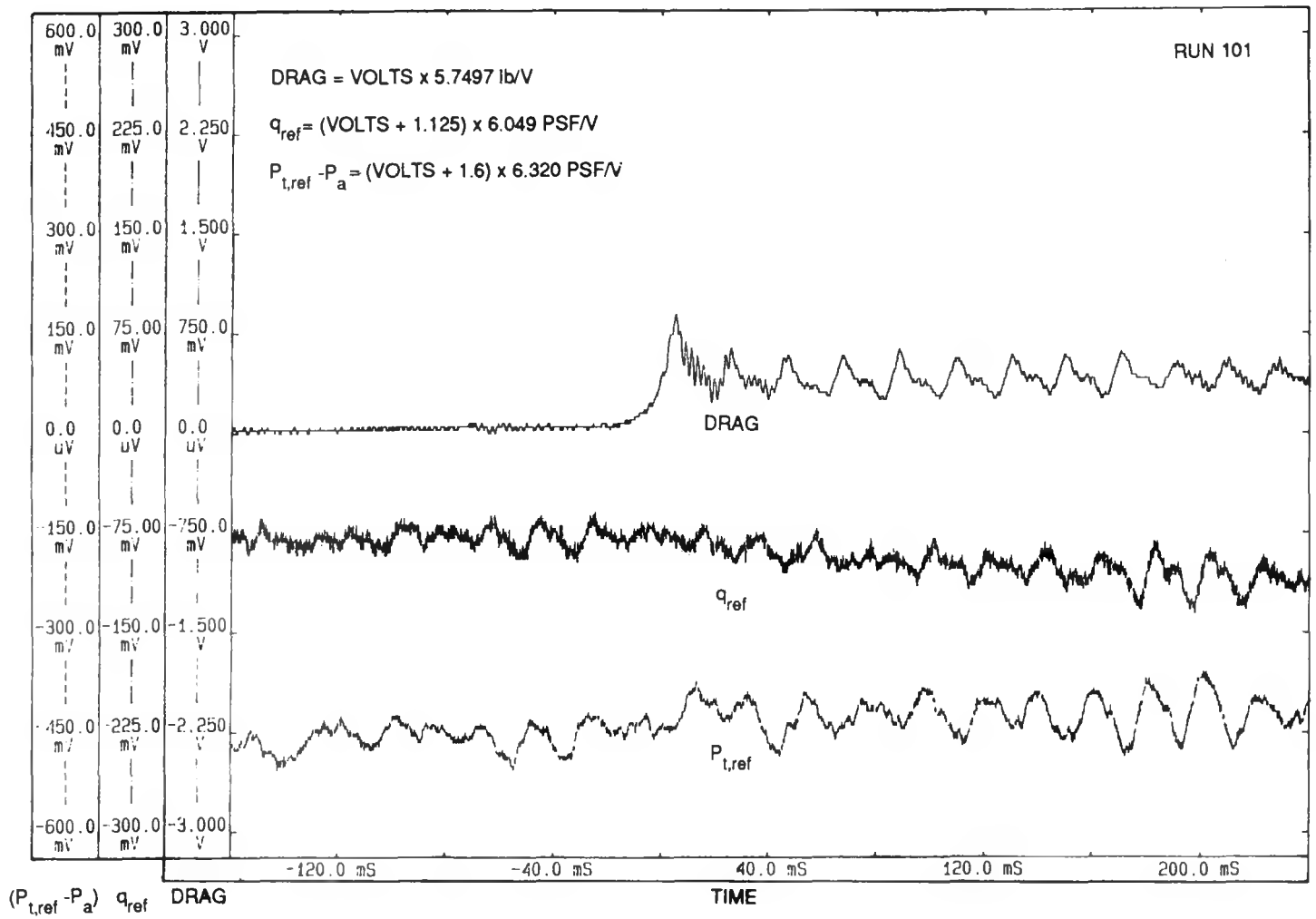

Figure 22. Transient Data for The 10" Parachute, Solid Wall Test Section

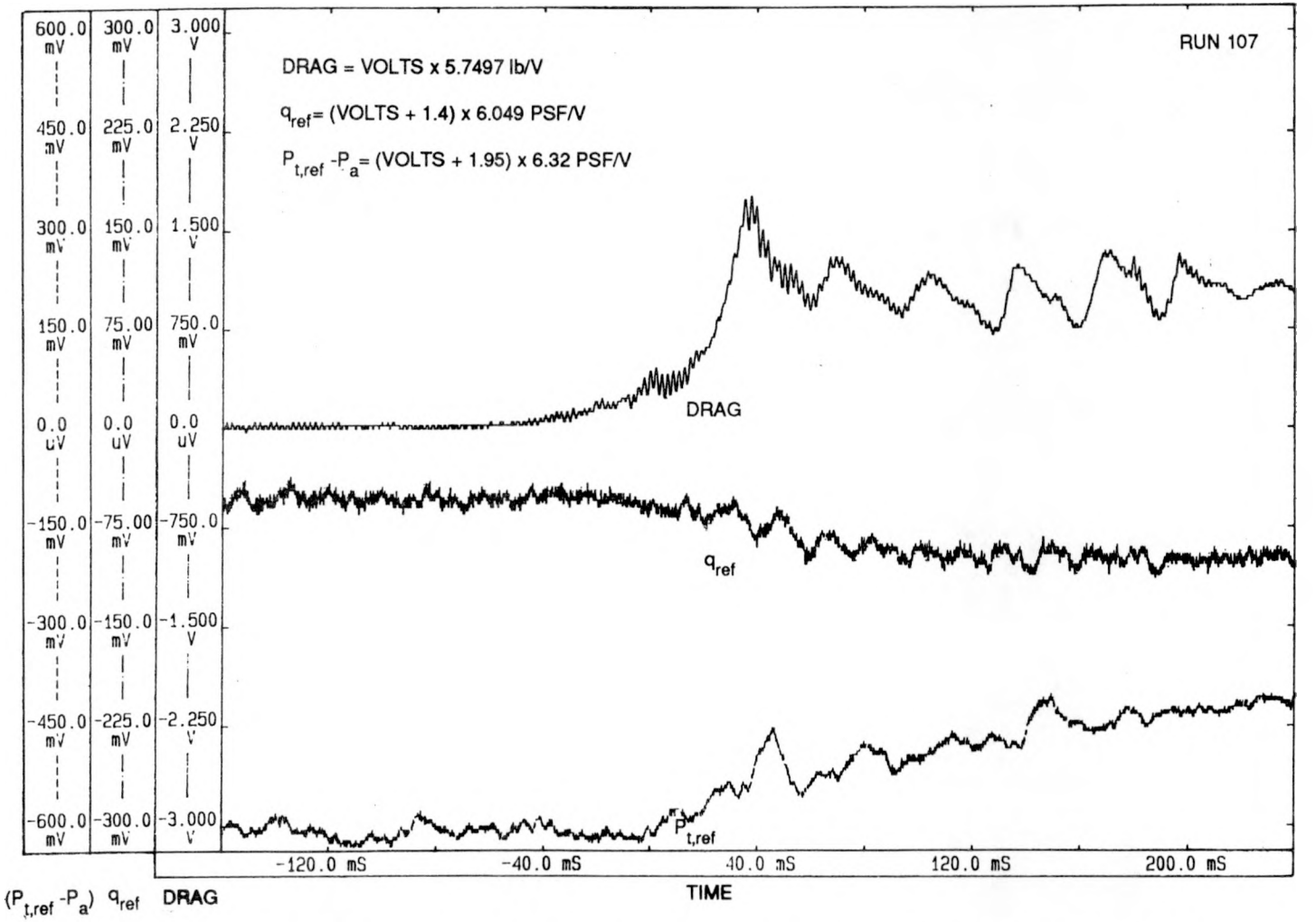

Figure 23. Transient Data for The 14.5" Parachute, Solid Wall Test Section

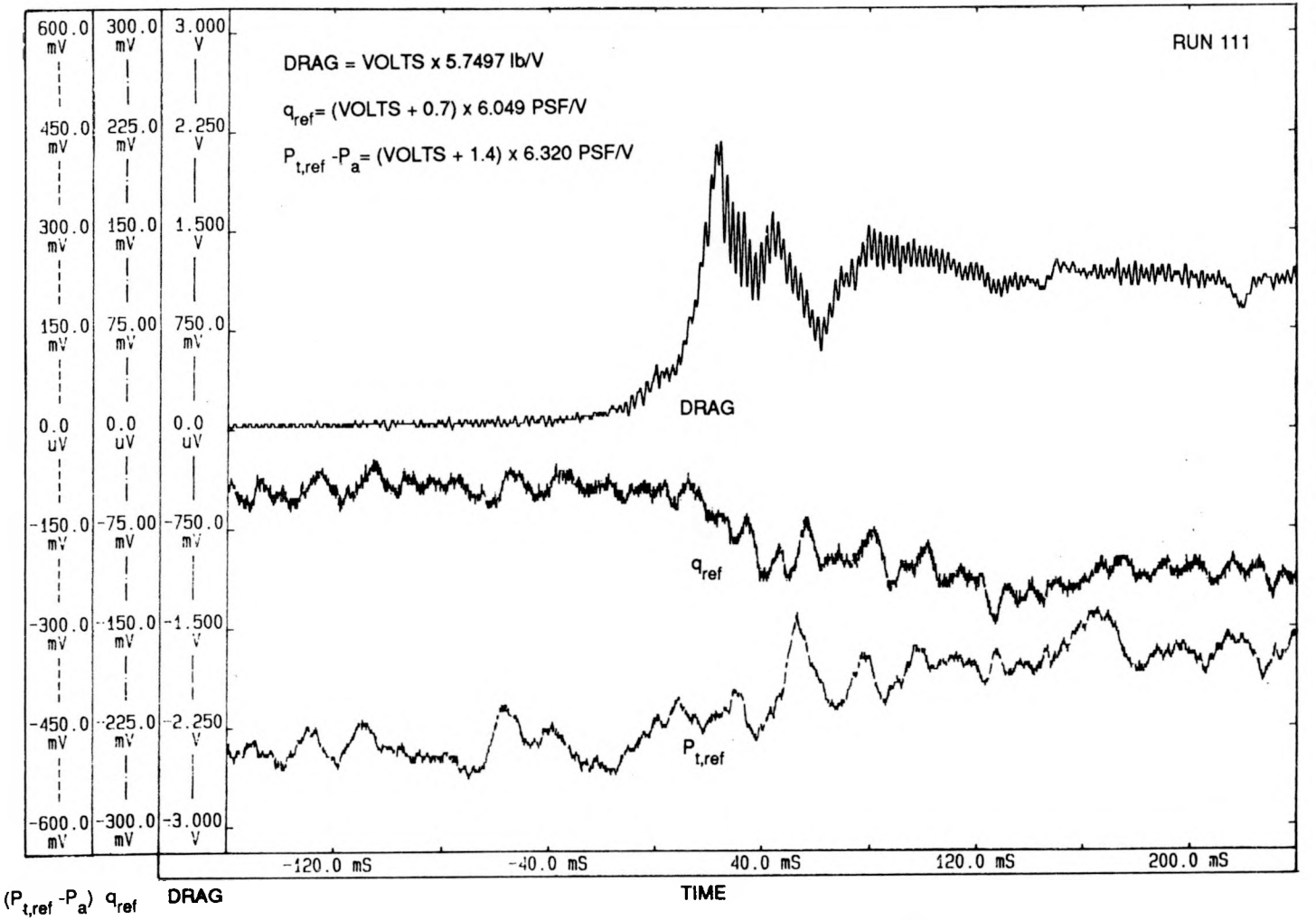

Figure 24. Transient Data for The 18" Parachute, Solid Wall Test Section

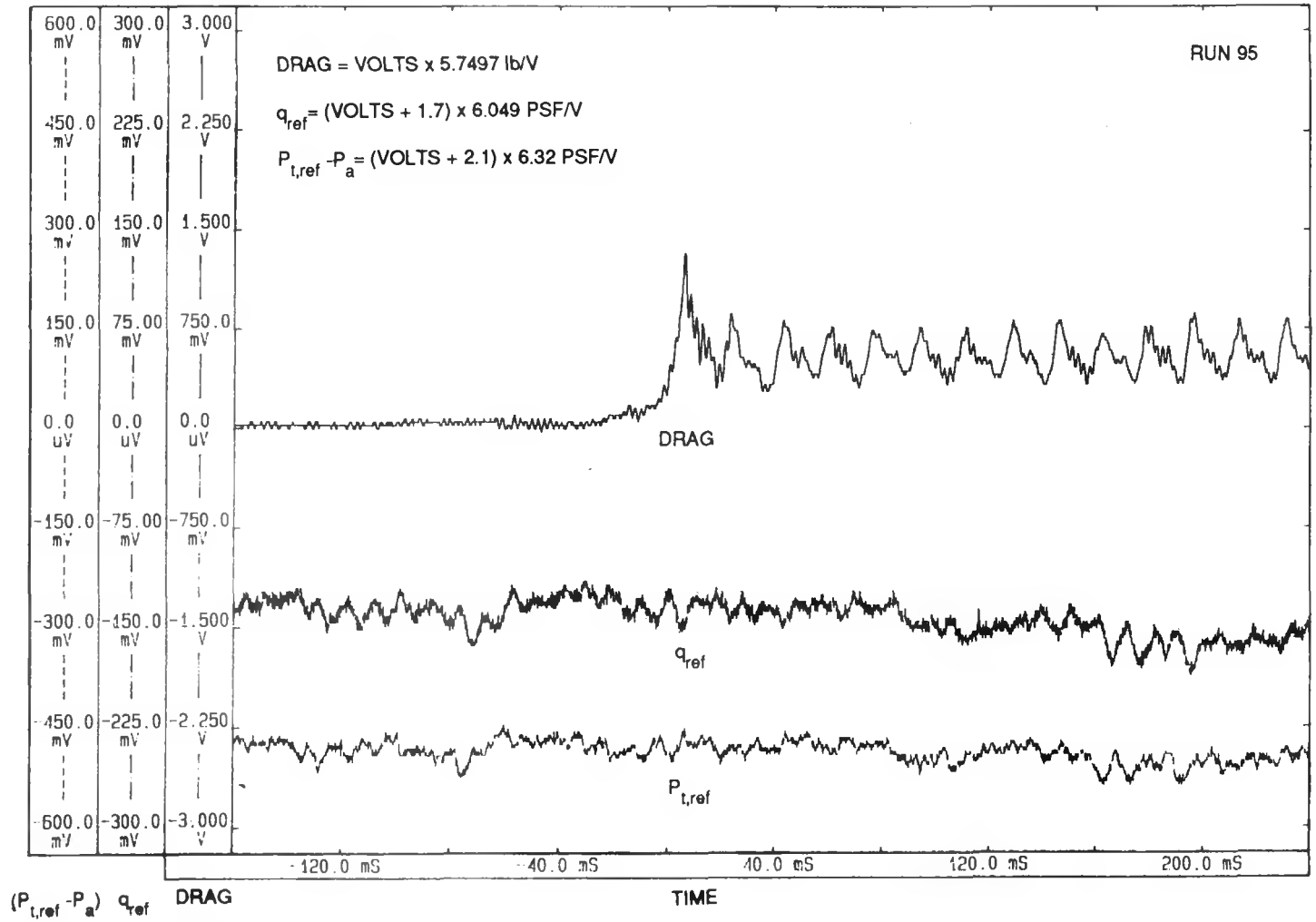

Figure 25. Transient Data for The 10" Parachute, 20% OAR Test Section

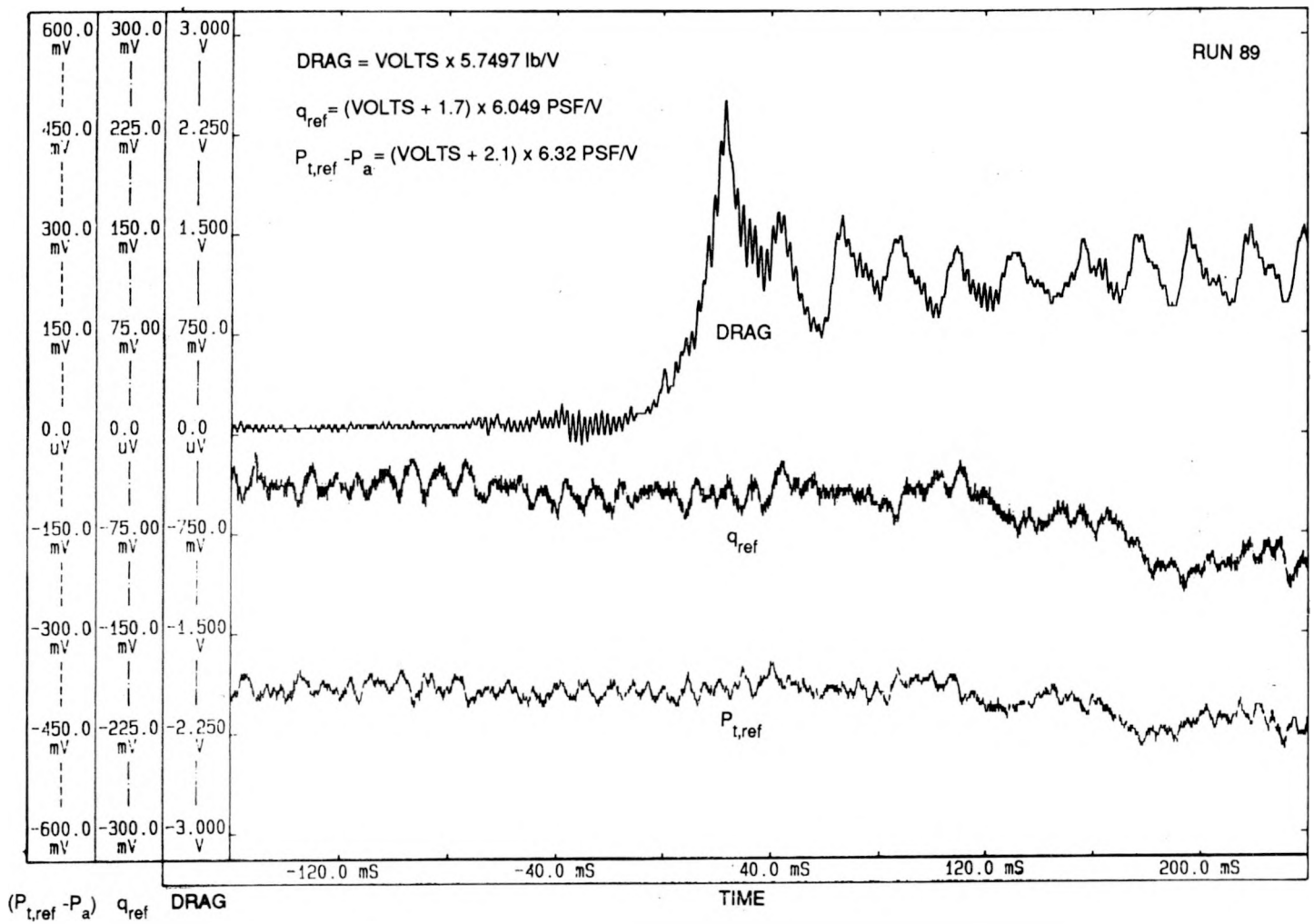

Figure 26. Transient Data for The 14.5" Parachute, 20% OAR Test Section

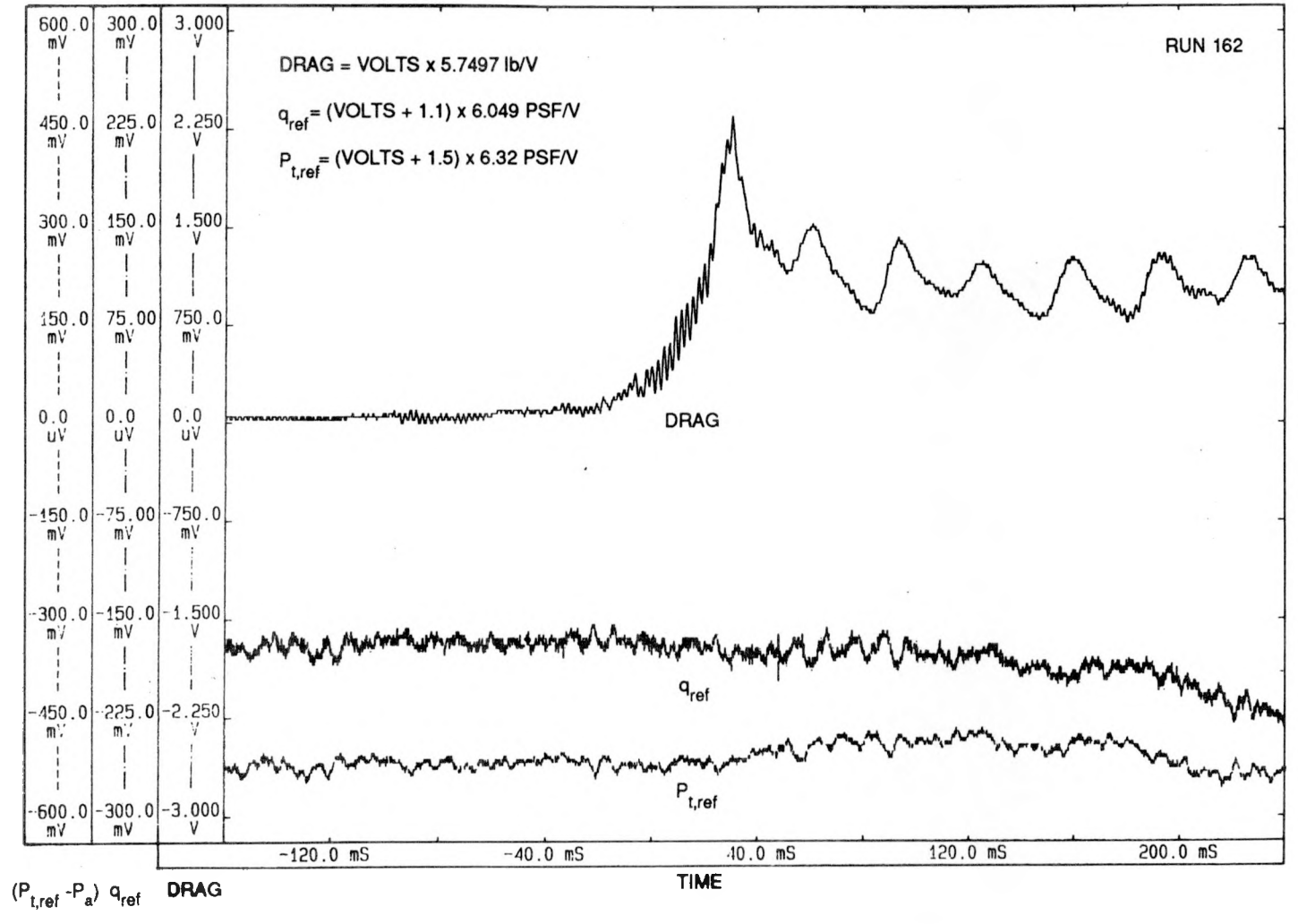

Figure 27. Transient Data for The 18" Parachute, 20% OAR Test Section

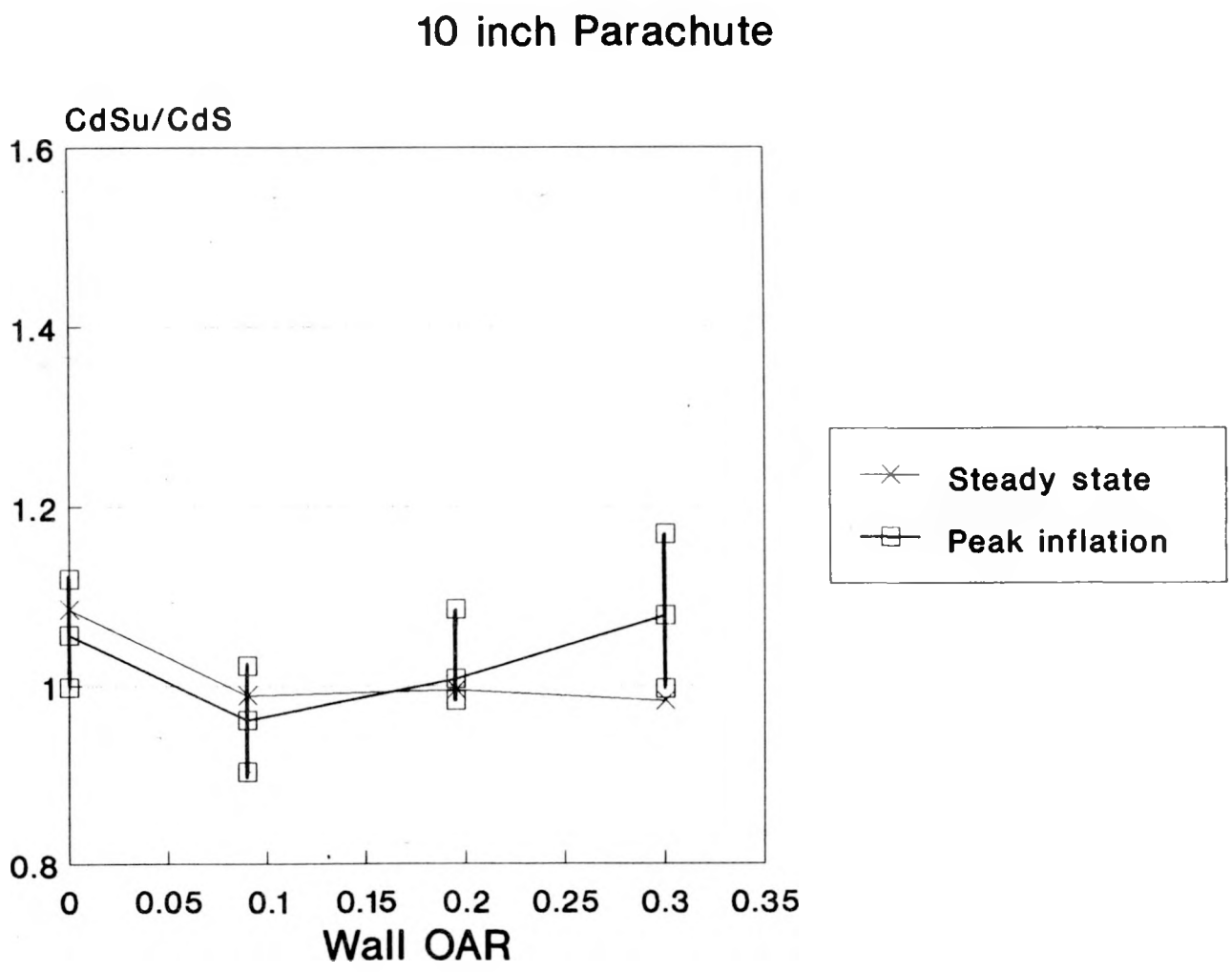

Figure 28. Blockage Correction as a Function of OAR for the 10 inch Parachute

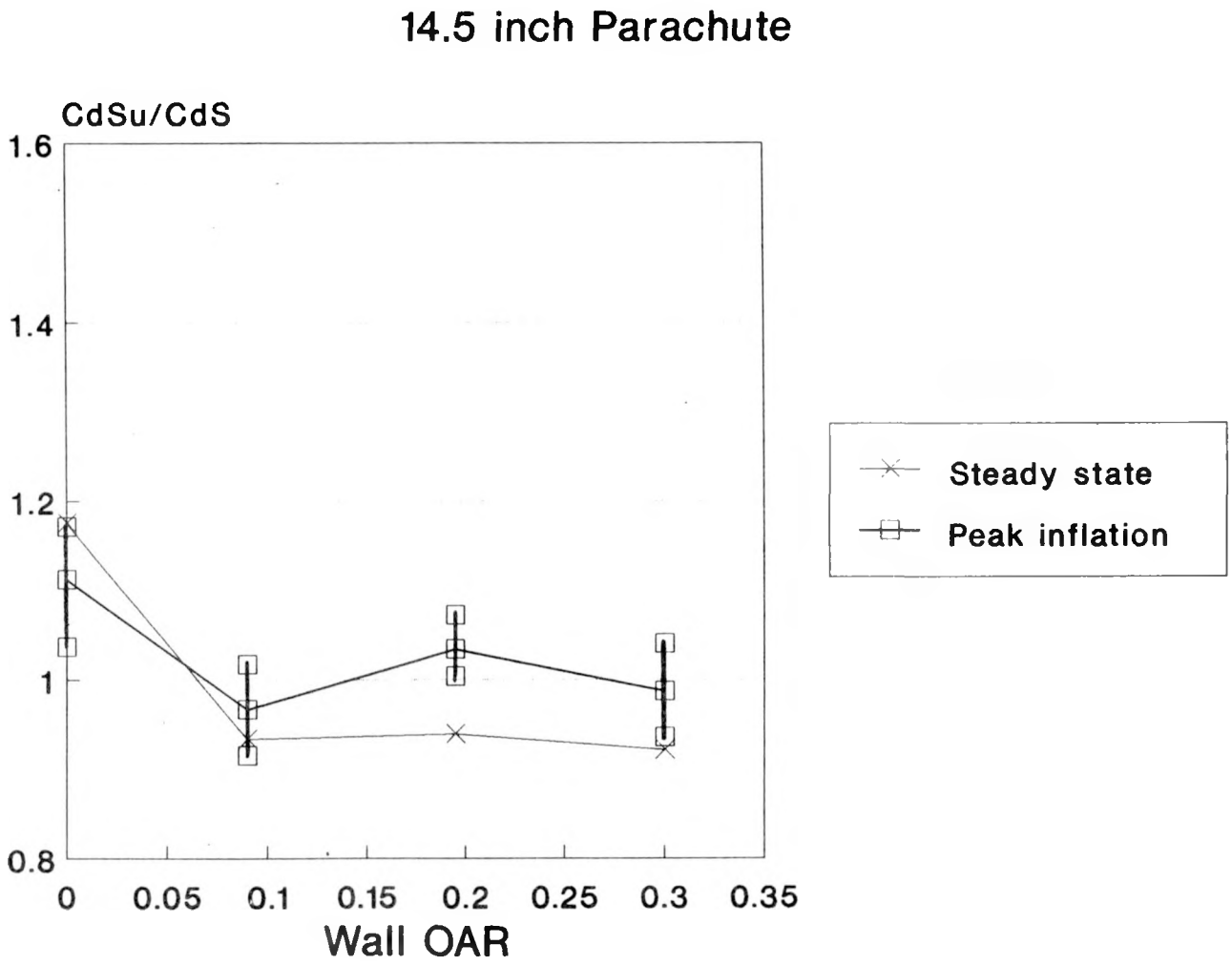

Figure 29. Blockage Correction as a Function of OAR for the 14.5 inch Parachute

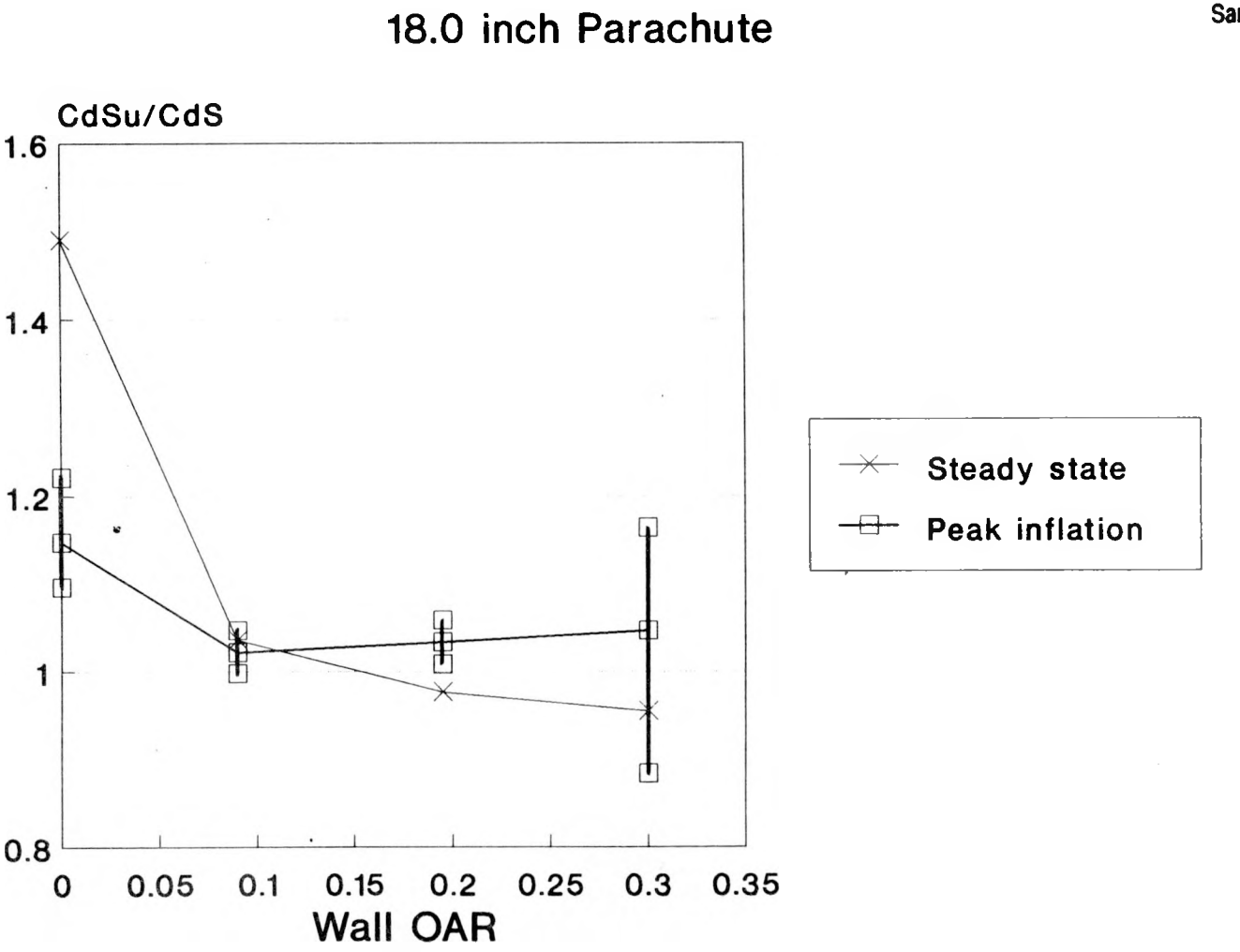

Figure 30. Blockage Correction as a Function of OAR for the 18.0 inch Parachute

Solid Wall

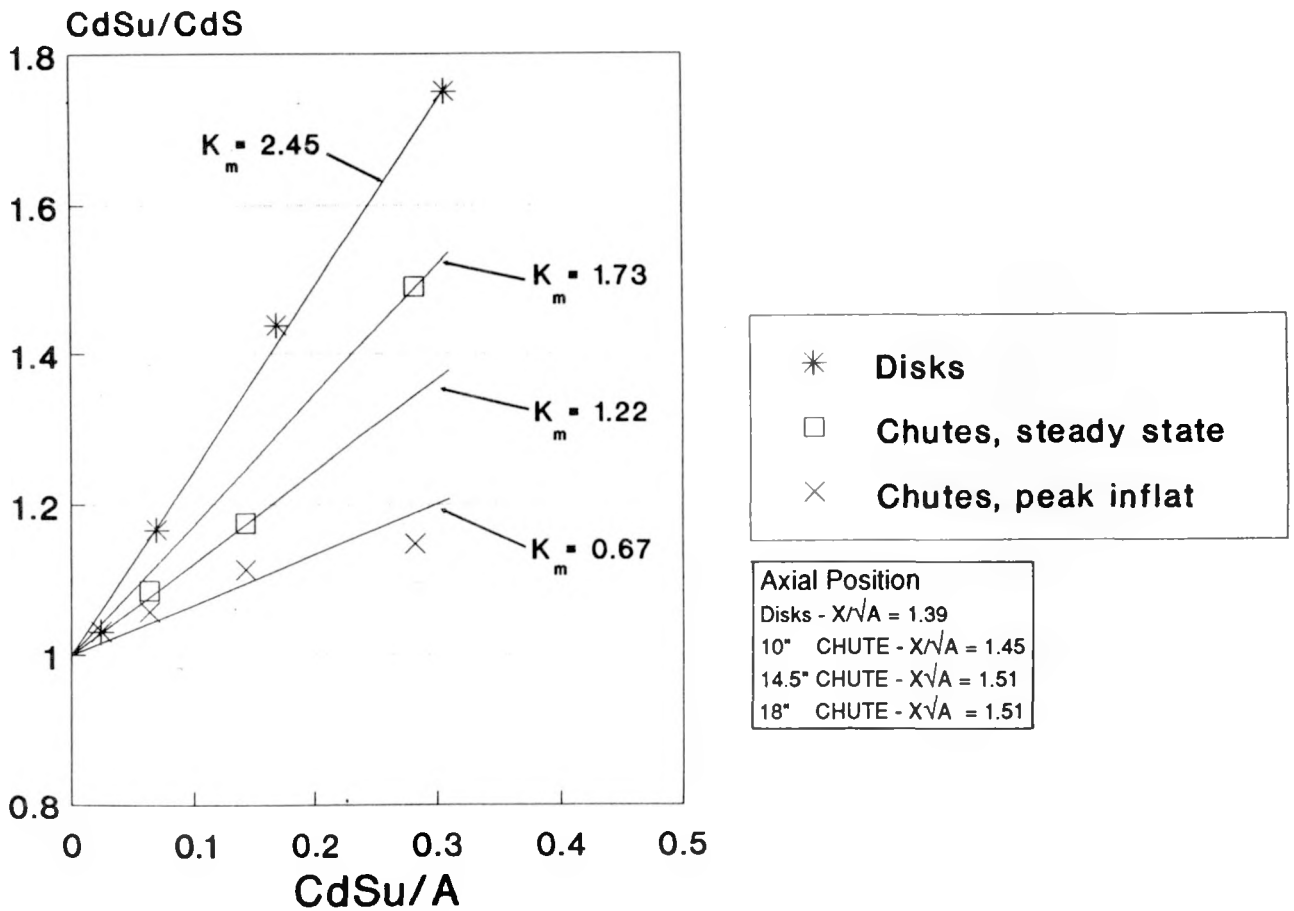

Figure 31. Blockage Correction for All Models, Solid Wall Test Section

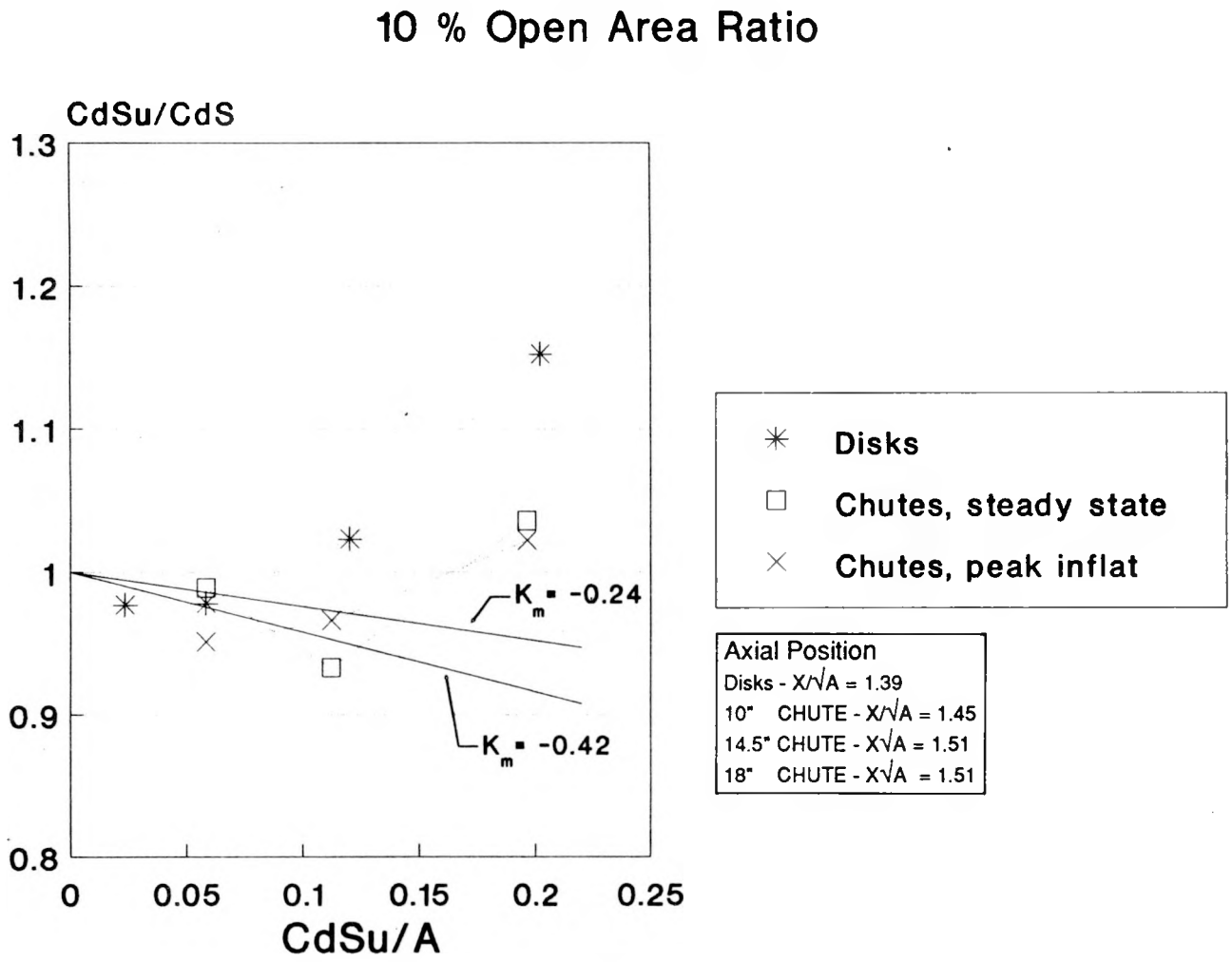

Figure 32. Blockage Correction for All Models, 10% OAR Test Section

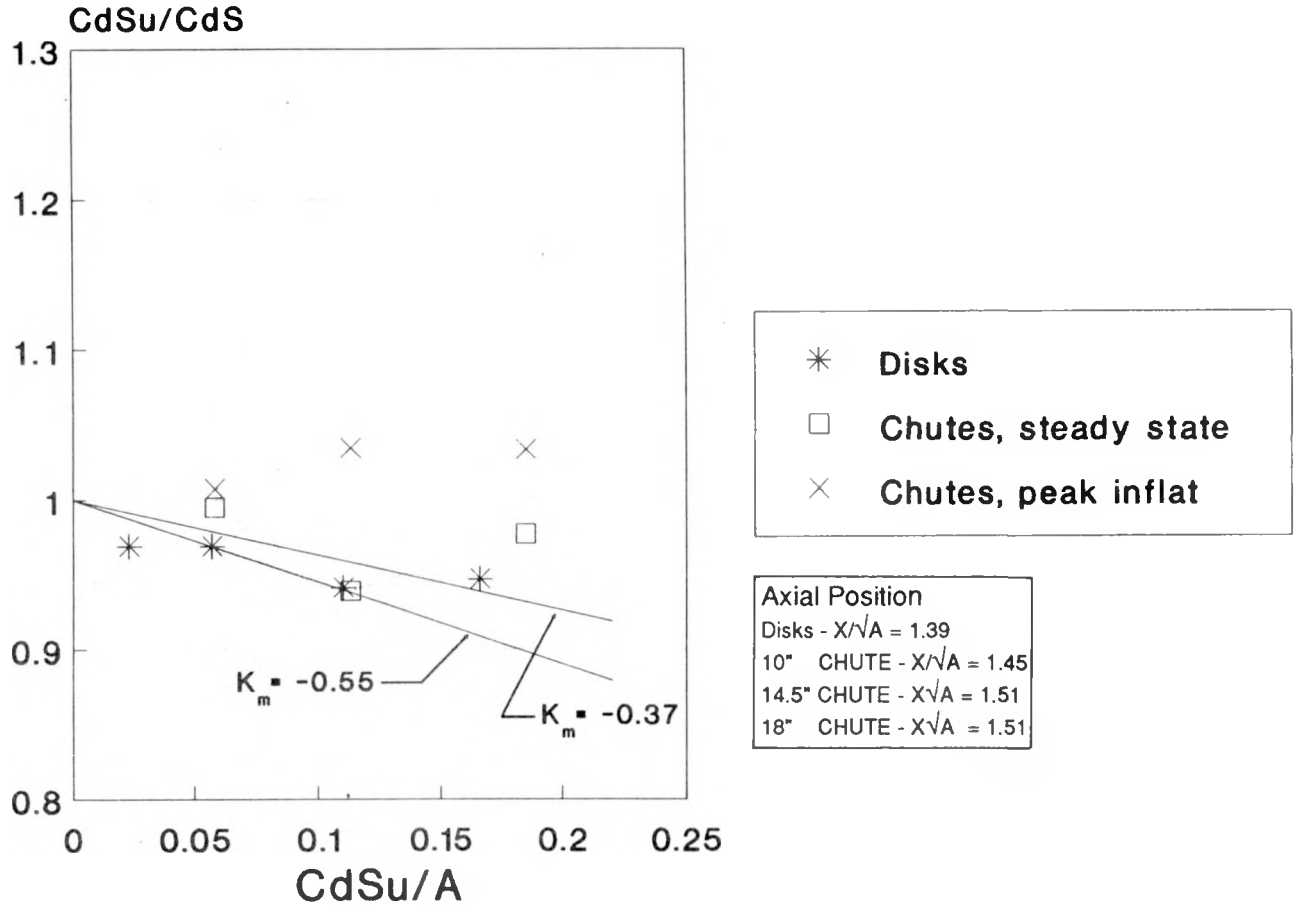

Figure 33. Blockage Correction for All Models, 20% OAR Test Section

30 % Open Area Ratio

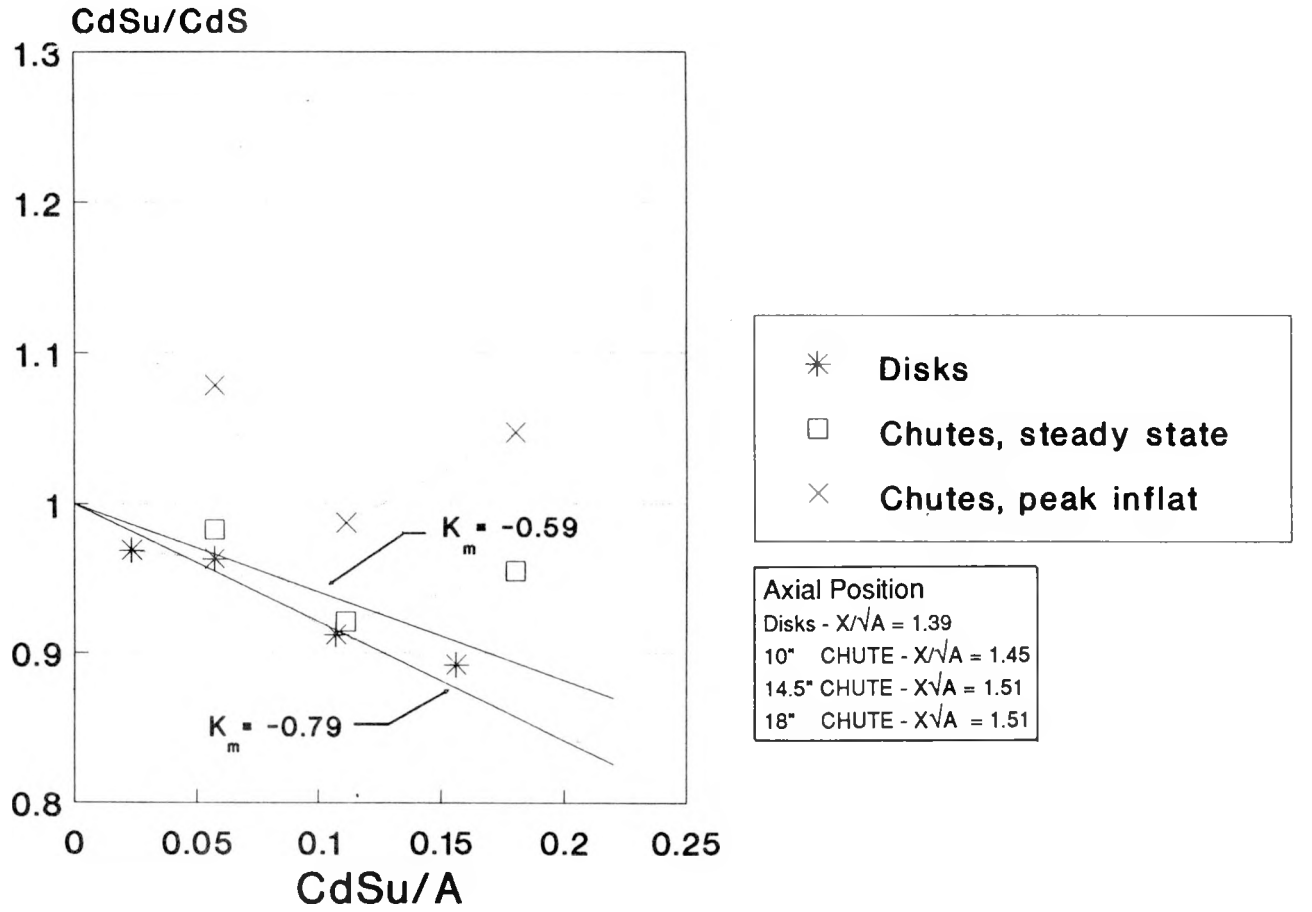

Figure 34. Blockage Correction for All Models 30% OAR

DSMA engineers constructors International

Sandia National Laboratories

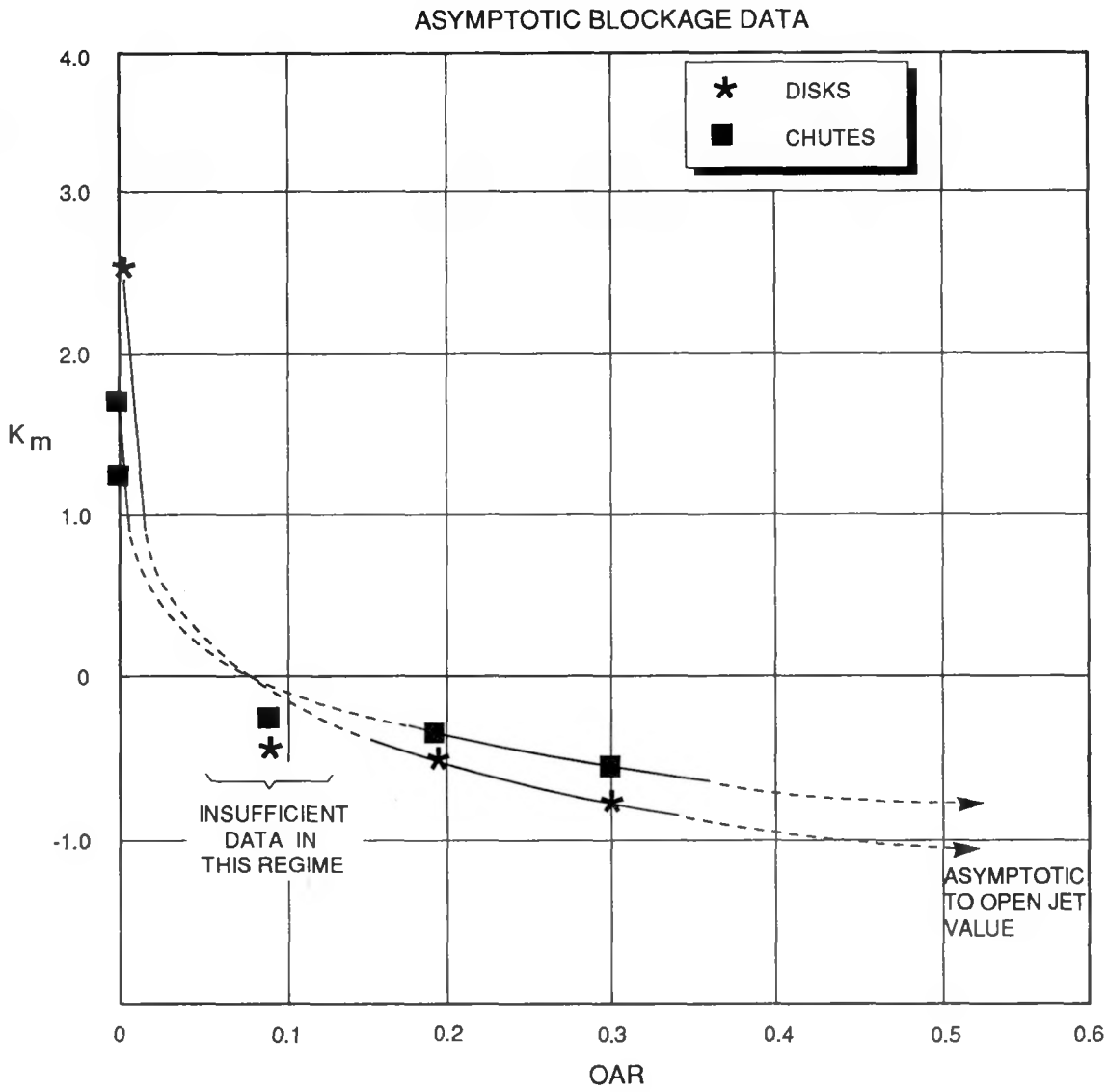

Figures 35. Asymptotic Maskell Blockage Correction as A Function of OAR

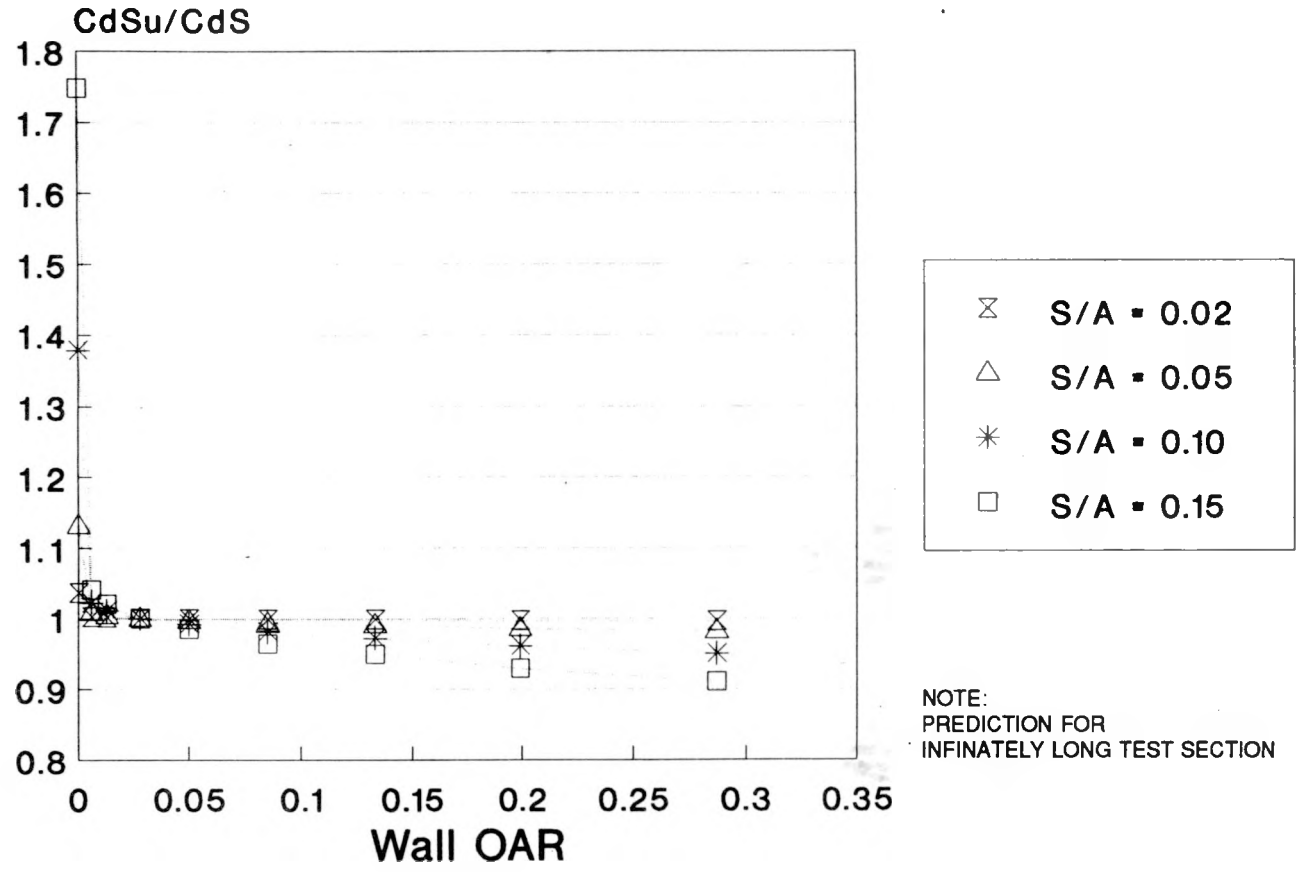

Figure 36. Theoretical Prediction of Blockage Correction as a Function of OAR

APPENDIX A

Calibration of the DSMA Model Wind Tunnel

INTRODUCTION

Prior to the start of the test program a calibration phase for the new test section was completed. This start-up phase included the following activities.

1. Evaluation of the flow in the test section diffuser and modifications to the diffuser to correct the flow separation.

2. Re-pitching the main fan blades and adding circuit loss elements to minimize the change in dynamic pressure during a parachute inflation.

3. Calibration of the two dynamic pressure measurement systems.

3. Measurement of the axial static pressure gradient and flow uniformity.

DIFFUSER FLOW

Initial runs with the 30% OAR wall configuration showed that there was some flow separation in the test section diffuser. This originated in corner flows but only appeared in the ceiling corners. The diffuser flow was evaluated both with corner fillets installed and vortex generators at the inlet to the diffuser. Two sizes of corner fillets and two sizes of vortex generators were employed; the most noticeable improvement was observed with the largest corner fillets. The vortex generators and large fillets were not significantly better than large fillets alone. Therefore the diffuser was configured with large corner fillets and no vortex generators for the remainder of the tests. Test section pressure fluctuations were judged to be acceptable with this configuration.

DYNAMIC PRESSURE CHANGE

Tuning of the circuit to minimize the change in dynamic pressure for constant fan RPM was done for the 30% OAR wall configuration. Three different fan blade pitches were used and various combinations of wire screen and fabric were installed on the upstream side of corner 2 to increase circuit losses. The dynamic pressure change was measured by comparing the dynamic pressure at a given fan speed with a flat disk model in the test section to the dynamic pressure with test section empty at the same fan speed.

A minimum wind speed of 30 m/sec at maximum fan speed and a maximum q change of 3.0% with 10% area blockage was established as the performance requirement for the successful configuration. The final configuration which gave the best performance and met the minimum wind speed requirement was with the fan pitched to a blade pitch setting of 8, and 4 layers of fabric and 2 layers of wire screen at corner number 2. The data for this configuration is summarized in Table A1.

CALIBRATION

The test section calibration constants were determined by positioning a pitot-static probe at an axial position of 3.28 feet and as close to the test section centre line as possible. As the probe was inserted through a slot in the slotted wall test sections, the probe was offset from the centre line by about half a slat width. The scanivalve system with the DSMA model wind tunnel data acquisition system was used to record the pressures from the nozzle reference section and the contraction reference system (see Figure 8). Two sets of wind tunnel calibration factors were calculated from this data.

For the nozzle reference system,

$$K_p = \frac{P_\infty - P_{ref}}{P_{tref} - P_{ref}}$$

$$K_q = \frac{P_{t\infty} - P_\infty}{P_{tref} - P_{ref}}$$

For the contraction reference system,

$$K_p = \frac{P_\infty - P_{c1}}{P_{c1} - P_{c2}}$$

$$K_q = \frac{P_{t\infty} - P_\infty}{P_{c1} - P_{c2}}$$

where: P_∞ is the static pressure from the pitot-static probe

$P_{t\infty}$ is the total pressure from the pitot-static probe

P_{ref} is the nozzle reference system static pressure

P_{tref} is the nozzle reference system total pressure

P_{c2} is the contraction exit static pressure

P_{c1} is the settling chamber static pressure

The calibration data is given in Table A2 and plotted in Figure A1. In Table A2 the pressure coefficients are calculated in the following way.

$$C_p = \frac{P_{measure} - P_{c2}}{P_{c1} - P_{c2}}$$

The calculated average value of K_q given in Table A2 was used to compute the dynamic pressure for each respective reference system for reduction of data during the main test program. The average value of K_p is also given in Table A2. K_p was not required for the present tests but is included in Table A2 for completeness and for possible future reference.

FLOW UNIFORMITY

During the commissioning phase the axial static pressure gradient was evaluated by examining the pressures measured with wall static taps in the middle slat on the left wall of the test section. Spot checks were also done with the pitot-static probe. The wall pressure data for all of the test sections is plotted in Figure A2. Note that the flap setting for the 10% OAR configuration was not optimum (too wide). The effect of the flaps on the static pressure distribution is shown for the 20% OAR wall. It can be seen from Figure A2 that the pressure gradient over the middle 4 feet of the test section is negligible.

Several limited traverses were made across the test section at X = 1000mm with the pitot-static probe. Traverse data for the 10% OAR and 20% OAR test sections is given in Figure A3.

Table A1: Dynamic Pressure Change with the 30% OAR Test Section

Run	Model	Area Blockage	Circuit Loss Factor	Dynamic Pressure Change
51	empty test section	0	3.29	0
53	200 mm diameter disk	6.1%	3.36	2.3%
54	250 mm diameter disk	9.5%	3.46	5.0%
52	300 mm diameter disk	13.6%	3.60	8.1%

Table A2: Calibration Data for all Test Sections

Run No.	Test Section	Nozzle Reference System delP (psf)	Ptref (Cp's)	Pref (Cp's)	Kq	Kp	Contraction Reference System delP (psf)	Pc1 (Cp's)	Pc2 (Cp's)	Kq	Kp
64	10%	9.82	.994	.015	1.064	-.063	10.03	.994	-.048	1.042	-.048
82	10%	3.86	1.005	.014	1.066	-.064	3.89	1.006	-.050	1.056	-.050
		6.02	1.005	.014	1.065	-.064	6.07	1.005	-.050	1.055	-.050
		8.27	1.006	.015	1.064	-.065	8.35	1.005	-.050	1.054	-.050
		10.55	1.004	.014	1.065	-.065	10.65	1.003	-.051	1.054	-.051
83	10%	3.84	1.007	.017	1.068	-.066	3.88	1.008	-.050	1.058	-.050
		6.03	1.004	.009	1.062	-.060	6.07	1.005	-.051	1.056	-.051
		8.26	1.005	.014	1.065	-.065	8.33	1.005	-.051	1.056	-.051
		10.53	1.004	.014	1.064	-.064	10.63	1.003	-.050	1.054	-.050

Table A2(cont): Calibration Data for all Test Sections

Run No.	Test Section	Nozzle Reference System delP (psf)	Ptref (Cp's)	Pref (Cp's)	Kq	Kp	Contraction Reference System delP (psf)	Pc1 (Cp's)	Pc2 (Cp's)	Kq	Kp
84	solid	10.10	1.005	.014	1.067	-.068	10.20	1.004	-.053	1.057	-.053
85	solid	3.88	1.008	.016	1.069	-.069	3.91	1.008	-.053	1.060	-.053
		6.02	1.005	.015	1.072	-.074	6.08	1.001	-.060	1.061	-.060
		8.28	1.005	.014	1.067	-.067	8.36	1.004	-.053	1.057	-.053
86	solid	10.57	1.005	.014	1.066	-.066	10.67	1.004	-.052	1.056	-.052
		3.91	1.005	.002	1.056	-.055	3.90	1.006	-.054	1.059	-.054
		6.06	1.009	.014	1.067	-.068	6.09	1.007	-.055	1.062	-.055
		8.28	1.004	.014	1.067	-.067	8.36	1.004	-.052	1.057	-.052
		10.54	1.003	.014	1.068	-.067	10.66	1.003	-.053	1.056	-.053
92	20%	9.99	1.005	.014	1.070	-.070	10.08	1.005	-.055	1.061	-.055
97	20%	3.82	1.007	.017	1.074	-.072	3.86	1.008	-.056	1.063	-.056
		5.92	1.006	.018	1.073	-.075	5.99	1.004	-.057	1.061	-.057
		8.14	1.002	.015	1.071	-.071	8.25	1.000	-.056	1.056	-.056
		10.41	1.004	.014	1.070	-.071	10.52	1.003	-.057	1.059	-.057
102	20%	3.81	1.006	.015	1.073	-.073	3.84	1.006	-.058	1.064	-.058
		5.94	1.008	.016	1.071	-.072	5.99	1.006	-.056	1.062	-.056
		8.27	1.020	.015	1.055	-.071	8.23	1.004	-.057	1.060	-.057
		10.45	1.007	.013	1.062	-.070	10.50	1.000	-.057	1.057	-.057
102	20%	3.81	1.006	.015	1.073	-.073	3.84	1.006	-.058	1.064	-.058
		5.94	1.008	.016	1.071	-.072	5.99	1.006	-.056	1.062	-.056
		8.27	1.020	.015	1.055	-.071	8.23	1.004	-.057	1.060	-.057
		10.45	1.007	.013	1.062	-.070	10.50	1.000	-.057	1.057	-.057
107	30%	10.38	1.005	.013	1.064	-.067	10.47	1.001	-.054	1.055	-.054

Table A2(cont): Calibration Data for all Test Sections

Run No.	Test Section	Nozzle Reference System delP (psf)	Ptref (Cp's)	Pref (Cp's)	Kq	Kp	Contraction Reference System delP (psf)	Pc1 (Cp's)	Pc2 (Cp's)	Kq	Kp
109	30%	3.76	1.005	.012	1.071	-.068	3.79	1.007	-.056	1.064	-.056
		5.77	1.000	.011	1.071	-.064	5.83	1.005	-.053	1.058	-.053
		8.04	1.009	.016	1.064	-.067	8.09	1.006	-.051	1.057	-.051
		10.25	1.001	.014	1.069	-.068	10.39	1.002	-.053	1.055	-.053
110	30%	3.74	1.008	.019	1.067	-.068	3.78	1.006	-.048	1.054	-.048
		5.65	.985	.016	1.079	-.067	5.83	.996	-.050	1.045	-.050
		7.98	1.003	.015	1.068	-.059	8.08	1.012	-.044	1.055	-.044
		10.25	1.003	.014	1.067	-.068	10.37	1.002	-.053	1.055	-.053
Average					1.067	-.068				1.057	-.053

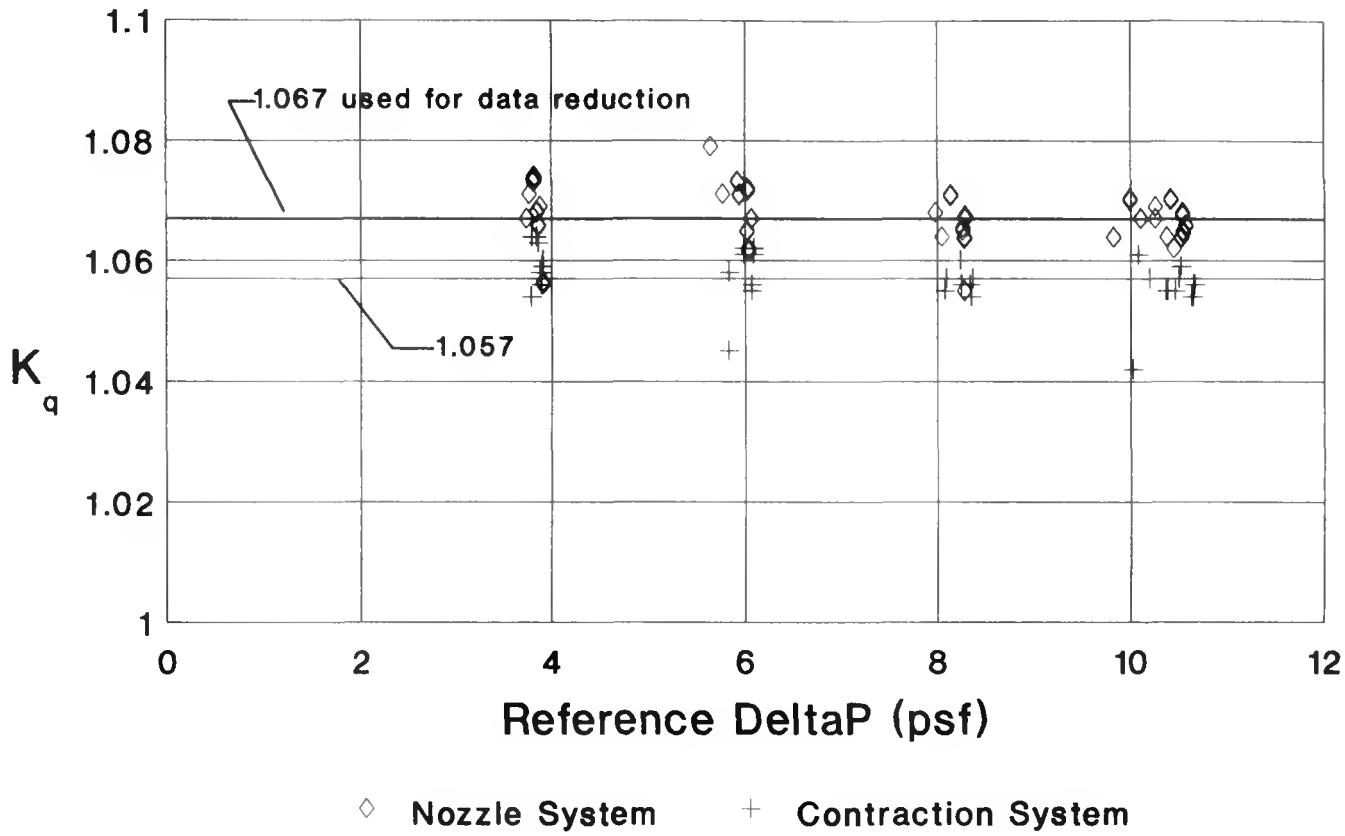

Figure A1. Test Section Dynamic Pressure Calibration Constant

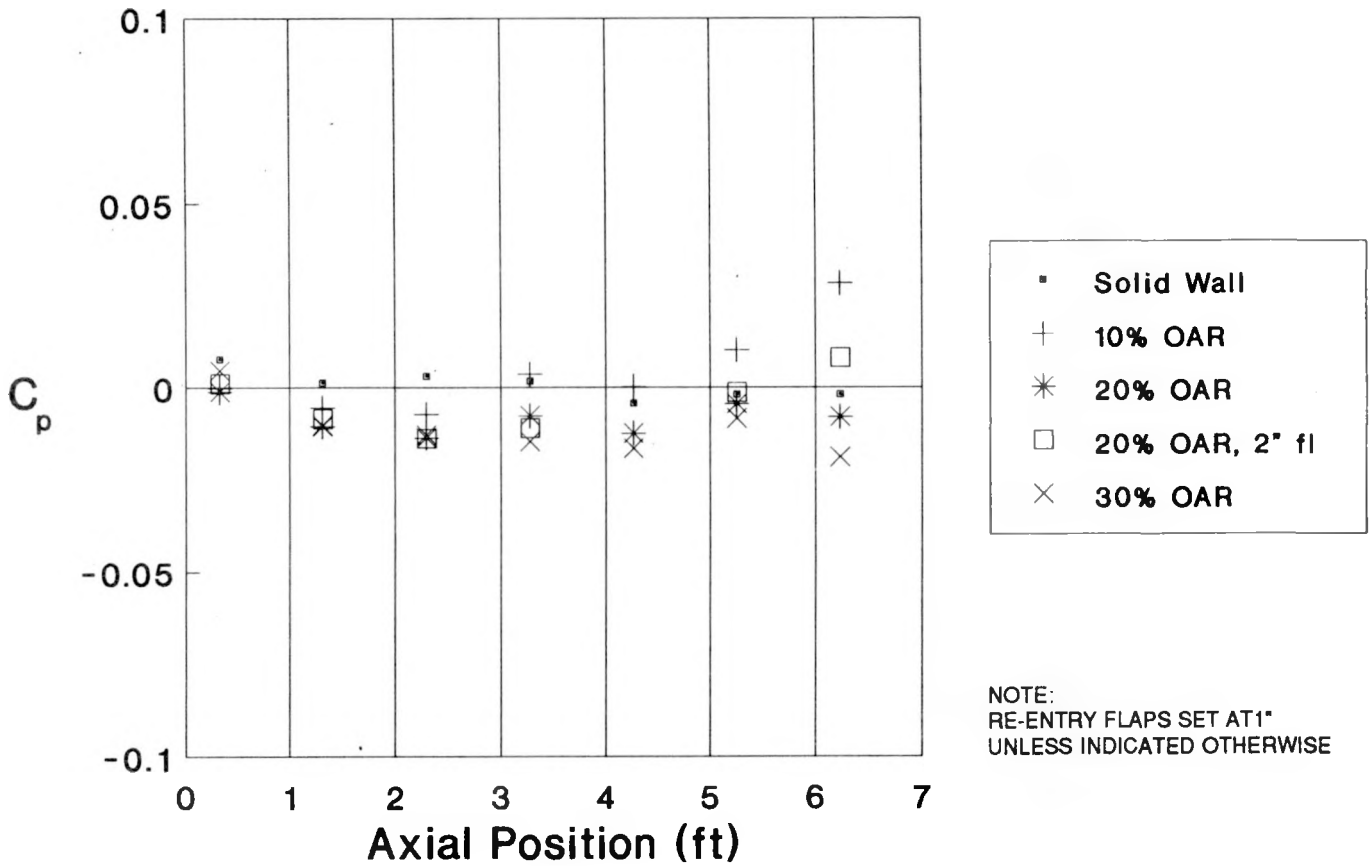

Figure A2. Axial Static Pressure Distribution

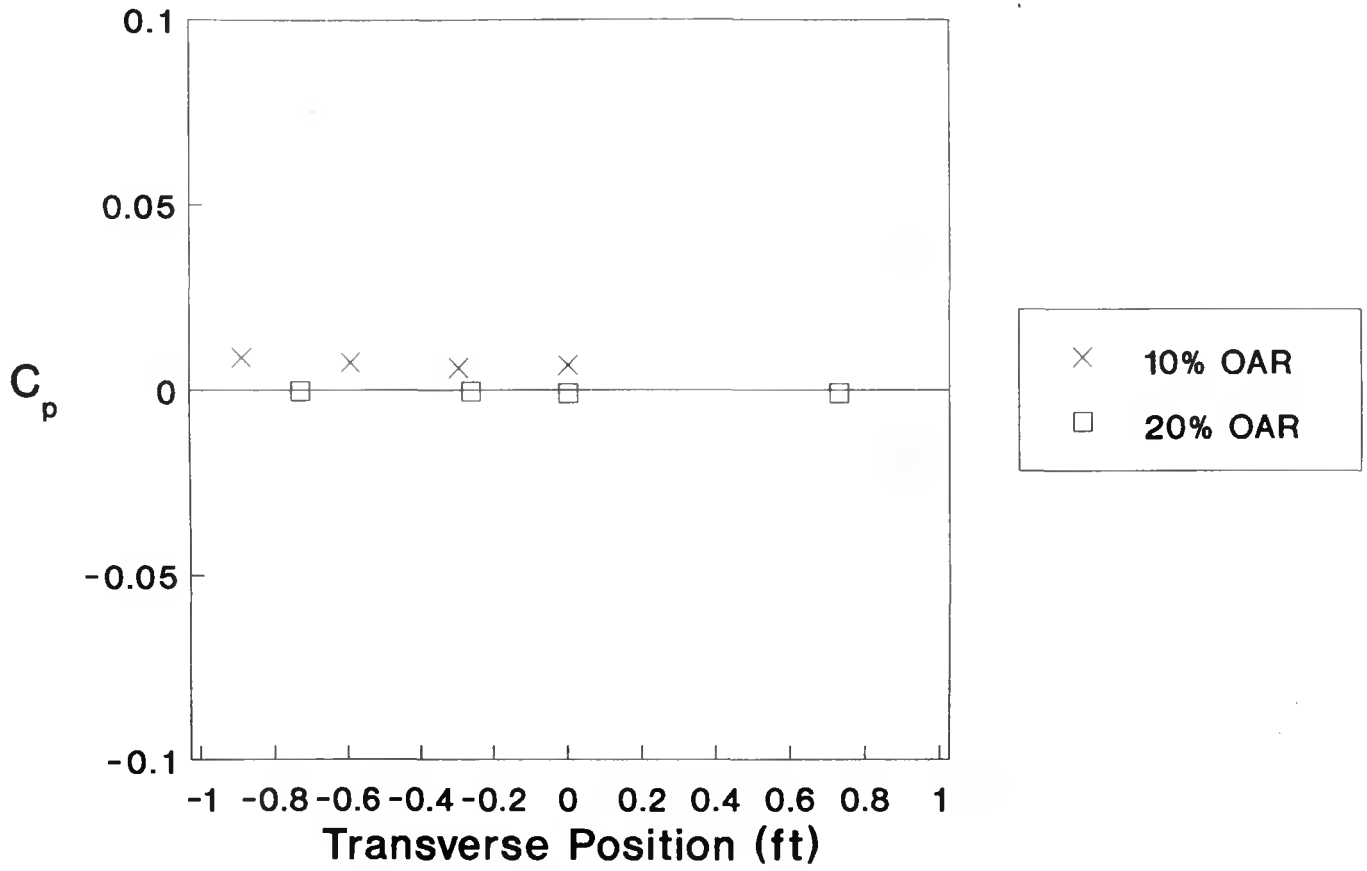

Figure A3. Transverse Static Pressure Distribution at X/√A = 1.39

APPENDIX B

Run Log

$K_Q = 1.057$

RUN	DATE	RPM	Q_{shaft} (ft-lb)	Patm (kPa)	T	MODEL	X (ft)	FLAP	T/S	COMMENTS
1	21/8/89	1462.5	9.548	99.05	29.4	10.1 "	4.85	1"	.30	Disk model. q = 2.25 volts
2.	"	1502.3	10.138	99.05	27.1	"	"	2"	"	
3	"	1538.5	10.618	"	28.9	"	"	3"	"	
4	"	1547.3	10.670	"	30.2	"	"	4"	"	rude scale flap set to 2"
5	"	1565.8	10.941	"	31.3	"	"	4"	"	repeat of 4 with correct flap
6	"	1580.7	11.234	"	28.8	"	"	5"	.3	
7	"	1513.9	10.221	"	30.6	"	"	2"	"	repeat of #2
8	"	1555.3	10.696	"	31.5	"	4.1	1"	0.3.	new axial position
9	"	1560.4	10.820	"	26.7	"	"	2"	"	
10	"	1580.1	11.114	"	27.7	"	"	3"	"	
11	"	1590.1	11.296	"	27.5	"	"	4"	"	
12	"	1597.5	11.416	"	27.5	"	"	5"	"	
13	"	1597.1	11.364	"	26.4	"	3.28'	5"	"	new axial position
14	"	1587.9	11.145	"	27.1	"	"	4"	"	
15	"	1585.2	11.077	"	27.1	"	"	3"	"	
16	"	1595.9	11.176	"	27.3	"	"	2"	"	
17	"	1578.5	10.926	"	27.8	"	"	1"	"	
18	"	1594.6	11.276	"	27.6	"	2.46	1"	"	no second strut
19	"	1577.3	10.926	99.1	28.6	10.1	2.46	2"	"	
"	"	1575.6	10.894	99.1	28.5	"	"	3"	"	
	"	1583.3	11.129	"	28.1	"	"	4"	"	

DSMA International Inc.
Toronto, Canada

Subject: Run Log SAUDIA TESTS

Design Report

Project No.
By
Date
Checked
Date
D.R. No.
Page
Of

$K_g = 1.067$ all models are shells

RUN	DATE	RPM	q lb/ft²	P_stn kPa	T °C	MODEL	X ft	FLAP	T/S	COMMENTS	
22	21/8/89	1579	11.020	99.1	27.9	10.1"	2.46	4"	0.30	sting support	
23	22/08/89	1530	11.067	99.5	25.4	4.5"	2.46	4"	0.30		
24	"	1486	10.320	"	24.8	7.2"	"	"	"		
25	"	1597.9	11.030	"	24.5	12.4"	"	"	"		
26	"	1550	10.352	"	24.5	12.4"	1.64	4"	0.30	new axial pos	$C_D S = 0.966$
27	"	1540	10.696	"	24.7	10.1"	1.64	"	"		$= .642$
28	"	1479.7	10.174	"	25.2	7.2"	"	"	"		.323
29	"	1479.1	10.216	"	25.4	4.5"	"	"	"		.128
30	"	1451.4	9.824	"	25.4	4.5"	0.82	"	"	.2cm axial pos	.130
31	"	1432.7	9.537	"	25.1	7.2"	"	"	"		.342
32	"	1453.7	9.346	"	25.3	10.1"	"	"	"		.720
33	"	1409.0	8.432	"	25.1	12.4"	"	"	"		1.182
34	"	1596.1	10.973	"	24.7	12.4"	3.28	"	"	new axial pos	0.864
35	"	1596	11.427	"	25.3	10.1"	"	"	"	(no	1.14 .593
36	"	1504	10.503	"	25.7	7.2"	"	"	"		1.12 .313
37	"	1461	9.997	"	25.5	4.5"	"	"	"		9/8 = 1.12 .126
38	"	1499.6	10.534	"	25.7	4.5"	4.10	"	"	new axial pos	
39	"	1535	10.978	"	26.1	7.2"	"	"	"		
40	"	1590	11.432	"	25.3	10.1"	4.1	"	"		
41	"	1597	11.114	"	25.8	12.4"	"	"	"		

DSMA International Inc.
Toronto, Canada

Design Report

Subject

Project No.
By
Checked
Date
Date
D.R. No.
Page
01

B-20002

$K_q = 1.057$ for parachute tests. X = position of sting nose

RUN	DATE	RPM	q lb/ft²	Patm mBa	T °C	MODEL	X ft	FLAP "	T/S	COMMENTS
42	22/08/89	1476	10.064	99.1	24.5	10" CHUTE	2.52	4"	.30	chute portioned to max D at 3.43'
43	"	1484.2	10.299	99.1	25.0	10"	"	"	"	inflation. $D_{peak} = -921.6$mV + 2.05V
			10.106	"			"			← after inflation $D_{ave} = -1.5105$mV + 2.06V
44	"	1482.8	10.247	"	25.0	10" CH	"	4"	0.3	repeat of 43 inflation only
45	"	1481.6	10.200	"	25.2	"	"	"	"	repeat of 43
			10.096	"	26.5					← after inflation
46	"	1503.9	10.294	"	25.0	14.5"	2.22	4"	0.3	max Diam @ 3.45' + .06'
47	"	1446.7	10.461	"	25.0	14.5"	"	"	"	inflation
		1502.9	10.211	"	26.5					← after inflation
48	"	1497.9	10.419	"	25.4	14.5"	"	"	"	repeat of 47
	"	1502.3	10.169	"	26.8	"				← after inflation
49	23/08/89	1495.7	10.560	99.1	23.4	14.5"	"	4"	0.3	repeat of 47
		1501.4	10.289	"	24.8					← after inflation
50	"	1155.5	6.108	"	22.5	18"	1.98	4"	0.3	inflation
		1156.1	5.773	"	23.0	"	"	"	"	← after inflation
51	"	1155.5	6.108	"	22.4	"	"	"	"	repeat of 50
		1156.1	5.800	"	22.8	"	"	"	0.3	← after inflation
52	"	1155.3	6.113	"	22.4	"	"	4"	0.3	repeat of 50
		1156.1	5.810	"	22.8	"	"	4"	"	← after inflation

DSMA International Inc.
Toronto, Canada

Subject

Design Report

Project No. | By | Date

Checked | Date

D.R. No. | Page | Of

8-20002

RUN	DATE	RPM	q	P_{atm} kPa	T °C	MODEL	X ft	FLAP "	T/S	COMMENTS
53	23/08/89	1476.2	9.767	99.4	24.3	10.1"	4.85'	1"	0.2	start of 0.2 wall
54	"	1505.7	10.169	"	24.2	"	"	2"	"	
55	"	1531.6	10.571	"	24.6	10.1"	"	3"	"	
56	"	1550	10.806	"	25.6	"	"	4"	"	
57	"	1564.5	11.098	"	25.2	"	"	5"	"	
58	"	1583.8	11.150	"	25.7	"	4.1'	5"	"	new location
59	"	1570.7	10.988	"	25.6	"	"	4"	"	
60	"	1581.8	11.129	"	25.7	"	"	3"	"	
61	"	1571.9	10.900	"	26.0	"	4.1"	2"	"	
62	"	1542.6	10.472	"	26.0	"	"	1"	"	$C_0S = .639$
63	"	1566.4	10.748	"	26.6	"	3.28'	1"	"	new location
64	"	1586.1	11.035	"	26.2	"	"	2"	"	
65	"	1584.4	10.983	"	26.4	"	"	3"	"	
66	"	1587.5	11.051	"	26.6	"	"	4"	"	
67	"	1584.8	11.025	"	26.8	"	"	5"	"	
68	"	1589.8	10.821	"	21.0	12.4"	"	4"	"	new dash
69	"	1486.5	10.064	"	26.4	7.2"	"	4"	"	" "
70	"	1430.3	9.475	"	26.0	4.5"	"	"	"	" "
71		1466.2	9.955	"	26.2	4.5"	2.46'	4"	"	
72	"	1497.3	10.252	"	26.0	7.2"	"	4"	"	

DSMA International Inc.
Toronto, Canada

Subject

Checked Date

By Date

Project No.

Design Report

D.R. No.

Page 01

9-20002

$K_q = 1.057$

RUN	DATE	RPM	q lb/ft²	Patm kPa	T °C	MODEL	X ft	FLAP	T/S	COMMENTS
73	23/08/89	1558.6	10.654	99.4	26.7	10.1" Δ	2.46	4"	0.2	
74	"	1561.3	10.660	99.4	26.5	"	2.46	"	"	
75	"	1570.7	10.372	"	26.6	"	"	"	0.2	
76	24/08/89	1467.4	9.151	100.0	24.6	12.4"	1.64	4"	0.2	
77	"	1492.2	9.944	"	24.0	10.1"	"	"	"	
78	"	1474.0	10.143	"	24.2	7.2"	"	"	"	
79	"	1466.6	10.132	"	24.2	4.5"	"	"	"	
80	"	1447.7	9.866	"	24.4	4.5"	0.82	"	"	
81	"	1438.3	9.556	"	25.3	7.2"	0.82	"	"	
82	"	1409.6	8.801	"	23.9	10.1"	"	"	"	
83	"	1343.2	7.548	"	23.6	12.4"	"	"	"	
84	"	1569.9	10.733	"	24.3	12.4"	4.1	4"	"	
85	"	1530.7	10.931	"	24.4	7.2"	4.1	4"	"	
86	"	1511.7	10.774	"	24.5	4.5"	4.1	"	"	
87	"	1160.9	6.222	"	22.5	18"CH	1.98'	4"	0.2	start of inflation; X = sting roll position 3.8% 24/8/89
		1161.7	5.862	"	23.1					← after inflation.
88	"	1159.6	6.217	"	22.5	18"CH	"	"	"	max inflated ϕ ② 3.59'
		1161.7	5.841	"	23.1					← after inflation
89	"	1501.4	10.691	"	23.5	14.5"	9.22'	"	"	
		1506.6	10.409	"	25.1					← after inflation 2.6% change in q

DSMA International Inc.
Toronto, Canada

Subject

Checked Date
By Date
Project No.

Design Report
D.R. No.
Page Of

B-20002

$k_g = 1.057$ for parachute runs X = position at sting nose.

RUN	DATE	RPM	q	Patm	T °C	MODEL	X	FLAP	T/S	COMMENTS
90	24/08/89	1501.6	10.649	100	24.2	14.5"	2.52'	4"	0.20	
		1507.2	10.367	"	25.5					← after inflation
91	"	1504.2	10.440	"	24.1	14.5"	"	4"	0.20	steady state only
92	"	1502.9	10.419	"	24.3	"	"	"	"	repeat of 91
93	"	1503.1	10.691	"	24.0	14.5"CH	"	"	"	spare skate (#2) inflation
		1508.6	10.393	"	25.4	"	"	"	"	
94	"	1466.8	10.153	"	23.6	10"CH	2.52'	4"	0.2	max q @ 3.43'
		1473.2	10.064	"	25.1	10"	"	"	"	← after inflation
95	"	1466.4	10.075	"	24.4	"	"	"	"	inflation
		1471.7	10.002	"	25.8	"				← after inflation
96	"	1396.9	9.161	"	25.9	4.5"	3.28'	1"	0.0	solid wall test section .135.
97	"	1347.5	8.488	"	24.2	7.2"	"	"	"	right flap not set
98	"	1331.8	8.310	"	24.0	7.2"	"	"	"	repeat of 97 .379
99	"	1257.4	7.172	"	23.3	10.1"	"	"	"	
100	"	1162.5	5.810	"	23.3	12.4"	"	"	"	
101	"	1199.6	6 724	"	23.2	10"CH		"	"	
		1202.3	6.645	"	23.8					
102	25/08/89	1201.0	6.875	100.4	21.5	10"CH	2.52	1"	0.0	inflation
		1202.7	6.812		22.1					← after inflation
103	"	1345.1	8.728	100.4	22.0	14.5"CH	"	1"	0.0	inflation $\frac{15}{4} = 27\%$
		1348.1	8.488		23.1					← after inflation

DSMA International Inc.
Toronto, Canada

Subject

Design Report

Project No. | By | Date
Checked | Date
D.R. No.
Page | Of

$K_q = 1.057$

RUN	DATE	RPM	q	Patm	T	MODEL	X	FLAP	T/S	COMMENTS
104	25/07/89	1344.3	8.697	100.4	22.2	14.5"CH	2.22'	1.0"	0.0	$\frac{\Delta q}{q} = 2.9\%$
		1349.0	8.441	"	23.4	"				← after inflation
105	"	956.6	4.192	"	21.3	18.0"CH	1.98'	1.0"	0.0	$\frac{\Delta q}{q} = 6\%$
		957.4	3.941	"	21.5					← after inflation
106	"	956.4	4.207	"	21.1	18.0"	"	"	"	
		957.4	3.931		21.4					← after inflation
107	"	956.4	4.197	"	21.0	"	"	"	"	
			3.941	"	21.3					← after inflation
108	"	5.779	1149.2	"	21.5	12.4" D	2.46	1.0"	"	
109	"	5.570	1130.9	"	21.6	12.4"	1.64	"	"	
110	"	5.559	1127.9	"	21.5	12.4" D	0.82	"	"	
111	"	1345.3	8.712	"	22.0	14.5"CH	2.22	"	"	
		1349.4	8.493	"	23.1	"				← after inflation
112	"	1446?	—	"	25.0	10." D	4.8'	1.0"	0.1	- DSMA leg trans not corrected.
113	"	1489	9.981	"	24.5	10." D	"	2.0"	0.1	
114	"	1519.7	10.252	"	25.0	10.1"	"	3.0"	0.1	
115	"	1518.0	10.263	"	25.0	"	"	4.0"	"	
116	"	1535.9	10.519	"	25.5	"	"	5.0"	"	
117	"	1547.9	10.571	"	25.4	"	4.1'	5.0"	"	
118	"	1545.1	10.524	"	25.6	"	4.1'	4.0"	"	
119	"	1552.7	10.587	"	25.9	"	"	3.0"	"	

B-20002

DSMA International Inc.
Toronto, Canada

Subject

Design Report

Project No.
By
Checked
Date
Date
D.R. No.
Page
Of

DSMA International Inc.
Toronto, Canada

Design Report

Subject

Project No.
By
Date
Checked
Date
D.R. No.
Page
Of

RUN	DATE	RPM	q	Patm kPa	T	MODEL	x ft	FLAP	T/S	COMMENTS
120	25/08/09	1530.3	10.284		25.8	10.1" D	4.1	2"	0.1	
121	"	1503.5	9.965		25.9	"	"	1"	"	
122	28/08/09	1501.8	10.070	100	23.8	10.1" D	3.28'	1"	0.1	
123	"	1515.4	10.164	100	24.4	"	3.28'	2"	0.1	
124	"	1519.9	10.226	"	24.7	"	"	3"	0.1	
125	"	1529.5	10.305	"	25.1	"	"	4"	0.1	
126	"	1517.8	10.127	"	25.5	"	"	5"	0.1	
127	"	1478.3	9.203	"	25.0	12.4"	3.28	4"	0.1	
128	"	1515.6	10.555	"	25.2	7.2"	"	4"	0.1	
129	"	1521.7	10.795	"	25.5	4.5"	"	4"	0.1	
130	"	1446.1	10.446	"	25.6	4.5"	2.46	4"	0.1	
131	"	1476.8	10.012	"	25.2	7.2"	"	4"	"	
132	"	1479.1	9.589	"	25.6	10.1"	"	"	"	
133	"	1413.9	8.337	"	25.8	12.4"	"	"	"	
134	"	1348.0	7.569	"	25.1	12.4"	1.98	"	"	
135	"	1428.9	8.900	"	25.1	10.1"	"	"	"	
136	"	1467.6	9.814	"	25.5	7.2"	"	"	"	
137	"	1482.4	10.205	"	25.7	4.5"	"	"	"	
138	"	1482.6	10.242	"	25.4	4.5"	0.82	"	"	
139	"	1437.5	9.365	"	25.8	7.2"	"	"	"	
140	"	1545.9	10.839	"	25.7	7.2"	4.1	"	"	

9-2002

RUN	DATE	RPM	q PSF	Patm kPa	T °C	MODEL	X ft	FLAP	T/S	COMMENTS
141	28/08/89	1567.0	10.760	100	26.1	10.1" D	4.1	4"	0.1	
142	"	1510.7	9.652	"	26.0	12.4" D	"	"	"	
143	"	1531.3	10.868	"	26.3	4.5" D	"	"	"	
144	"	1536.1	10.900	"	25.9	4.5" D	4.85	4"	"	
145	"	1546.9	11.025	"	27.1	"	"	3"	"	
146	"	1520.3	10.707	"	26.1	"	4.1	3"	"	
147	"	1518.8	10.701	"	26.2	"	"	2"	"	
148	"	1512.7	10.571	"	26.3	"	"	1"	"	
149	"	1183.4	6.337	"	25.1	10" CH	3.09	4"	"	← move of string / inflation 3.98' after inflation chute position
		1184.2	6.269	"	25.4	"				
150	"	1183.4	6.348	"	25.1	10 "CH	"	4"	0.1	
		1185.2	6.301	"	25.5	10 "CH				
151	"	1183.2	6.379	"	24.5	"	3.09	1"	"	← new flap.
		1185.2	6.259	"	25.0	"				
152	"	1181.6	6.363	"	24.2	"	"	1"	0.1	repeat of 151
		1183.6	6.264		24.9	"	"			
153	"	1183.2	6.316	"	25.1	"		4"	0.1	string support in chute at 2.36'
		1185.4	6.254	"	26.0	"	1.85'	"	"	← after inflation
154	"	14.77.1	10.044	"	27.4	"	"	"	"	repeat of 153 with higher q.
		1479.9	9.866	"	29.7	"				

DSMA International Inc.
Toronto, Canada

Subject

Design Report

Project No.
By
Checked
Date
Date
D.R. No.
Page 01

2002-8

$K_q = 1.057$ X = row of string for chute

RUN	DATE	RPM	q PSF	Patm kPa	T	MODEL	X	FLAP	T/S	COMMENTS
155	28/08/84	1475.0	10.049	100	26.8	10" CH	2.52'	4"	0.1	
		1479.5	9.913	100	28.0					
156	"	1474.2	10.023	100	26.8	"	"	"	"	repeat of 155
		1478.8	9.929	"						
157	"	1476.2	10.017	100	27.1	"	"	"	"	repeat of 155
		1480.7	9.924							
158	"	1540.6	10.968	100	27.0	14.5"CH	2.22	4"	4	3.54' - max chute ϕ
		1546.9	10.547	100	28.7					
159	"	1541.4	10.936	"	27.7	"				
		1546.5	10.571							
160	"	1158.6	5.982	"	26.2	18" CH	1.98'	4"	4	3.54' - max chute ϕ
		1160.5	5.622		26.5					
161	"	1159.2	6.019	"	25.9	"	"	"	1	repeat of 160
		1161.3	5.627		26.2					
162	"	1159.0	6.008	"	25.6	"	"	"	"	repeat of 160
		1161.3	5.653		26.1					
163	"	1543.6	11.009	"	26.5	14.5"CH	2.22	4"	"	
		1549.0	10.633	"	28.1					
164	"	1543.8	10.968	"	27.3	"	"	"	"	repeat of 158
		1548.2	10.618	"	28.7	"	"	"	"	
165	"	1543.9	10.952	"	27.8	"	"	"	"	repeat of 158
		1547.9	10.654	"	29.0	"	"			

DSMA International Inc.
Toronto, Canada

Subject

Design Report

Project No. | By | Date | Checked | Date | D.R. No. | Page | Of

RUN	DATE	RPM	q	Patm	T	MODEL	x	FLAP	T/S	COMMENTS
166	29/09/89	1530.1	10.623	99.2	25.4	7.2" D	3.28	4"	0.1	
167	"	1523.8	10.487	99.2	25.7	"	"	1"	0.1	
168	"	1590.0	11.657	99	80.3°F	EMPTY		4"	0.0	wall pressures, empty tunnel. manifold on q - SCANI gain = 20
169	"	1582.6	11.704	"	80.2°F	"		1"	0.0	repeat of 168 - flap at 1"
170	"	1186.5	5.873	"	79.5°F	12.4" D	3.28	1"	0.0	5 sec averaging
171	"	1191.6	5.956	"	78.7	"	"	"	"	repeat of 170 10 sec averaging
172	"	1187.1	5.914	"	78.5°F	"	"	"	"	repeat of 170 15 sec averaging
173	"	1289.6	7.324	"	78.7°F	10.1" D	"	"	"	5 sec averaging - all remaining solid wall ports
174	"	1404.9	9.015	"	79.7°F	7.2" D	"	"	"	
175	"	1490.2	10.247	"	80.5°F	4.5" D	"	"	"	
176	"	1506.8	10.440	"	81.4	4.5" D	2.46'	1"	"	support strut installed
177	"	1409.8	8.984	"	82.3	7.2" D	"	"	"	
178	"	1314.7	7.345	"	81.5	10.1" D	"	"	"	
179	"	1188.5	5.857	"	80.6°F	12.4" D	"	"	"	
180	"	1585.2	11.625	"	81.3°F	EMPTY		1"	"	- sting support in. - nose at 715 mm
181	30/09/89	1579.7	11.594	99.	77.2°F	EMPTY		4"	0.2	5 sec sampling
182	"	1586.7	10.534	99	79.9 °F	12.4" D	3.28	4"	0.2	5 sec sampling
183	"	1581.1	49465Pa	99	27.8°C	"	"	"	"	10 sec averaging
184	"	1584.4	10.440	"	80.6 °F	"	"	"	"	15 sec averaging
185	"	1597.3	11.035	"	80.7°F	10.1" D	"	"	"	10 sec averaging

DSMA International Inc.
Toronto, Canada

Subject

Design Report

Project No. | By | Date

Checked | Date

D.R. No. | Page | Of

$k_q = 1.057$

RUN	DATE	RPM	q PSF	Patm	T °F	MODEL	X ft	FLAP	T/S	COMMENTS
186	30/04/89	1548.6	10.774	99	83.0F	7.2" D	3.28	4"	0.2	
187	"	1540.2	10.754	99	83.3	4.5" D	"	"	"	
188	"	1498.4	10.237	"	77.2°C	14.5"CH	9.22	4"	0.2	inflation - 3.54' max chute ϕ
		1502.7	9.965		28.1	2.2				
189	"	1498.6	10.216	"	27.2	14.5"CH	"	"	"	repeat of 188
		1503.3	9.955							
190	"	1496.5	10.200	"	27.2	"	"	"	"	repeat of 189
		1501.4	9.950	"	"					
191	"	1580.9	11.453	"	79.8F	EMPTY	—	1"	0.2	repeat of 181 with 1" flap.
192	"	1584.2	11.437	"	81.5F	EMPTY	—	1"	0.2	steng support in
193	"	1581.4	11.385	"	82.9F	"	—	4"	0.2	repeat of 192
194	"	1536.7	10.639	"	83.9F	4.5" D	2.46	4"	0.2	
195	"	1535.0	10.461	"	84.0F	7.2" D	"	4"	0.2	
196	"	1576.2	10.571	"	84.3	10.1" D	"	4"	0.2	
197	"	1592.8	10.320	"	84.7	12.4" D	"	"	"	

DSMA International Inc.
Toronto, Canada

Subject

Design Report

Project No. | By | Date
Checked | Date
D.R. No.
Page | Of